

**Structural and Biophysical Studies
of
Adhesive Binding by Classical Cadherins**

Von der Naturwissenschaftlichen Fakultät
der Gottfried Wilhelm Leibniz Universität Hannover
zur Erlangung des Grades

Doktorin der Naturwissenschaften
Dr. rer. nat.

genehmigte Dissertation

von
Dipl.-Biochem. Julia Brasch
geboren am 16. Januar 1982 in Braunschweig

2011

Referent: Prof. Dr. rer. nat. Bernd Otto

Korreferent: Prof. Dr. rer. nat. Walter Müller

Drittprüfer: Prof. Dr. Lawrence S. Shapiro

Weitere Prüfer: Prof. Dr. rer. nat. Hans-Jörg Jacobsen

Tag der Promotion: 21. April 2011

The present study was carried out at the Institute of Molecular Biophysics and Biochemistry, Columbia University in the City of New York, in the Laboratory of Prof. Dr. Lawrence Shapiro in collaboration with Prof. Dr. Bernd Otto, at the Institute of Biochemistry, Tiermedizinische Hochschule Hannover.

Parts of this thesis have been published in:

Brasch J, Harrison OJ, Ahlsen G, Carnally SM, Henderson RM, Honig B, Shapiro L. (2010) **Structure and binding mechanism of vascular endothelial cadherin, a divergent classical cadherin.** *Journal of Molecular Biology*, 408 (1): 57-73.

Harrison OJ, Jin, X, Hong S, Bahna F, Ahlsen G, **Brasch J**, Wu Y, Vendome J, Felsovalyi K, Hampton CM, Troyanovsky RB, Ben-Shaul A, Frank J, Trojanovksy SM, Shapiro L, Honig B. (2010) **The extracellular architecture of adherens junctions revealed by crystal structures of type I cadherins.** *Structure*, 19 (2): 244-56.

Harrison OJ, Bahna F, Katsamba PS, Jin X, **Brasch J**, Vendome, J, Ahlsen, G, Carrol KJ, Price SR, Honig B, Shapiro L. (2010) **Two-step adhesive binding by classical cadherins.** *Nature Structural Molecular Biology*, 17 (3): 348-57.

Ciatto C, Bahna F, Zampieri N, CanSteenhouse HC, Katsamba PS, Ahlsen G, Harrison OJ, **Brasch J**, Jin X, Posy S, Vendome J, Ranscht B, Jessel TM, Honig B, Shapiro L. (2010) **T-cadherin structures reveal a novel adhesive binding mechanism.** *Nature Structural Molecular Biology*, 17 (3): 339-47.

Zusammenfassung

Cadherine stellen eine große Familie von transmembranen Adhäsionsrezeptoren auf Zelloberflächen dar, deren erlesene Bindungsspezifitäten für die Formation und Instandhaltung der Gewebearchitektur von Vertebraten und Invertebraten verantwortlich sind. Circa 100 nicht klassische und 19 klassische Cadherine sind in Wirbeltiergenomen kodiert. Klassische Cadherine gliedern sich in zwei Unterfamilien: Typ I und II, von denen beide Kalzium abhängige Zelladhäsion vermitteln, die morphologischen Prozessen in Wirbeltieren zu Grunde liegen. Typ I Cadherine sind zumeist großflächig in Keimblättern und Epithelien exprimiert, wohingegen Typ II Cadherine im sich entwickelnden und erwachsenen zentralen Nervensystem (ZNS) weitaus feingliedriger und auch überlappend exprimiert sind. Vaskulär-endotheliales (VE) Cadherin, ein divergentes Mitglied der Typ II Familie, vermittelt homophile Zelladhäsion ausschließlich im Endothel, das die Blutgefäße auskleidet und ist unabkömmlich für vaskuläre Angiogenese und Instandhaltung der Vaskulatur. Für bakteriell produzierte VE-cadherin Ektodomän Fragmente wurde ein Adhäsionsmodell vorgeschlagen, bei dem sich das Protein auf derselben Zelloberfläche lateral zu Trimeren organisiert, die mit Trimeren nebeneinander liegender Zellen *trans* adhäsive Hexamere bilden. Dieses Modell weicht stark vom allgemein akzeptierten Bindungsmechanismus anderer Cadherine ab, der als ‚strand swap‘ Mechanismus bezeichnet wird, da er auf dem Austausch N-terminaler Regionen der extrazellulären cadherin (EC) ähnlichen Domänen zwischen zwei Protomeren besteht, aber keine Bildung von Trimeren involviert. Die vorliegende Dissertation befasst sich mit der detaillierten Charakterisierung des adhäsiven Bindungsmechanismus von VE-cadherin Ektodomänen, die in Säugetierzellen produziert wurden. Biophysikalische Studien, wie analytische Ultrazentrifugation, Größenausschlusschromatographie, Lichtstreuungsdetektion und Aggregation von Liposomen sowie spektroskopische Rasterkraftmikroskopie von Proteinen in Lösung und Elektronen-mikroskopie künstlicher Zellverbindungen, zeigen, dass VE-cadherin den ‚strand swap‘ Mechanismus klassischer Cadherine adoptiert, indem ausschließlich *trans* adhäsive Dimere gebildet werden. Zusätzlich wurde gefunden, dass die beschriebenen Trimere Artefakte repräsentieren, deren Bildung durch die Abwesenheit von Glykosylierung bei bakteriell produzierten Proteinen hervorgerufen wurde. Die Kristallstruktur der adhäsiven Domänen EC1-2 von VE-cadherin mit einer Auflösung von 2.1Å enthüllte Homodimere, deren Formation der ‚strand swap‘ Mechanismus zu Grunde liegt. Die adhäsive Interaktionsseite ist einzigartig, da sie Charakteristika von Typ I und II Cadherinen vereint, was zu einer unüblichen Konfiguration des Dimers führt. VE-cadherin stellt daher einen strukturellen Außenseiter der Typ II Cadherine dar. Eine Studie, die homo- und heterophile Interaktionen von Typ II Cadherinen untersuchte, schlägt zum ersten Mal einen Bindungscode für diese Zelladhäsionsproteine vor, der die Spezifität ihres heterophilen Bindungsmusters entschlüsselt. Interessanter Weise wurde auch eine Interaktion zwischen Typ I N- und Typ II VE-cadherin, identifiziert, die unabhängig vom ‚strand swap‘ Mechanismus ist, und eine neuartige Form einer *cis*-Interaction verspricht.

Schlüsselwörter: Zell-Zell-Adhäsion / Cadherine / Kristallstruktur.

Abstract

Cadherins constitute a large family of cell surface transmembrane adhesion receptors whose binding specificity is important in generation and maintenance of tissue architecture in vertebrates and invertebrates. About 100 nonclassical cadherins and approximately 18 classical cadherins are encoded in vertebrate genomes. Classical cadherins, comprised of two subfamilies the type I and type II cadherins, mediate calcium dependent cell-cell adhesion that is essential for morphogenesis in vertebrates. Type I cadherins are typically expressed broadly in germ layers or epithelia, whereas type II cadherins have a finely grained expression pattern, which is overlapping and primarily restricted to the developing and adult nervous system. A divergent member of the type II cadherin family, vascular endothelial (VE) cadherin, mediates homophilic adhesion in the vascular endothelium and is crucial for vascular angiogenesis, maintenance and restoration of vascular integrity after injury. In the past a binding model for VE-cadherin has been proposed based on data from bacterially produced ectodomain fragments in which the protein forms trimers laterally on the same cell surface, which bind to trimers presented by juxtaposed cells to form adherent hexamers. This model is substantially different from the well characterized binding mechanism of other classical cadherins, which is mediated by N-terminal extracellular cadherin (EC) domains in a three dimensional domain swapping mechanism, termed the ‘strand swap mechanism’, and involves no trimer interactions. Here I report extensive studies of purified mammalian produced VE-cadherin ectodomains to elucidate the adhesive binding mechanism of this crucial protein. Biophysical studies such as analytical ultracentrifugation, size exclusion chromatography and multi angle light scattering in addition to liposome aggregation and atomic force microscopy imaging studies and cryo electron microscopy of artificial junctions reveal that VE-cadherin forms adhesive *trans* dimers between monomers emanating from opposing cell surfaces and not hexamers. Trimerization of bacterially produced protein is found to be artifactual due to lack of glycosylation. I present the 2.1Å resolution crystal structure of VE-cadherin adhesive domains EC1-2 which reveals that the strand swap mechanism common to classical cadherins underlies homodimerization. The adhesive interface of VE-cadherin is unique as it features characteristics of both cadherin subfamilies. Two tryptophan residues are exchanged which is reminiscent of type II cadherins, but an extended non polar interface region specific to type II subfamily members is absent as observed for type I cadherins, resulting in an unusual overall dimer organization. VE-cadherin can therefore be described as a structural outlier among classical cadherins. A systematic binding study of homophilic and heterophilic interactions of type II cadherins, including VE-cadherin, was performed and reveals evidence for a new binding code which appears to govern the specificity of these important CNS cell adhesion proteins. In addition, for the first time, a strong heterophilic interaction between type I N-cadherin and type II VE-cadherin could be identified, which appears to be strand swap independent and may represent a novel *cis* interaction between these cadherins.

Key words: Cell-cell adhesion / cadherins / crystal structure.

Index

List of commonly used abbreviations	9
Chapter 1: Introduction	10
1.1 Cell adhesion in multicellular organisms	11
1.1 The cadherin superfamily of calcium dependent cell adhesion molecules	11
1.2 General features of classical cadherins	14
1.3 Molecular basis of cadherin-cadherin binding	19
1.4 Cadherins utilize a 3D domain swapping mechanism for adhesion.....	21
1.5 T-cadherin structures reveal a novel adhesive binding mechanism.....	23
1.6 Specificity and promiscuity of adhesive interactions between cadherins	25
1.7 Classical cadherins are the core molecules of adherens junctions	27
1.8 Vascular endothelial cadherin, a divergent classical cadherin.....	31
1.8.1 Special features of the vascular endothelium.....	31
1.8.2 VE-cadherin plays a pivotal role in the vascular endothelium.....	32
1.8.3 Hexamer model for VE-cadherin binding.....	34
1.9 Aims of this work.....	36
Chapter 2: Materials and Methods	37
2.1 Protein Production.....	38
2.1.1 Mammalian protein production.....	38
2.2.5 Atomic force microscopy imaging.....	46
2.2.6 Protein crystallography	47
2.2.7 Surface plasmon resonance	49
2.3 Biochemical Methods.....	52
2.3.1 N-terminal sequencing	52
2.3.2 Mass Spectrometry.....	52
2.3.3 SDS-PAGE.....	52
2.3.4 Removal of N-linked glycan with Endoglycosidase H.....	53
2.3.5 Complex immunoprecipitation assays	54
Chapter 3: Protein Production	55
3.1 Mammalian protein production in human embryonic kidney cells 293F and 293 GNT1	56
3.2 VE-cadherin ectodomains are highly glycosylated.....	60
3.3 Bacterial protein production in <i>Escherichia coli</i>	65
3.3.1 VE-cadherin protein fragments expressed in <i>E. coli</i>	65
3.3.2 Classical cadherin fragments expressed in <i>E. coli</i>	67
3.3.3 Preparation of C-terminally tagged classical cadherins	70
Chapter 4: Full length VE-cadherin ectodomains form dimers similar to those of classical cadherins.....	72

4.1 Biophysical studies of the adhesive binding mechanism of native VE-cadherin ectodomains.....	73
4.2 Biophysical behavior of VE-cadherin in sedimentation equilibrium analytical ultracentrifugation	73
4.3 Analytical size-exclusion chromatography	76
4.4 Multi angle light scattering	79
4.5 Liposome aggregation assays with cadherin ectodomains.....	80
4.6 Electron microscopy studies of <i>in vitro</i> VE-cadherin junctions	83
4.7 Atomic force microscopy imaging studies of VE-cadherin ectodomains.....	86
4.8 VE-cadherin EC4 domain enables multimerization only when glycosylation is absent	89

Chapter 5: Structure of the homophilic binding interface of a VE-cadherin EC1-2 adhesive fragment 94

5.1 EC1-2 domains are responsible for strand swap mediated homodimerization	95
5.2 Screening and optimization of crystals of VE-cadherin EC1-2	97
5.3 Crystal structure of chicken VE-cadherin EC1-2 reveals a strand swapped dimer.....	103
5.4 The VE-cadherin strand swapped interface is unique	107
5.4.1 VE-cadherin uses a different set of residues for <i>trans</i> dimerization than other classical cadherins	108
5.4.2 Analysis of structural superpositions of VE-cadherin with type I and II cadherins	111
5.5 Investigation of other interfaces in the VE-cadherin crystal structure.....	115

Chapter 6: Binding affinities and adhesive specificity in the type II cadherin subfamily 118

6.1 Comparison of VE-cadherin and type II cadherin homophilic binding affinities in analytical ultracentrifugation experiments	119
6.2 Adhesive specificity of type II cadherins in surface plasmon resonance assays	120
6.2.1 Identification of a suitable tag for immobilization of VE-cadherin for SPR	123
6.2.2 Identification of running buffer for VE-cadherin in SPR experiments.....	130
6.2.3 Assessing homophilic VE-cadherin binding in SPR-experiments.....	130
6.2.4 Homophilic and heterophilic adhesive binding of type II cadherins	135
6.3 Heterophilic adhesive binding between type I subfamily members and VE-cadherin	137
6.4 Co-immunoprecipitation assays to detect cadherin high affinity binding.....	142

Chapter 7: Homophilic adhesion without the cadherin strand swap motif..... 145

7.1 Background and significance	146
7.2 Strand swap site directed T-cadherin mutations do not affect adhesive binding	146
7.3 Context of the mutational data in the published work	150

Chapter 8: Discussion	151
8.1 VE-cadherin adhesion is mediated by a classical cadherin dimer.....	152
8.2 Variations on a common binding mechanism in classical cadherins	155
8.3 Adherens junction assembly – differences within the classical cadherin subfamilies.	157
8.4 Type II cadherin specificity – a code to crack.....	159
8.5 Interactions between cadherins in vascular endothelial cells	162
9. Future Directions	164
10. List of References	166
11. Table of Figures.....	173
12. List of Tables	175
13. Acknowledgements.....	176
14. List of Publications.....	177
15. Curriculum vitae	178

List of commonly used abbreviations

Abbreviation	Description
A pool	Adductor motor pool
Å	Angström
AFM	Atomic force microscopy
AUC	Analytical ultracentrifugation
A*-strand	N-terminal section of the A-strand used for strand swapping
Avi-tag	C-terminal tag (GGGLNDIFEAGKIEWE)
Avi*bio-tag	Biotinylated C-terminal tag (GGGLNDIFEAGKIEWE, Lys biotinylated)
BSA	Buried solvent accessible area
C _α	Carbon alpha atom of amino acid
CAM	Cell adhesion molecule
C-cadherin	Compact embryonal stage cadherin
Cis	Lateral association between proteins on the same cell or liposome surface
CM-dextran	Carboxymethyl-dextran
CYS-tag	C-terminal tag (GGGC)
C9-tag	C-terminal tag (GGGTETSQVAPA)
Da	Dalton
DGS-NTA (Ni)	1,2-dioleoyl- <i>sn</i> -glycero-3-[(N-(5-amino-1-carboxypentyl)iminodiacetic acid)-succinyl] nickel salt
DOPC	1,2-dioleoyl- <i>sn</i> -glycero-3-phosphocholine
E9.5	Embryonic stage day 9.5
E-cadherin	Epithelial cadherin
EC-domain	Extracellular cadherin domain
EDC	1-ethyl-3-(3-dimethylaminopropyl)-carbodiimide
eF motor pool	External Femorotibialis motor pool
EM	Electron microscopy
FLAG-tag	C-terminal tag (DYKDDDDK), FLAG owned by Sigma
GPI-anchor	Glycosylphosphatidylinositol anchor
HEK 293 F cells	Human embryonal kidney cells line 293 fast growth
HEK 293 GNTI	HEK-cells 293 lacking enzyme N-acetylglucosamine transferase I
K _D	Dissociation constant as measure for binding affinity
K _{D(i)}	Isodesmic dissociation constant
MALDI	Matrix-assisted laser desorption/ ionisation
MALS	Multi angle light scatterin
MN-cadherin	Motor neuron cadherin
N-cadherin	Neural cadherin
NHS	N-hydroxysuccinimide
NTA	Nitrilotriacetic acid (chelating agent)
Ni-NTA	Nitrilotriacetic acid chelating Nickel (II)
P	Crystallographic point group
PAGE	Poly acrylamid gel electrophoresis
P-cadherin	Placental cadherin
Pdb	Protein data bank
PDEA	2-(2-pyrdinyldithio) ethaneamine
PISA	Protein interactions, surfaces and assemblies
r. m. s. d.	Root mean square deviation
RU	Response Unit
SDS	Sodium Dodecyl Sulfate
SPR	Surface Plasmon Resonance
T-cadherin	Truncated cadherin
TCEP	Tris(2-carboxyethyl)phosphine
TOF	Time of flight
Trans	Association between two opposing cells or liposomes
VE-cadherin	Vascular endothelial cadherin
1d4	Antibody recognizing C9 antigen
3D	Three dimensional

Chapter 1:

Introduction

1.1 Cell adhesion in multicellular organisms

Every multicellular organism is constituted of heterotypic cells arranged into specific tissues, which form the basis for the formation of organs and complex tissue architectures (Gumbiner, 1996; Takeichi, 1991). Selective organization of cells within and between these tissues is governed by the process of cell adhesion through which cells bind to adjacent cells or to extracellular structures (Gumbiner, 1996; Takeichi, 1991). Cell surface associated glycoproteins, termed cell-adhesion molecules (CAMs), are responsible for these processes. CAMs adhere either to other CAMs on surfaces of adjacent cells to mediate cell-cell adhesion or instead to components of the extracellular matrix to mediate cell-matrix adhesion (Takeichi, 1991). Interactions of CAMs are highly specific and can be either homophilic, in which identical CAMs bind to each other, or heterophilic, in which binding occurs between distinct proteins. Specific interactions at the molecular level are thought to underlie tissue morphogenesis and architecture on the cellular level.

Since the first observations of selective cell adhesion (Steinberg and Gilbert, 2004) several major families of CAMs have been identified. Integrins and integrin ligands are primarily responsible for cell-matrix adhesion (Tuckwell and Humphries, 1993). Calcium independent cell-cell adhesion is mediated by members of the immunoglobulin-like superfamily, including nectins and NCAMs (Goridis and Brunet, 1992; Takai et al., 2008) in addition to smaller families of adhesion molecules such as claudins and connexins (Cruciani and Mikalsen, 2006; Koval, 2006). The major family of adhesion proteins responsible for calcium dependent cell-cell adhesion in vertebrates and invertebrates are the cadherins. Cadherins are essential during all stages of development for intercellular adhesion and cell sorting and are expressed in virtually all solid tissues in the adult where they are responsible for maintenance of tissue architecture (Patel et al., 2003; Suzuki, 1997; Takeichi, 1990, 1991). This important family of cell adhesion proteins will be the focus of this thesis.

1.1 The cadherin superfamily of calcium dependent cell adhesion molecules

Cadherins, which mediate cell-cell adhesion dependent on calcium ions, constitute a large superfamily of more than 350 proteins (Hulpiau and van Roy, 2009). Members of this superfamily are expressed in all vertebrates and invertebrates and are found even in choanoflagellates, the closest known unicellular relative of animals (Abedin and King, 2008). Most are thought to function in cell adhesion or recognition processes. Cadherins are all membrane associated glycoproteins, most being single-pass transmembrane proteins, which

have at least two tandem repeats of a characteristic structural element, the extracellular cadherin-like (EC) domain in their extracellular region (Nollet et al., 2000). The overall protein domain organization, number of EC domains present in the molecule and other sequence characteristics vary widely between different cadherins, allowing division of this family into several subfamilies (Figure 1 and (Nollet et al., 2000)). The classical type I and II cadherins constitute the best characterized of these. Classical cadherins are single-pass transmembrane proteins with an extracellular region comprised of five EC domains and are linked to the actin cytoskeleton by a highly conserved cytoplasmic domain that interacts with adaptor proteins called catenins. Classical cadherins are expressed exclusively in vertebrates throughout all stages of development including in the adult and are essential for tissue morphogenesis. Type I and type II classical cadherins are the focus of this thesis work and will be described in detail in subsequent sections. Other subfamilies have been less studied, but have similarly important roles. Protocadherins represents the largest subfamily of cadherins in mammals with more than 60 different proteins, which are primarily expressed in the central nervous system where their diversity may be important for neural patterning (Hulpiau and van Roy, 2009; Sano et al., 1993). Desmocollin and desmoglein subfamily members are localized together in the same cellular structure in vertebrate animals, referred to as the desmosome, which is a specialized cell-cell junction found mostly in tissues subject to mechanical stress, that is anchored to intermediate filaments intracellularly (Huber, 2003). Flamingo cadherins are unusual in the superfamily in that they are seven-pass transmembrane receptors. These are involved in planar cell polarity processes in both vertebrates and invertebrates (Usui et al., 1999). In addition, there are a few solitary atypical cadherin superfamily members which, too, mediate cell-cell adhesion, but cannot be grouped into the aforementioned subfamilies. These include the invertebrate ‘classical’ cadherins such as *Drosophila melanogaster* DN- and DE-cadherins (Hynes and Zhao, 2000), as well as FAT and dachsous proteins (Sopko and McNeill, 2009). They are comprised of large numbers (>5) of EC domain repeats intermixed with other structural motifs. Another solitary member of the cadherin family is truncated (T-) cadherin (Figure 1), which shows an overall extracellular domain organization closely similar to that of classical cadherins with the caveat that T-cadherin lacks the cytoplasmic domain, which is replaced by a glycosylphosphatidyl inositol (GPI)-anchor (Ranscht and Dours-Zimmermann, 1991).

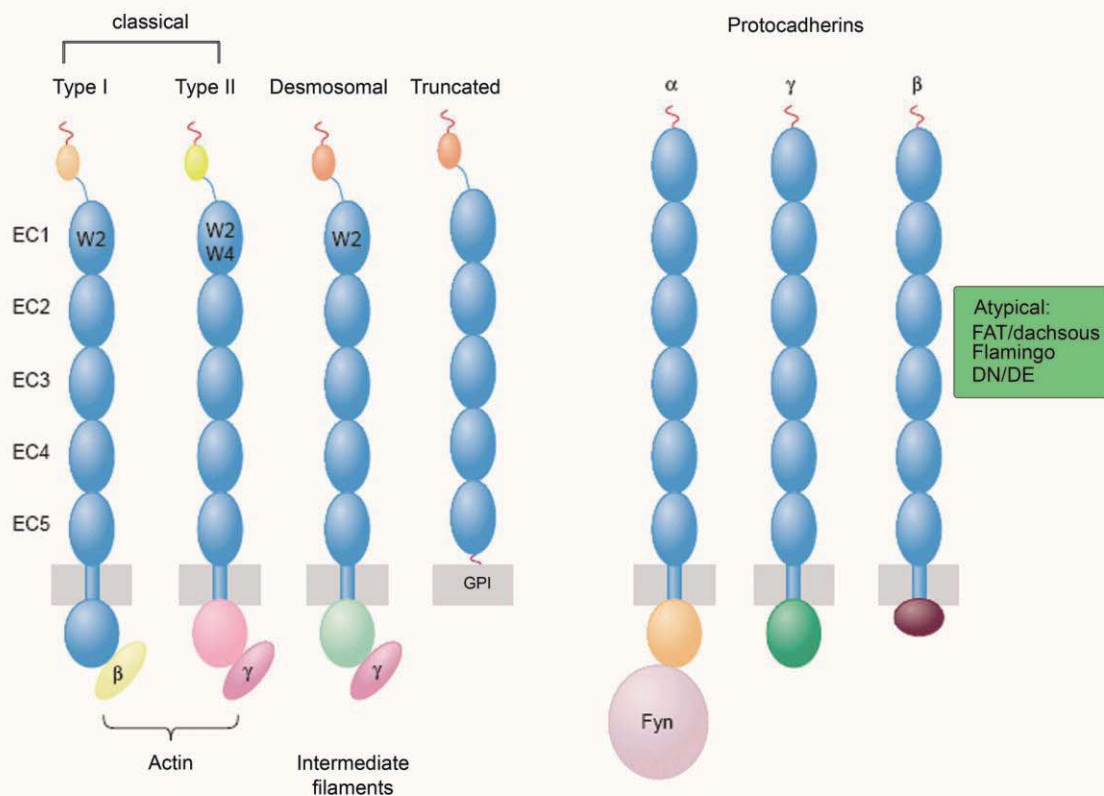


Figure 1: Schematic representation of the domain organization of various subfamilies of the superfamily of cadherins. All cadherins share the structural repeat composed of 110 amino acids (blue ovals) known as extracellular cadherin-like (EC) domains and most of these are transmembrane proteins with short cytoplasmic domains except Truncated (T) cadherin, which is attached to the plasma membrane via a GPI-anchor. Type I, II and desmosomal and T-cadherin are all expressed as pro-proteins with an EC like prodomain (small ovals) which is removed on the cell surface by furin like proteases. Intracellular binding partners of classical cadherins like β - and γ -catenin are indicated by yellow and pink ovals, respectively. Cadherins in this superfamily are grouped into subfamilies according to number of EC domains, conserved tryptophans and cytoplasmic domains. Shown are classical type I and II cadherins, T-cadherin and three major families of the protocadherins. Examples for atypical cadherin subfamilies are listed in the green box. See text for further detail. Schematic adapted from Patel *et al.* (2003).

1.2 General features of classical cadherins

Classical cadherins are divided into two groups, type I and type II, on the basis of differences at the level of sequence and genomic organization (Nollet et al., 2000). Both type I and type II classical cadherins mediate calcium-dependent cell-cell adhesion and show some degree of homophilic specificity in that adhesion between identical cadherin subtypes is favored, at least to some extent, over that between different cadherins (see Section 8.4 for discussion). Type I and II cadherins are expressed in solid tissues of all vertebrates, but they exhibit different types of distribution regarding their expression pattern. Type I cadherins have rather broad expression patterns, which are separated by germ layers and tissue types (Nakagawa and Takeichi, 1998), whereas type II cadherins are predominantly expressed in finely grained, often overlapping patterns in the central nervous system (Price et al., 2002; Suzuki et al., 1991), in which they occur often in combinations of two or more subsets per single cell (Price et al., 2002). A notable exception is the type II cadherin-5 (VE-cadherin) that is found to be expressed exclusively in the vascular endothelium (See Introduction 1.8, (Breier et al., 1996; Lampugnani et al., 1992). 18 classical cadherins have been identified so far in mouse and human, five of which are type I cadherins: Epithelial (E-), Neural (N-), Placental (P-), Retinal (R-) and Muscle (M-) cadherin and 14 are type II cadherins vascular endothelial (VE-) cadherin (sometimes referred to as cadherin-5), cadherin-6, -7, -8, -9, -10, -11, -12, -18, -19, -20, -22 and -24 (Hulpiau and van Roy, 2009; Posy et al., 2008). The phenotypes of knockout mice for individual classical cadherin subtypes tend to reflect the different types of expression patterns observed for type I and type II cadherins. Effects of type I cadherin inactivation are severe, at least in the cases of E- and N-cadherin. E-cadherin null embryos die at the preimplantation stage due to failure of adhesion and compaction in the blastocyst, while N-cadherin null embryos die during gestation due to severe cell adhesion defects in the heart and also show malformation of the neural tube (Charlton et al., 1997). Both knockouts underscore the essential role for classical cadherin-mediated calcium dependent adhesion throughout development. In contrast, type II cadherin knockout phenotypes tend to be more subtle. For example, cadherin-6 and cadherin-8 knockout mice are viable but show defects in compartmentalization in the CNS and kidney development or in cold sensation, respectively (Inoue et al., 2001; Suzuki et al., 2007). The VE-cadherin knockout phenotype will be discussed in a later Section 1.8.2.

Table 1: Classical type I and II cadherins identified in mouse and human.

Classical type I cadherins	Classical type II cadherins
E-cadherin	VE-cadherin /cadherin-5 ^a
N-cadherin	cadherin-6
P-cadherin	cadherin-7
R-cadherin	cadherin-8
M-cadherin	cadherin-9
	cadherin-10
	cadherin-11
	cadherin-12
	cadherin-18 ^b
	cadherin-19
	MN-cadherin / cadherin-20 ^a
	cadherin-22
	cadherin-24

^a These cadherins are more commonly known under the first listed name.

^b Human Cadherin-18 is sometimes referred to as cadherin-14.

All classical cadherins share the same overall protein organization (Figure 1 and 2) and are expressed as inactive pro-proteins, with an N-terminal pro-domain resembling a cadherin EC-like domain fold, which is removed by furine proteases on the cell surface yielding mature protein that is active in adhesion (Koch et al., 2004). The mature protein is comprised of a large extracellular domain, commonly referred to as the ectodomain, a single pass class I transmembrane domain and a short cytoplasmic tail of approximately 150 amino acids in length, which is highly conserved on the sequence level (Figure 2)(Nollet et al., 2000). Mature ectodomains are composed of five successive EC domains with approximately 110 amino acids each connected by interdomain linkers, reminiscent of beads on a string. A wide array of structural data revealed that these EC domains are each composed of a seven stranded β -barrel (Boggon et al., 2002; Ciatto et al., 2010; Harrison et al., 2010a; Harrison et al., 2010b; Haussinger et al., 2004; Nagar et al., 1996; Patel et al., 2003; Patel et al., 2006; Shapiro et al., 1995), in which the strands are by convention named A to G from the most N-terminal to the most C-terminal strand (Figure 2b and c).

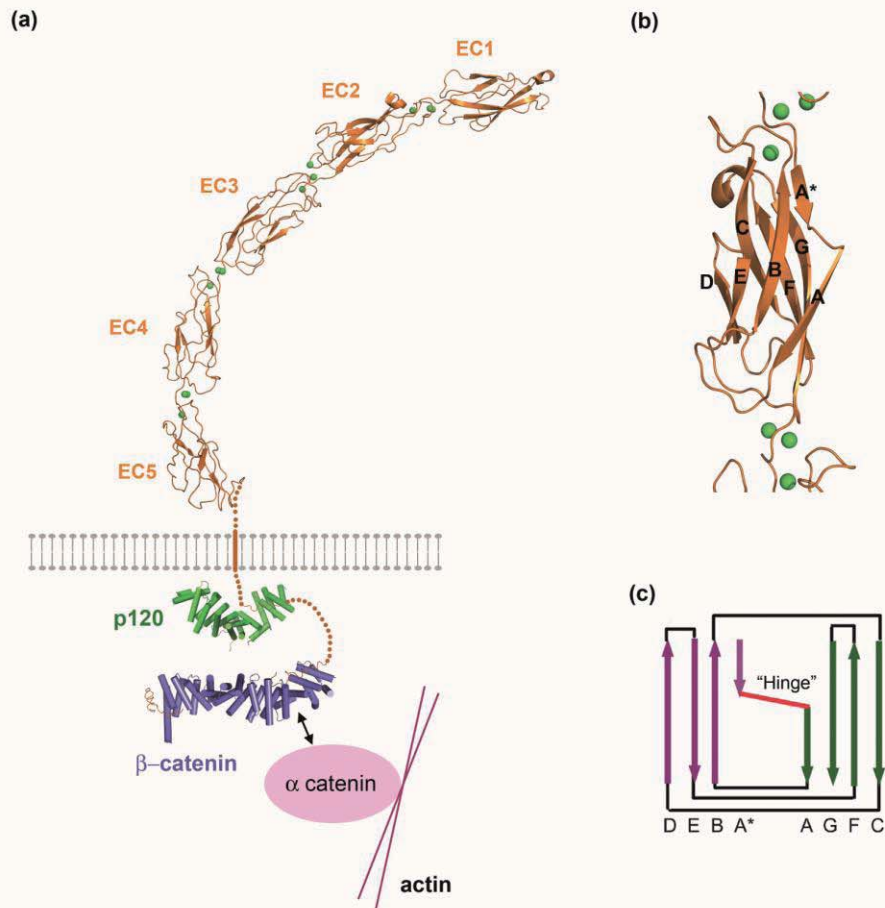


Figure 2: Domain organization and structural architecture of classical cadherins. (a) Depicted is the extracellular domain from C-cadherin as ribbon diagram spanning EC1-5 with calcium ions (shown as green spheres) coordinated between successive domains (pdb: 1L3W). Structure of stalk, transmembrane and cytoplasmic domain are unknown at present time (dotted orange line). Intracellular binding partners p120 (green barrels representing α -helices, pdb 3L6X) and β -catenin (blue barrels representing α -helices, pdb: 1I7X) are positioned schematically. β -catenin interacts with α -catenin which links extracellular cadherin-adhesion to actin filaments. Sizes of proteins chosen are for schematically purposes only and do not represent actual relative size. (b) Extracellular cadherin (EC) domain 2 of C-cadherin (pdb: 1L3W) shown as ribbon diagram with β -strands labeled from A- to G-strand, including A*-strand. Position of coordinated calcium ions (green spheres) indicated. (c) Schematic representation of the EC2, showing the assembly of β -strands (arrows) into the two β -sheets (purple and green) which form EC-domains. Hinge region separating A-strand and A*-strand is indicated in red. Representation adapted from Posy *et al.* (2008) and Shapiro *et al.* (1995). See text for further detail.

The A strand is further divided into an N-terminal portion (the A* strand) and a C-terminal portion (the A strand), which hydrogen bond to the B and G strands, respectively (Figure 2b). Three atomic resolution structures of full length classical cadherins (Boggon et al., 2002; Harrison et al., 2010b) gave detailed information about the arrangement and conformation of the cadherin ectodomain, which was found in each to adopt a highly similar crescent shaped, curved form (Figure 2a). Successive EC-domains bind three divalent calcium ions in their interdomain linker regions (Figure 2), principally via carboxylate side chains of acidic residues in three motifs, conserved on sequence level for all classical cadherins: DRE, in the EC domain preceding the interdomain linker, DXND directly in the linker region and DXD localized in the EC domain posterior to the linker (Figure 2 and 3) (Boggon et al., 2002; Nagar et al., 1996). Electron microscopy studies of cadherin ectodomains in presence and absence of calcium (II) revealed, that it is crucial for locking the orientation of successive EC domains to each other into a rigid curved overall shape; in the absence of calcium ectodomains are folded into globular shapes (Pokutta et al., 1994). In addition, cell-cell aggregation experiments of cadherin expressing cells showed that removal of calcium (II) resulted in abrogation of adhesion (Takeichi et al., 1988), which confirms its role for the biological importance of these proteins. Notably, the binding to calcium also protects the ectodomains of cadherins, especially the interdomain linker regions, from proteolytic digestion (Takeichi, 1991). These rigid cadherins ectodomains engage in binding interactions across intercellular contacts to mediate adhesion and are linked to the cytoplasm through interactions of the cadherin cytoplasmic tail with armadillo proteins β - or γ - and p120-catenin (Figure 2a and (Gentil-Dit-Maurin et al., 2010; Huber and Weis, 2001; Ishiyama et al., 2010; Lampugnani et al., 1995; Ozawa et al., 1989)). These adaptor proteins enable the indirect attachment of cadherins to the cytoskeleton via further intracellular protein interactions with proteins such as α -catenin (Figure 2a) (Kobielak and Fuchs, 2004). p120 catenin also has a well defined role in regulation of cadherin trafficking (Liu et al., 2007; Reynolds and Carnahan, 2004).

1.3 Molecular basis of cadherin-cadherin binding

Early *in vitro* studies showed that a variety of cell lines that do not normally form aggregates in suspension could be induced to aggregate in a calcium dependent manner by transfection with cDNA encoding cell surface type I or type II classical cadherins (Breviario et al., 1995; Hatta et al., 1988; Nagafuchi et al., 1987; Takeichi et al., 1988). Blocking studies also demonstrated that calcium dependent adhesion between cells in culture or in embryonic tissues could be disrupted by addition of antibodies against the cadherin ectodomain (May et al., 2005; Vestweber and Kemler, 1985; Volk et al., 1984). Together with subsequent experiments, including mutational analyses and gene deletion studies, these assays established the role of molecular interactions between cadherins in driving calcium dependent cell-cell adhesion. These interactions occur between cadherin ectodomains presented on opposing cells. Purified ectodomain fragments were found to associate homophilically in a variety of assays (Harrison 2010b, 2010a, Katsamba 2009, Ahrens 2003, Boggon 2002, Nagar 1996). Additionally, while interactions between the cadherin cytoplasmic domain and the cytoskeleton were found to be essential for proper cellular cohesion (Gentil-dit-Maurin 2010, Kintner 1992, Nagafuchi 1989), recently it has been found that in cryo EM and transfection studies (Harrison et al., 2010b; Hong et al., 2010; Ozaki et al., 2010), cadherin ectodomains attached to the plasma membrane are sufficient for initial cell-cell adhesion.

The binding interface between cadherin ectodomains that underlies homophilic classical cadherin adhesion has been extensively characterized by atomic resolution structures of adhesive ectodomain fragments from classical type I (Boggon et al., 2002; Harrison et al., 2010a; Harrison et al., 2010b; Haussinger et al., 2004; Nagar et al., 1996; Shapiro et al., 1995) and type II (Patel et al., 2006) cadherins. In crystal structures of each type, dimers are observed between molecules oriented as if interacting across the intercellular space, in which two cadherin protomers bind to each other via their membrane distal EC1 domains (Figure 3a). The dimers are two fold symmetrical and EC1 domains are arranged approximately parallel producing, due to the curvature of the protomers, an overall *trans* dimer orientation. In all native classical cadherin dimers, the amino terminal residues of the A-strand, designated the A*-strand, are exchanged between both protomers (Figure 3b) and are held in place by intermolecular hydrophobic and ionic interactions as well as hydrogen bonds. This arrangement is referred to as the strand swapped cadherin dimer. The exchange of β -strands is stabilized by docking of one tryptophan residue (Trp2) in type I cadherins or two tryptophan

residues, Trp2 and Trp4, in type II cadherins into a hydrophobic acceptor pocket of the partnering molecule (Figure 3b).

Type I and type II cadherins share the mechanism of strand swapping, but there are a few major differences in the detail which may underlie adhesive specificity between the two subfamilies (see Section 1.6). Type II cadherins have in contrast to type I cadherins an extended hydrophobic region along the entire face of the EC1 domain whereas type I cadherins form contacts only close to the site of A*-strand swapping near the apex of the domain (Patel et al., 2006). Also, the size of the acceptor pocket of type I cadherins is rather small accommodating a single Trp2 side chain, whereas the acceptor pocket of type II cadherins has to accommodate Trp2 and Trp4 and thus is significantly larger (Patel et al., 2006). These differences suggest potential steric incompatibility of type I and type II cadherins with regard to adhesive dimer formation.

Biological importance of the strand swapped dimer observed in crystal structures of classical cadherins has been confirmed by a number of methods. Sequence analyses show that Trp2 in type I cadherins and Trp2 and Trp4 in type II cadherins as well as the respective residues lining the acceptor pocket are found to be highly conserved within classical cadherins (Figure 3c). Mutation of Trp2 in type I cadherins (Kitagawa et al., 2000; Tamura et al., 1998) or either Trp2 or Trp4 in type II cadherins (Harrison et al., 2010b; May et al., 2005) to alanine is sufficient to abrogate strand swap mediated adhesion. In agreement with these results, alteration of one of the alanine residues lining the acceptor pocket to a large methionine in order to ‘occupy’ the pocket (Tamura et al., 1998) or addition of indole-3-acetic acid, which is the soluble analogue of the tryptophan side chain, resulted in loss of adhesive function in both cell based experiments (Tamura et al., 1998) and studies with purified cadherin proteins (Perret et al., 2002). Additionally, the N-terminal amino group of the cadherin engages in an intermolecular salt bridge in the dimer configuration, which is conserved for type I and II classical cadherins. Extension of the mature N-terminus by one or two residues prevents formation of the salt bridge and was shown to result in loss of adhesive binding (Bibert et al., 2002; Boggon et al., 2002; Harrison et al., 2010a; Ozawa et al., 1990). Cross-linking studies with E- and N-cadherin also detected the strand swap dimer (Harrison et al., 2005; Troyanovsky et al., 2003).

More generally, the critical role for the EC1 domain suggested by structures of the adhesive dimer is also supported by several lines of evidence. The involvement of N-terminal regions alone for *trans* adhesion was also observed in rotary shadowing electron microscopy experiments of full length type I E- and N-cadherin and type II VE-cadherin ectodomains conducted by Engel and collaborators (Ahrens et al., 2003; Pertz et al., 1999; Tomschy et al., 1996). In addition, fluorescence resonance energy transfer (FRET) experiments with purified E-cadherin supported overlap of EC1 domains only (Sivasankar et al., 2009). In a more physiologically relevant context, He *et al.* (2003) and Al-Amoudi *et al.* (2008) visualized the organization of desmosomal cadherins, which show the same overall domain organization as classical cadherins, in desmosomes of mouse and human skin, respectively (Figure 4a). Fitting of strand swapped C-cadherin *trans* dimer structures into electron tomography reconstructions of sections of mouse neo-natal and human skin, confirmed that N-terminal domains are employed also *in situ* (Figure 4b). In the tomograms, cadherins adopted the dimer arrangement observed in crystal structures and these therefore are very likely to be the biological relevant adhesive binding unit for classical and desmosomal cadherins.

1.4 Cadherins utilize a 3D domain swapping mechanism for adhesion

The strand swap mechanism described here for cadherin adhesive binding is an example of 3D domain swapping (Bennett et al., 1995; Shapiro et al., 1995), because the swapped A* β -strand, is replaced by the exact same domain from the partnering protomer and vice versa. The swapped domain has in monomer and homodimer configuration an identical residue environment, provided by intramolecular or intermolecular interactions, respectively. Domain swapping resulting in dimer formation is accompanied by an entropy loss, which can be compensated by a less energetically favorable monomeric conformation. In the case of cadherins this is likely to be caused by a strained conformation of the A-strand in the monomer configuration, which is eased in the dimer (Vendome et al., 2010). 3D domain swapping in cadherins is likely to be responsible for the relatively low binding affinities observed for type I E-, N- and C-cadherin and type II cadherin-6, which are found to be in the micromolar range (Chappuis-Flament et al., 2001; Ciatto et al., 2010; Harrison et al., 2010a; Harrison et al., 2010b; Katsamba et al., 2009). This is because the closed monomer form can act as a form of ‘competitive inhibitor’ by sequestering the A-strand. The low affinity of cadherin homophilic binding is thought to be important for specificity in adhesion, since higher affinity dimerization mechanisms would be less sensitive to small differences in interfacial residues between mismatched molecules (Chen et al., 2005).

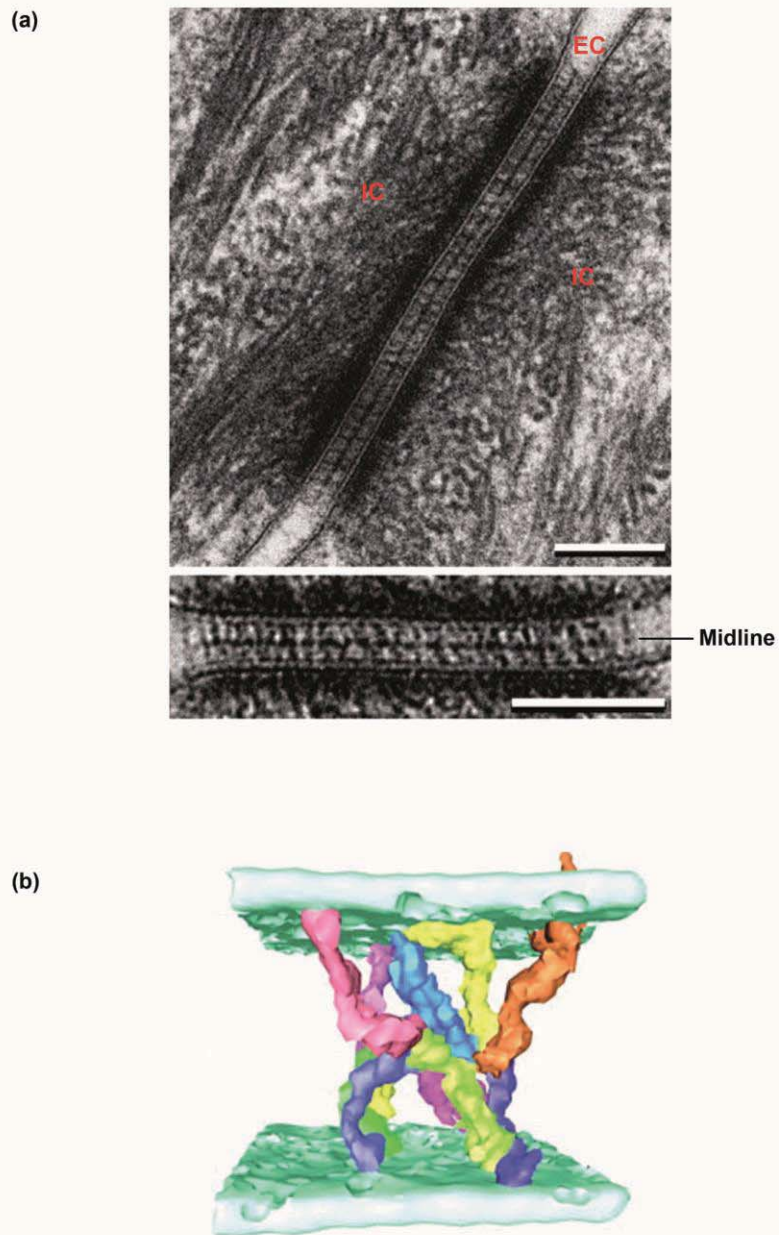


Figure 4: EC1 domains govern cadherin mediated adhesion in classical type I and desmosomal cadherins. (a) Electron micrograph showing the cellular structure of a desmosome. Note the dark midline which indicates overlapping amino-terminal domains indicated in the inset. EC: extracellular intermembrane space and IC for intracellular. Scale bars depicted represent 100nm. (b) C-cadherin dimers, are fitted into electron tomography reconstructions showing that only EC1 domain governs trans adhesion. Adapted from He *et al.* (2003). See text for detail.

1.5 T-cadherin structures reveal a novel adhesive binding mechanism

Recently, the crystal structure of the adhesive interface of a divergent vertebrate cadherin, T-cadherin, has been determined (Ciatto et al., 2010). The structure, comprising domains EC1-2, revealed a novel interface adopting an overall X shaped configuration (Figure 5a), which is characterized by a symmetrical contact region centered around the calcium linker region (Figure 5a). Domains EC1-2 are oriented almost parallel to each other with hydrophobic, ionic and hydrogen bonding interactions involving residues of the EC1 domain, the interdomain linker and domain EC2 (Figure 5b). The area of the EC1 domain involved in this interface is almost the same as found in the strand swapped dimer of classical cadherins, which was described above. However, the analogous region to the A* strand in classical cadherins is found not to be swapped between protomers. Instead, Ile2, at the same position as key residue Trp2 in type I cadherins (Figure 3c), is docked into a small hydrophobic pocket in its own protomer and no strand exchange occurs. Extensive mutagenesis studies targeting this novel interface revealed in biophysical assays, cell aggregation assays and axon guidance experiments (Ciatto et al., 2010) that the X interface is crucial to T-cadherin adhesion, suggesting this interface to be the biological adhesive interface.

Interestingly, this interface was also observed in E-cadherin and cadherin-6 mutants, in which strand swap adhesion was impaired (Harrison et al., 2010a). Mutations specifically disrupting the X interface in type I E-cadherin and type II cadherin-6 whilst leaving the strand swap interface intact, lead to loss of adhesive binding in short time scale SPR and cell aggregation experiments without lowering the binding affinity in long time scale sedimentation equilibrium AUC analysis. Further biophysical experiments suggested that exchange between monomer and dimer was slowed in these mutants. This leads to a model, in which the X-dimer interface acts as a binding intermediate, which positions the A-strands in close apposition for strand swapping (Figure 5c).

Interestingly, despite the fact that EC1-domains alone are responsible for *trans* adhesive strand swapped binding and are able to form dimers at high concentration in protein crystals (Patel et al., 2006; Shapiro et al., 1995), deletion mutagenesis studies revealed, that EC1 domains alone are not sufficient to mediate *trans* dimerization of cells and require, in addition, presence of domain EC2 in order to mediate adhesion (Shan et al., 2004). The requirement for EC2 may reflect its involvement in the X dimer interface, though other effects of EC2 removal such as changes in EC1 folding or orientation can not be ruled out.

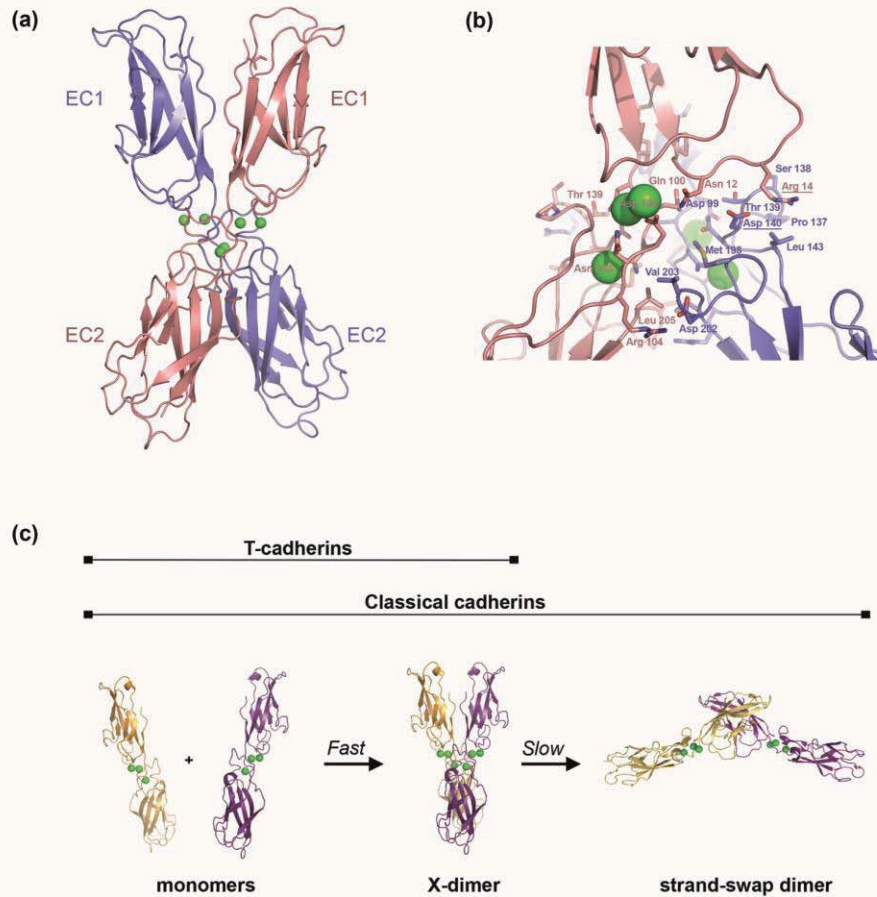


Figure 5: The adhesive interface found in T-cadherin adopts an X-shaped conformation. (a) The adhesive dimer in T-cadherin involves a region around the calcium binding site and adopts an overall symmetric configuration resembling an 'X'. Structure shown in ribbon presentation, one protomer shown in salmon, the other in blue, calcium ions as green spheres. (b) Close up of the adhesive binding site found in T-cadherin. One protomer is shown in salmon, the other in blue and calcium ions are depicted as spheres. Residues buried in the X-dimer interface are represented as sticks. Adapted from Ciatto *et al.* (2010). (c) Same interface as for the T-cadherin adhesive dimer found in strand swap impaired classical cadherins. This led to the proposal of a two step binding model for classical cadherins. Cadherin monomers associate first with 'fast' kinetics into an intermediate X-dimer configuration shared with the interface observed for T-cadherin. This configuration positions EC1 domains parallel to each other enabling the kinetically 'slow' formation of the strand swap dimer. One protomer shown in yellow ribbon presentation, the other in purple. Adapted from Harrison *et al.* (2010).

1.6 Specificity and promiscuity of adhesive interactions between cadherins

Numerous studies suggest that within and between each subfamily of vertebrate classical cadherins proteins bind homophilically to each other, preferring binding to the same or similar subtype (Boggon et al., 2002; Ciatto et al., 2010; Harrison et al., 2010a; Harrison et al., 2010b; Katsamba et al., 2009; Nagar et al., 1996; Patel et al., 2006; Price et al., 2002; Shan et al., 2004; Shan et al., 2000; Shapiro et al., 1995; Shimoyama et al., 1999; Shimoyama et al., 2000; Takeichi et al., 1988). This provides a potential simple and efficient mechanism, to segregate identical cells into homogenous tissues (Patel et al., 2003).

In multiple cell aggregation studies it was found that cells transfected with type I cadherins fail to intermix with cells expressing type II cadherins and in all cases form separate cell aggregates (Duguay et al., 2003; Foty and Steinberg, 2005; Katsamba et al., 2009; Patel et al., 2006; Shimoyama et al., 2000). These results suggest that type I and type II cadherin binding is orthogonal, because there were no cross reactions found between subfamilies, and may be explained by the substantial differences in the adhesive interface between these subfamilies (Section 1.3).

Within type I cadherins, an example for homophilic binding was described by Nose et al (1989). Lungs of mouse embryos consist of epithelial cells expressing E- and P-cadherin and mesenchymal cells expressing N-cadherin. After dissociation of the lung tissues with trypsin, it was observed that these cells were able to re-assemble into a lung like tissue within which epithelial and mesenchymal cells were segregated. Further, this group found that L-cells expressing recombinant E-cadherin added after homogenisation colocalized with epithelial, but not with mesenchymal cells in the reconstituted structures showing that cadherin subtype expression could determine sorting in a tissue-like environment. Similar sorting of cells based on type I cadherin sub-type was observed in aggregation assays of mixtures of transfected cells singly expressing either E- or P cadherin, or E and N-cadherin (Nose et al., 1990; Shan et al., 2000). However, other experiments, mostly involving cell aggregation or co-culture assays revealed heterophilic binding between chicken and mouse N- and R-cadherin (Matsunami et al., 1993), chicken N- and E-cadherin (Volk et al., 1984), chicken and human E- and P-cadherin (Murphy-Erdosh et al., 1995) and chicken R- and P-cadherin and N- and P-cadherin (Duguay et al., 2003), suggesting, that type I cadherin binding is considerably more promiscuous. Recent studies from Katsamba and Carroll et al (2009) reproduced in biophysical surface plasmon resonance (SPR) using purified E- and N-cadherin the

heterophilic binding behavior of type I E- and N-cadherin *in vitro*, which appears to be delicately regulated by homodimerization and heterodimerization affinities.

The type II subfamily has an even more elaborate heterophilic binding pattern than found for type I cadherins. A well characterized example of homophilic selectivity for type II cadherins was reported by Price et al (2002). Type II cadherins are expressed throughout the CNS during development and adult stages and are found to be expressed in motor pools in the spinal cord, which are functional subsets of motor neurons clustered in the lateral motor column (Price et al., 2002). Neurons within a motor pool are electrically coupled to each other (Price et al., 2002) and control a single muscle target in the limbs. Cadherins are found to be expressed either alone or in subsets of different combinations of two or more subfamily members in motor pools. For example, motor neuron (MN-) cadherin (chicken homolog to human and mouse cadherin-20) expression becomes restricted to the Adductor (A) pool during segregation of motor pools (Price et al., 2002). *In ovo* electroporation studies, which re-introduced MN-cadherin expression into the neurons of other segregated motor pools in the lateral motor column, found that MN-cadherin mis-expression resulted in intermixing of the A and external Femorotibialis (eF) pool exclusively, whereas other pools remained separated from each other. Reintroduction of MN-expression into the eF neurons removed any differences in cadherin expression between these pools *in vivo*. The A and eF neurons were then expressing the exact same set of type II cadherins whereas for the other motor pools cell surface differences were maintained, which suggests a complex fine tuned degree of adhesive specificity introduced by type II cadherins (Price et al., 2002).

Shimoyama et al (2000) conducted a systematic cell aggregation study that revealed not only homophilic, but also heterophilic binding behavior of type II cadherins. The study was conducted with eight transfected L-cell lines of which each expressed one of the human type II cadherins 6, 7, 8, 9, 10, 11, 12 and 14. All of the type II cadherins tested exhibited equal homophilic binding behavior, in that they all formed approximately the same aggregate size, except cadherin-9 and -10 which had lower initial expression levels. Heterophilic cell aggregation assays conducted on all possible cadherin pairs of the eight proteins resulted in one of three outcomes: Some cadherin pairs aggregated homogeneously, from which similar adhesive specificity was concluded; others were found in heterogeneous partially mixed aggregates, from which was assumed that these cadherins share part of their binding specificities; or complete segregation was observed, where no binding specificity is in

common between the two cadherins tested. For example, cells expressing cadherin-6 were found in homogeneous aggregates with those expressing cadherin-9, in heterogeneous aggregates with those expressing cadherin-10 and showed no intermixing with cadherin-11 expressing cells. These assays indicated a complex pattern of type II specificity although they were conducted only on cadherin pairs. *In vivo* type II cadherins are found to be expressed in a complex pattern, sometimes with multiple cadherins on the same cell, which makes a highly complex homo- and heterophilic interaction pattern likely. This may be important since type II cadherins are expressed in the developing brain and spinal cord, with notable regional expression patterns in the cerebral cortex, cerebellum and thalamus as well as in motor pools as described above (Price et al., 2002; Redies et al., 2003; Suzuki, 1997).

Domain shuffling experiments using either type I or type II cadherins revealed that inherent cadherin specificity is governed by adhesive domain EC1 (Nose et al., 1990; Patel et al., 2006; Shan et al., 2000). Type I and II chimera proteins were produced for these experiments, which were composed of domain EC1 ('head') of one cadherin and the 'body' (EC2-4) of another. Their binding behavior was assessed by cell aggregation assays and it was found that cells expressing cadherins with matched EC1-domains, e.g. E-cadherin wild type and E-cadherin EC1 chimera or cadherin-6b wild type and its EC1 chimera, formed homogenous aggregates of wild type and chimera proteins and in contrast, proteins which had mis-matched EC1 domains ('heads'), but matched domains EC2-4 ('bodies') formed separate aggregates (Patel et al., 2006). Based on these experiments and other studies (Chen et al., 2005; Klingelhofer et al., 2000; Posy et al., 2008) it was proposed that adhesive specificity is governed exclusively by amino terminal EC1 domains. This is in agreement with the localization of the strand swapped adhesive interface in the EC1 domain and suggests that differences between cadherin subtypes in the interface region may underlie specificity.

1.7 Classical cadherins are the core molecules of adherens junctions

Adherens junctions are intercellular structures which play a pivotal role in cell-cell adhesion and their major transmembrane components are classical cadherins (Farquhar and Palade 1963; McNutt and Weinstein 1973; Takeichi 1991). In particular, cell-cell junctions found in the intestinal epithelium are well studied and electron microscopy of these shows an interesting arrangement of adherens junctions with other cell-cell junctions in what is referred to as the junctional complex (Figure 6a). Most apical positioned are tight junctions (O) which

are formed by claudins and occludins and seal the underlying tissues from the intestine lumen (Koval, 2006). Sub-apical to those are located the zonula adherens (ZA), which represent a specialized form of cadherin mediated adherens junction. In addition, smaller adherens junction clusters of cadherins are also found distributed along the entire lateral part of the cell (Ozaki et al., 2010).

Further toward the basal side of the lateral membrane are desmosomes, in which as mentioned above the cadherin superfamily members desmogleins and desmocollins mediate adhesion between cells and are connected via intracellular proteins to intermediate filaments, visible as electron-dense plaques in the micrographs (Al-Amoudi and Frangakis, 2008; He et al., 2003). Zonula adherens a type of adherens junctions that are observed in intestinal epithelium link cells together in a belt extending around the sub apical zone, which assembles cells into sheets, allowing coordinated tissue movements across entire epithelial layers (Harris and Nelson, 2010). In addition, other examples for specialization of cadherin mediated adherens junctions are intercalated discs, which are found in the cardiac muscle, puncta adherentia which are adherens junctions found bordering synapses and adherens junctions in the vascular endothelium, which will be described in greater detail in Section 1.8. In all adherens junctions, opposing cell membranes are positioned parallel to each other with an intermembrane spacing of approximately 150-300Å (Farquhar and Palade, 1963; Harrison et al., 2010b; McNutt and Weinstein, 1973) and a high extracellular concentration of protein, representing cadherin ectodomains, is observed between the membranes. This assembly is accompanied by cytoplasmic plaques, representing the intracellular assembly of proteins and F-actin (Farquhar and Palade, 1963; McNutt and Weinstein, 1973).

Extracellular domains of cadherins mediate *trans* adhesion in adherens junctions via the well understood strand swap binding mechanism as described above. However, the understanding of the molecular mechanism underlying lateral, *cis*, assembly of cadherins has been less clear. A potential *cis* interaction was described for the first time by Boggon et. al. (2002) for C-cadherin and has been very recently extensively studied additionally for E- and N- type I classical cadherins (Harrison et al., 2010b). Together, these studies suggest that the assembly of ectodomains in a molecular layer formed by a single *cis* interface in addition to the swapped *trans* interface that was observed in the crystal structures of type I E-, N- and C-cadherin represent the arrangement of cadherins in adherens junctions (Figure 6b) (Boggon et al., 2002; Harrison et al., 2010a). The *cis* interface was identified to be an interaction between

EC1, comprising a region opposite the strand swap interface involving strands C, F and G and residues of the quasi β -helix of one protomer, and strands B, D and E of EC2 of the following protomer (Figure 6c). The biological relevance of this interface for junction formation was tested by mutagenesis studies of E-cadherin mutants, in which hydrophobic core residues found in this interface, Val81 (EC1) and Leu175 (EC2), were substituted with negatively charged Asp residues to introduce repulsion and specifically inhibit *cis* interactions while leaving *trans* interactions functional. Crystal structures of two domain fragments of E-cadherin *cis* mutant protein lacked the assembly of the molecular layer which was observed for all previous two domain and five domain type I cadherin structures, and, notably, even for strand swap mutants adopting X shaped dimer confirmations (Harrison et al., 2010a). In a cellular context, wild type E-cadherin formed stable, non fluctuating adherens junctions, whereas the mutant protein was found to produce highly mobile and unstable junctions, which the mutant protein diffused in and out of quickly (Harrison et al., 2010b). In addition, cryo EM studies of wild type and *cis* mutant proteins showed clearly, that despite the fact that both molecules were able to aggregate liposomes similarly well, only wild type E-cadherin arranged into an ordered array at intermembrane contact sites, closely resembling the molecular layer seen in the crystal structures (Figure 6d, left panel). The mutant protein was concentrated at junctions, but was shown to be unordered (Figure 6d, right panel). Together, the cell and liposome studies suggest that passive diffusion or cytoplasmic interactions alone are not sufficient to induce clustering of cadherins into ordered junctions, which is most likely driven by suggested *cis* interface.

This *cis* interface observed for type I cadherins, or similar potential *cis* interface, could not be identified in type II cadherin crystal structures (Patel et al., 2006) or in electron tomography studies of desmosomal cadherins. Nonetheless, a comparable ectodomain-mediated clustering mechanism may operate, because both of these cadherin subfamilies are known to form adherens junctions or desmosomal junctions, respectively (Al-Amoudi and Frangakis, 2008; He et al., 2003; Kiener et al., 2006; Uehara, 2006).

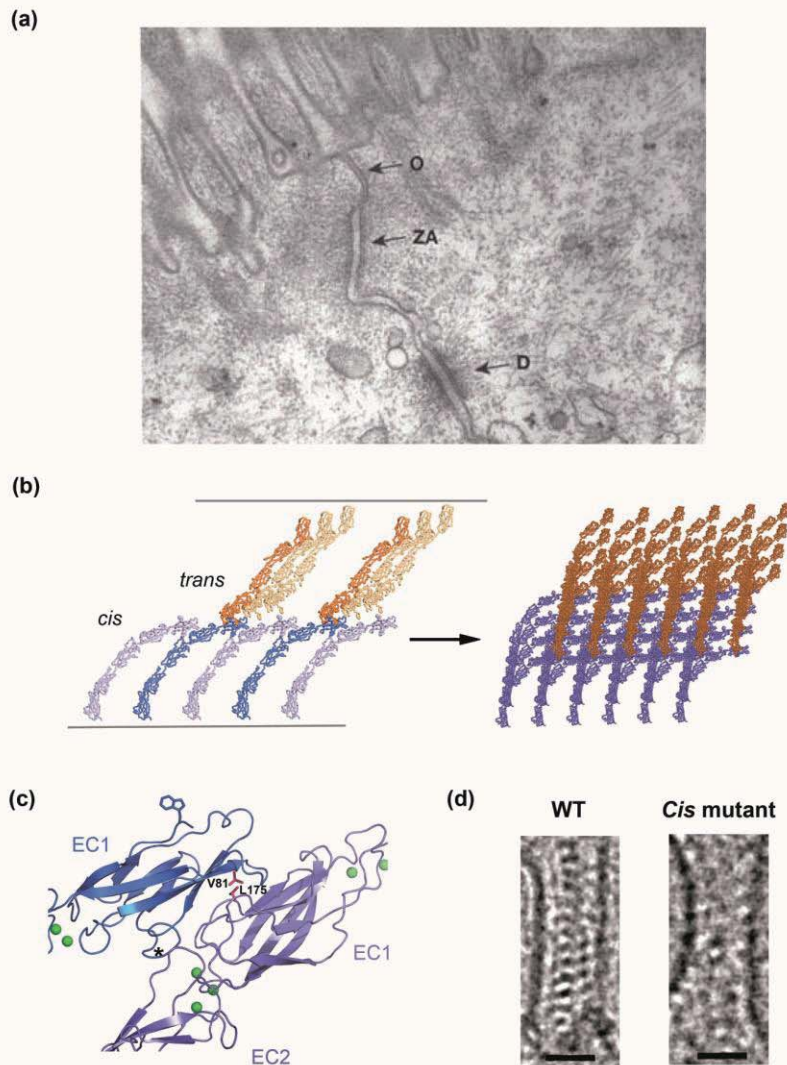


Figure 6: Cadherins are the major cell adhesion protein in adherens junction. (a) Electron micrograph showing three forms of cell-cell junctions: O:Occludens: Tight junction, ZA: zonula adherens, D: Desmosome. Adapted from Farquhar and Palade (1963). (b) Crystal structures of classical cadherins revealed molecular interactions crucial to formation of adherens junction. Two interactions are necessary: *trans* adhesive interactions mediated by EC1 domains alone, and lateral, *cis*, interactions mediated by EC1 and EC2 domains of adjacent molecules. (c) Close up of the *cis* interface between two adjacent cadherin protomers. Hydrophobic residues which have been targeted by mutagenesis studies to disrupt the interface are represented as purple sticks: Val81 and Leu175. Asterisk indicates position of quasi β -helix, which is specific to type I cadherins and contributes to this interface. (d) Close up of artificial junctions formed between liposomes. Junctions formed by wild type protein are well ordered (left panel) and resemble protomer arrangement observed in the crystal structures. Proteins in which the residues shown in (c) are mutated to Asp, still form junctions, but they are unordered and fail to organize properly. See text for further detail. Adapted from Harrison *et al.* (2010).

1.8 Vascular endothelial cadherin, a divergent classical cadherin

1.8.1 Special features of the vascular endothelium

Under physiological conditions, fluids, cells and nutrients are exchanged between the blood compartment and surrounding tissues. Endothelial cells line the vasculature and represent a selective barrier separating blood from the underlying tissues as they control the passage of blood proteins, cells such as leukocytes, and fluids (Harris and Nelson, 2010). Passage of these is achieved by specialized transport vesicles and by coordinated disassembly, ‘opening’, and assembly, ‘closure’, of adherens junctions (Dejana et al., 2009). The endothelium is also the site for angiogenesis, which involves remodelling and extension of the vasculature (Harris and Nelson, 2010) and junctions found in this monolayer do function not only as barrier, but also as signalling structures which limit growth and apoptosis and regulate vascular homeostasis (Dejana, 2004). Thus, many pathological diseases such as atherosclerosis, diabetes, brain stroke and disease states like inflammation, allergy and hypertension and also tumor metastasis (Dejana et al., 2009; Harris and Nelson, 2010) are found to involve abnormal permeability of the endothelium layer.

Cell-cell junctions in endothelial cells are less rigidly organized than those found in epithelial cells despite the mechanical stress and shear forces they endure (Sato and Ohashi, 2005), likely so they can accommodate the high degree of change these cells undergo during blood vessel formation, maintenance and remodelling (Dejana, 2004; Gavard, 2009). Endothelial cells contain tight junctions and adherens junctions, which are, in contrast to those in epithelial cells, intermingled in that tight junctions are not exclusively found at the apical side of the intercellular cleft (Dejana et al., 2009; Harris and Nelson, 2010). Tight junctions play a role especially in endothelial cells in stringent barriers, i.e. those of the blood-brain barrier, and in addition regulate the permeability of the monolayer. Adherens junctions are more important during initial cell-cell contact, establishment and maintenance of adhesion and also for remodelling processes (Harris and Nelson, 2010). Interestingly, it is suggested that adherens junctions are formed first and tight junctions occur once the junction is stabilized (Harris and Nelson, 2010), which is supported by the fact that in some cell systems blocking of adherens junctions ablates correct formation of tight junctions (Dejana et al., 2009). Vascular endothelial (VE) cadherin, a divergent type II cadherin, is the endothelial-specific protein in adherens junctions (Breier et al., 1996; Dejana et al., 1996; Lampugnani et

al., 1992; Vittet et al., 1997) and claudin-5 is the major component of tight junctions in the endothelium.

1.8.2 VE-cadherin plays a pivotal role in the vascular endothelium

VE-cadherin is found in vertebrate species including birds, fish, amphibia and mammals and plays a pivotal role in the vascular endothelium. Endothelial cells express, in addition to VE-cadherin, type I N-cadherin and low levels of P-cadherin, but exclusively VE-cadherin is found to be concentrated in adherens junctions (Figure 7a and b)(Kapadia, 1984; Uehara, 2006), whereas N-cadherin is found to be dispersed over the cell surface and absent from cell-cell contacts (Gentil-Dit-Maurin et al., 2010; Jaggi et al., 2002; Liaw et al., 1990; Navarro et al., 1998; Salomon et al., 1992). VE-cadherin knockout mice die during gestation at E9.5 due to disintegration of primitive vasculature (Carmeliet et al., 1999) and, furthermore, VE-cadherin gene null mutations in murine embryonic stem cells lead to a dispersed endothelium lacking organized vasculature in embryonic bodies (Vittet et al., 1997). Similarly, depletion of VE-cadherin in zebrafish embryos resulted in collapse of initial vascular networks as vessels could not form cell-cell junctions critical for lumen formation (Dejana, 2004).

In another set of experiments, in which antibodies directed against VE-cadherin were injected into adult mice, permeability of the vasculature increased, leukocyte trafficking was enhanced and the vasculature disassembled, which resulted in death within 24 hours post injection (Corada et al., 1999; May et al., 2005). In contrast, knockout mice for claudin-5, which is the major component of tight junctions in the vascular endothelium, had a normal overall morphology of the vasculature, but died within 10 hours after birth due to dysfunction of the blood brain barrier. Overall, these experiments suggest a crucial, specific, non-redundant role for cell-cell adhesion mediated by VE-cadherin. This important protein is also involved in regulation of cellular processes like cell contact inhibition, leukocyte trafficking (Navarro et al., 1995), signaling processes (Harris and Nelson, 2010) and control of vascular permeability (Corada et al., 2001).

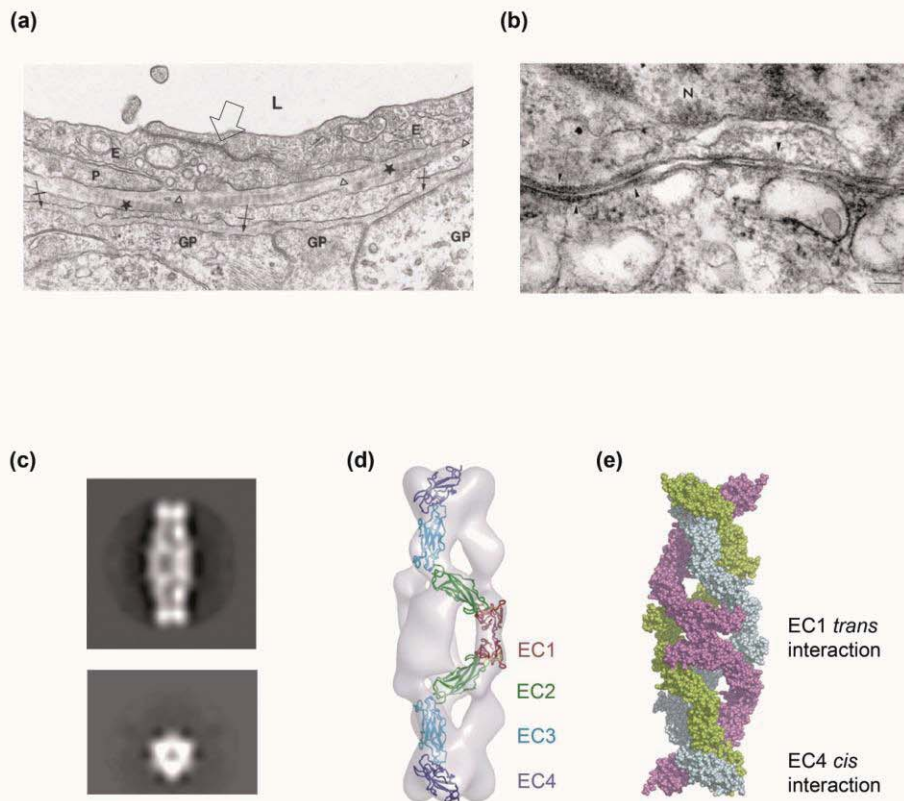


Figure 7: VE-cadherin, the major adhesion molecule of the vascular endothelium, is proposed to form adhesive hexamers. (a) Transverse section of a capillary in white matter of mouse spinal cord. L=lumen of capillary; E= endothelial cell; P=pericyte; GP=glial processes; arrowheads=basement membrane; crossed arrows=lower basement membrane; asterisks=collagen fibers in perivascular space; white arrow indicates adherens junction between endothelial cells. Adapted from Kapadia *et al.* (1984). (b) EM micrographs of immunological gold stainings of VE-cadherin in adherens junctions in the vasculature. Arrow heads indicate junctions. Adapted from Uehara *et al.* (2005). (c) Bacterially produced human VE-cadherin EC1-4 adopt the structural architecture of a cigar shaped hexamer. in EM micrographs, averaged images are depicted. (d) Homology model of VE-cadherin based on the C-cadherin structure can be fit into the electron density map showing a *trans* dimerization. EC domains are labelled for orientation. (e) Two different protein interactions are found in the hexamer. A *trans* interaction involving EC1 domains alone (also shown in panel (d)). In addition, a second novel trimeric interface can be observed, a *cis* interface, which appears to be mediated by domain EC4 alone. The hexamer can be imagined to be an adhesive dimer formed by two *cis* trimers. (c)-(e) adapted from Hewat *et al.* (2007). See text for detail.

Interestingly, N-cadherin, which is co-expressed with VE-cadherin on endothelial cells, was not able to rescue the severe defects caused by VE-cadherin removal, although it is a potent cell-cell adhesion protein in other important tissues. Gentil-dit-Maurin et al (2010) conducted a study with embryonic bodies, in which VE-cadherin expression was silenced and N-cadherin adhesive behavior observed. Embryoid bodies expressing VE-cadherin showed angiogenesis sprouting whereas bodies lacking VE-cadherin did not. N-cadherin also failed in these experiments to mediate sprouting in place of VE-cadherin once silenced, which supports VE-cadherin's non-redundant role for adhesion in the vasculature. N-cadherin is found to be dispersed evenly over the cell surface in presence of VE-cadherin (Jaggi et al., 2002; Salomon et al., 1992), but localized to junctions when VE-cadherin was not expressed (Gentil-Dit-Maurin et al., 2010; Navarro et al., 1998). In *in vitro* transfection experiments, immunofluorescence staining of endothelium cells and different transfected cell lines co-expressing N-cadherin and VE-cadherin (Jaggi et al., 2002; Navarro et al., 1998) revealed that VE-cadherin excludes N-cadherin actively from junctional localization, which is the reason for its even distribution on the cell surface. A study by Jaggi et al (2002) provided additional insight, showing that the effect VE-cadherin has on type I N-cadherin is specific; it has no effect on other type I cadherins like E- and P-cadherin, because in immunofluorescence staining of cells co-expressing E- and VE-cadherin or P- and VE-cadherin, these proteins were found to co-localize at cell-cell contacts (Jaggi et al., 2002). This is the first time that competition between cadherins for clustering at junctions was observed. Nonetheless, N-cadherin can in presence of VE-cadherin still homophilically adhere to cells expressing N-cadherin only, which suggests that N-cadherin homophilic adhesion might be responsible for connection of the endothelial-monolayer to the surrounding cell types such as smooth muscle cells or pericytes (Navarro et al., 1998).

1.8.3 Hexamer model for VE-cadherin binding

VE-cadherin shares several features with classical type II cadherins including exon and intron arrangement on the DNA level and the overall domain organization of the protein (Nollet et al., 2000). It also has a small prodomain, an ectodomain composed of domains EC1-5, a single transmembrane domain and a short cytoplasmic tail similar to type II cadherins. In addition VE-cadherin is associated in endothelial cells with β -, γ - and p120 catenins (Gentil-Dit-Maurin et al., 2010; Lampugnani et al., 1995; Lim et al., 2001; Potter et al., 2005) which promote interactions via α -catenin to F-actin for classical cadherins (see above).

Surprisingly, despite these similarities, bacterially produced VE-cadherin ectodomain fragments spanning domains EC1-4, purified from inclusion bodies, were not found to form adhesive dimers like other classical type II cadherins (Harrison et al., 2010b; Patel et al., 2006). Instead, several experimental approaches including cryo electron microscopy (Hewat et al., 2007; Lambert et al., 2005; Legrand et al., 2001) and solution biophysics experiments such as chemical cross linking, analytical size exclusion chromatography and equilibrium analytical ultracentrifugation (Bibert et al., 2002) revealed a novel hexameric binding model for these VE-cadherin fragments in which six molecules associated in an approximately cylindrical arrangement. Single particle 3D reconstruction of EM-micrographs (Figure 7c) yielded 24Å resolution electron density map, into which a homology model of VE-cadherin was fitted (Figure 7d). This shed light on the VE-cadherin hexamer binding configuration (Figure 7e), which was found to adopt a compact elongated cigar like shape with a length of 233Å corresponding to the length of two EC1-4 domain proteins in tandem (Hewat et al., 2007). Protomers were oriented as if emanating from juxtaposed cells, with three molecules on each side (Figure 7e). Two different contact sites were identified in the hexamer: one involves a *trans* EC1 domain contact which was suggested to be mediated by strand swapping similar to that of classical cadherins forming anti parallel dimers; and the other was a novel trimeric interaction involving domain EC4 (Figure 7e). It appears that the EC4 contact is lateral, so that VE-cadherin ectodomains on the same cell surface would assemble into *cis* trimers, which form a dimer together with a *cis* trimer from the opposing cell to produce a final hexameric assembly. So far, however, the hexameric arrangement has been observed only for purified, bacterially expressed ectodomain fragments and the biological relevance of this novel VE-cadherin binding model remains to be determined.

1.9 Aims of this work

The work described in this thesis will focus primarily on the investigation of the adhesive binding mechanism of VE-cadherin, a divergent type II cadherin crucial to the formation and maintenance of the vascular endothelium. No atomic level structure of the VE-cadherin binding interface is available and a novel binding mechanism has been proposed for which biological importance needs to be investigated. The binding affinities and specificities of other type II classical cadherins will also be investigated, as will the binding mechanism of the atypical classical cadherin T-cadherin.

Specific experimental aims are:

(1) VE-cadherin full ectodomains and a fragment containing the putative trimerization site will be expressed in a mammalian expression system to provide natively glycosylated soluble protein, which will be used in an extensive biophysical approach such as sedimentation equilibrium analytical ultracentrifugation (AUC), analytical size exclusion and multi angle light scattering (MALS) to characterize the adhesive binding mechanism and to test the hexamer binding model.

(2) Fragments of the VE-cadherin ectodomain will be expressed in bacteria to identify the minimal adhesive binding unit of VE-cadherin and structural studies will be performed to determine the structure of the *trans* adhesive interface.

(3) The homodimerization binding affinities of a set of five additional type II cadherins in addition to VE-cadherin, all produced in bacteria, will be assessed by equilibrium AUC experiments to determine general binding trends in the classical cadherin family.

(4) To determine the relative binding specificities inherent to type II cadherins and assess the degree of promiscuous binding, surface plasmon resonance experiments will be conducted. In addition, the ability of VE-cadherin to heterophilically interact with other type II subfamily members and with type I cadherins, with which it is coexpressed *in vivo*, will be tested.

(5) To test the dependency of T-cadherin mediated adhesion on the strand swap mechanism common to classical cadherins, in order to test models from structural studies suggesting that T-cadherin uses a non-swapped dimerization mechanism. I will introduce strand swap targeted mutations into T-cadherin and simultaneously into mouse type I E-cadherin and type II cadherin-6 so that the impact of these mutations on adhesive binding can be assessed by equilibrium AUC.

Chapter 2:
Materials and Methods

2.1 Protein Production

Plasmid construction, protein expression and purification for all proteins produced in mammalian and bacterial systems that were used in the biophysical and biochemical studies in this work are described in this section.

2.1.1 Mammalian protein production

2.1.1.1 Plasmid construction

Coding sequences for human VE-cadherin EC1-5 (Asp1-Asp542, all numbering according to the mature proteins), EC3-5 (Ile204-Asp542) and chicken VE-cadherin EC1-5 (Asp1-Glu545) were amplified by polymerase chain reaction (95°C for 2' activation polymerase; 40 cycles of 95°C 30'' dissociation, 63°C 1' annealing, 68°C 2' extension; final extension at 68°C for 10min, stored at 4°C) from cDNA libraries (human VE-cadherin from human heart library, Invitrogen and chicken cDNA library clone pgp 1n.pk007.i4, Delaware Biotechnology Institute) using KOD Hot start DNA polymerase (Novagen) according to manufacturer's instructions with primers at a concentration of 10pM. A Kozak sequence (gtt gtt) was included before the start methionine; signal sequence and prodomain encoding regions found in naive cadherin sequences were replaced by the signal sequence of CD33 (MPLLLLWAGALA) and the transmembrane and cytoplasmic domains were replaced by a hexa histidine tag. All proteins were cloned into the KpnI/NotI restriction sites (enzymes from New England Biolabs) of the episomal expression vector pCEP4 (Invitrogen). An expression construct encoding wild-type mouse E-cadherin (Asp1-Ala544), cloned in the same manner, was produced as described in Harrison et al (2010b). Point mutations W2A W4A in VE- and W2A K14E in E-cadherin were introduced by site directed mutagenesis using the Quickchange method (Stratagene). DNA sequences of produced plasmids were validated by Sanger DNA sequencing (Genewiz, Inc.).

2.1.1.3 Tissue culture

All proteins referred to as 'mammalian produced' were expressed either in adherent human embryonic kidney (HEK) 293 Fast Growth (F) cell lines or in 293 N-acetylglucosamine transferase I deficient (GNTI) cell lines. HEK 293 F produce proteins with native N-linked glycosylation, whereas HEK 293 GNTI- cells produce proteins with limited N-linked

glycosylation (Man₅GlcNac₂) (Reeves, J. 2002). Both cell lines, which will be referred to together as HEK 293 cells, were cultured in advanced glutamine free DMEM/F12 medium (Gibco, Invitrogen) freshly supplemented with 100µg/ml Penicillin/Streptomycin (Gibco, Invitrogen), 4mM L-Glutamine (Gibco, invitrogen) and 10% Newborn calf serum (<10 days old, Fisher Scientific) in a Thermo Scientific Hepa class 100 incubator at 37°C in presence of 5% CO₂ and 90% humidity. This medium composition will be referred to as DMEM/F12, when composition is altered, supplements added will be specified. Cells were maintained by splitting 1:10 every seven days by removing medium, dissociating with pre-warmed trypsin 0.05% (1X) with EDTA (Gibco, invitrogen) for 5 minutes, pelleting the cells by spinning at 1000g at 25°C for 6 minutes and resuspension in 10mL of DMEM/F12. For replating, 1mL of cell suspension was transferred to 75cm² flask with vented caps (Corning) containing 20mL DMEM/F12 pre-warmed medium.

2.1.1.4 Transfection of HEK 293 cells

For transfection cells were lifted and pelleted as described in the previous section, resuspended in 20mL of DMEM/F12 without Penicillin and Streptomycin supplements and seeded into a 6 well plate of 2cm² per well surface area to grow until they reached approximately 80% confluency. On the day of transfection cells were transfected with 6µg cadherin-pCEP4 expression construct plasmid DNA prepared with the HiSpeed Maxi prep kit according to the manufacturer's instructions (Qiagen) using Lipofectamine 2000 following the instructions provided by the company (Invitrogen). On the following day, transfectant medium was removed from cells and cells were resuspended in 2mL of DMEM/F12 and transferred into a 75cm² flask containing 25mL of DMEM/F12. Selection for successfully transfected cells was begun 48 hours after transfection by supplementing the medium with 200µM Hygromycin B (MediaGrowth, Fisher Scientific) as pCEP4 carries the resistance gene for this aminoglycoside. Transfected stable cell lines were cultured in the presence of 200µM Hygromycin at all times.

2.1.1.5 Protein Expression

Cells transfected as described above secrete the respective soluble cadherin proteins into the conditioned medium, so once cells reached confluence in 75cm² flasks, medium was tested for presence of hexa-histidine tagged cadherins by Western Blotting and immunological

detection by horseradish peroxidase (HRP) labeled monoclonal antibody against the His tag (Qiagen, see Section 2.3.3.2 below). Once protein expression was validated, the relevant cell culture was expanded to a 10 layer cell Stack flask with tissue culture surface totaling in 6360cm² surface area (Corning). Cells were cultured in 1 liter DMEM/F12 + 200µM Hygromycin B per cell stack farm and every 14 days the culture split in half as described before, 200mL of trypsin solution are needed per split. Dissociated cells were spun down in 50mL Corning graduated plastic tubes at 1000g for 6min at 25°C and were resuspended in DMEM/F12 for replating in cell stack farms. Each time, conditioned media were collected before trypsinization. and cell debris was removed by 20 minute spins at 13000g at 4°C. Conditioned media were then stored at -80°C until 4 liters of were collected for purification.

2.1.1.6 Protein purification

Supernatants were thawed on ice and filtered using a 1L 0.22µm PES funnel filter (Corning) and vacuum prior purification. Supernatants were supplemented with 500mM sodium chloride (Sigma), 20mM Tris-Cl pH8.0 (Fisher Scientific), 3mM calcium chloride (J.T. baker, Fisher Scientific) and 10mM imidazole pH8.0 (Fisher Scientific), then were transferred to 4L plastic beaker (Nalgene) covered by Styrofoam lid, in which a Wheaton BiStir stirrer (Model 356887, ‘floating stir bar’) was inserted. Hexa-histidine tagged cadherins were collected by nickel batch affinity purification through addition of 20mL nickel (II) charged IMAC Sepharose 6 fast flow resin (GE Healthcare), which was equilibrated in 500mM sodium chloride, 20mM Tris-Cl pH8.0, 3mM calcium chloride, 10mM imidazole pH8.0. After incubation for 3 hours at 4°C under gentle stirring, resin was extracted by passing through a 7cm diameter Kontes column (Kimble Chase, ~250mL) using gravity and washed with 20 column volumes total of 500mM sodium chloride, 20mM Tris-Cl pH8.0, 3mM calcium chloride and 12.5mM imidazole to remove non specifically bound contaminant serum proteins. Resin was transferred to a XK 16 column (GE Healthcare) and connected to an AKTA FPLC 900 (GE healthcare) operated by Unicorn software. After an additional 20 column volumes of washing, proteins were eluted by increasing the imidazole concentration to 75mM (GE Healthcare) in ~5 column volumes. Protein elution was monitored by absorbance at a wavelength of 280nm. Eluted proteins were dialyzed in 10 MWCO snake skin dialysis tubing (Thermo Scientific) for 18 hours at 4°C in 5L of 100mM sodium chloride, 20mM Tris-Cl pH8.0, 3mM calcium chloride. For further purification the protein was flown over a Mono S ion exchange column HR10/10 (GE Healthcare) to remove high molecular

weight contaminants, which were found to bind tightly the column. Cadherins uniformly were found in the flow through and were collected and then passed over an anion exchange column MonoQ MQ HR10/10 (GE Healthcare) to remove residual contaminants. The protein was concentrated to a volume of approximately 3mL using Amivon 50K MWCO Spin concentrators (Millipore). Proteins were spun at 4000g in 3min intervals at 4°C until desired volume of 3mL was reached. The last step of purification was size exclusion chromatography by a HiLoad 26/60 Superdex S200 prepgrade column. The peak containing the protein of interest was collected and purified protein was concentrated using same method as described above, tested for purity by SDS-PAGE (see below) and flash frozen in liquid nitrogen in aliquot sizes of 15-30µL. All proteins were in a final buffer of 150mM sodium chloride, 10mM Tris-Cl pH8.0 and 3mM calcium chloride.

2.1.2 Bacterial protein production

2.1.2.1 Plasmid construction

Coding sequences of two and three domain wild type cadherin proteins were amplified by PCR (95°C for 2' activation polymerase; 40 repetitions of 95°C 30'' dissociation, 63°C 1' annealing, 68°C 1' extension; final extension at 68°C for 10min, stored at 4°C) from cDNA libraries (human VE-cadherin from human heart library, Invitrogen and chicken cDNA library clone pgp 1n.pk007.i4, Delaware Biotechnology Institute, mouse proteins from mouse multiple tissue cDNA (MTC) panel I libraries, clontech) using KOD Hot start DNA polymerase (Novagen) according to manufacturer's instructions with primers at concentration of 10pM. Mouse cadherin-6, -8, -9, -10, -11 and VE-cadherin EC1-2 and chicken VE-cadherin and cadherin-6b as well as human VE-cadherin EC1-2 and mouse cadherin-8 EC1-3 fragments were cloned in frame with an N-terminal hexa His tagged SUMO protein into the BamHI/NotI sites of the bacterial pSMT3 T7 polymerase expression vector (Invitrogen). Quickchange site-directed mutagenesis (Stratagene) was used to introduce all point mutations, extensions or to delete parts of the N-terminus. The same method was applied to remove extra bases between the encoded protease site (Gly-Gly) and the amino terminus of the encoded protein to ensure correct mature cadherin N-termini. Constructs encoding Avi-tagged proteins (Avidity) were prepared by inclusion of a sequence encoding the Avitag at the cadherin fragment C-terminus immediately prior to the stop codon. All plasmids were transformed into XL10-gold *E. coli* (Stratagene), positive colonies selected with Kanamycin and plasmid DNA

generated by Mini prep (Qiagen) according to the companies instruction. Correct DNA sequences were validated as for mammalian plasmids.

2.1.2.2 Protein Expression

Verified pSMT3plasmids encoding cadherin fragments were transformed into E. coli Rosetta2DE3 pLysS strains (Novagen) for expression following the manufacturer's manual. Small cultures of 3mL LB medium (Miller, granulated LB-broth, EMD) were prepared with 50µg/mL Kanamycin and 34µg/mL Chloramphenicol, inoculated with one colony of bacteria and incubated for 18h at 37°C shaking at 200rpm to grow. 100µL of this culture were used to inoculate a starter culture of 300mL LB with the same antibiotic composition, which was also incubated for 18h at 37°C. A glycerol stock of each culture was prepared where 1.2mL of culture were supplemented with 30% glycerol to be stored at -80°C. For protein expression, 25mL of the starter culture were used per Liter of expression culture for a batch of 12Liters total. Once OD₆₀₀ of 0.6 was reached by the bacterial culture, protein expression was induced by adding 100µM IPTG and temperature lowered to 18°C for a total of 18h of expression, shaking at 200rpm for all proteins but cadherin-6 (wild type, tagged protein and mutants), for which the temperature was kept at 37°C for an additional 5hours instead (Harrison 2010a).

To obtain biotinylated Avi-tagged cadherins, pSMT3-cadherin with sequence encoding the Avi-tag at the C-terminus was co-transformed with BirA plasmid (Chloramphenicol resistance) which encodes for the biotin ligase and into E. coli strain BL21 (Invitrogen). Expression was as described above, with the addition that medium was supplemented with IPTG and 50µM Biotin.

Bacteria were harvested in 1L buckets at 4,000g for 20min at 4°C, supernatants discarded and pellets retained for lysis and purification as described below..

2.1.2.3 Bacterial Protein Purification

Bacterial pellets were resuspended in 250mL of 500mM sodium chloride, 20mM Tris-Cl pH8.0, 3mM calcium chloride and 20mM imidazole pH8.0. Cells were lyzed by sonication on ice for a total of 6 minutes in intervals of 15sec of pulse with 45sec rest with Branson Digital Sonifier. Cell debris was pelleted and lysates cleared by centrifugation for 30min at 20,000g

at 4°C. His-tagged SUMO-cadherin fusion proteins were collected from lysates by flowing over 5mL of nickel charged IMAC sepharose 6 Fast Flow resin (GE Healthcare). Resin with captured protein was washed with 40 column volumes of the same buffer and His-tagged SUMO-cadherin fusion proteins were eluted by increasing the imidazole pH8.0 concentration in the buffer to 250mM for a total volume of ~50mL (10 column volumes). His-SUMO tags were removed during dialysis in 50mM sodium chloride for E-, N-, T-cadherins and cadherin-6 and 100mM sodium chloride for cadherins 8, 9, 10, 11 and VE-cadherin and 20mM Tris-Cl pH8.0 and 3mM calcium chloride by specific proteolytic cleavage after the Gly-Gly motif by 2µg/mL ubiquitin ligase protein I (Invitrogen), leaving all proteins in this study with native N-termini unless specifically altered.

Hexa His-SUMO tags and uncut fusion proteins were removed from the dialyzates by batch binding for 30min at 25°C with rotation to 5mL of nickel charged resin (as above) preequilibrated in respective dialysis buffer. Cadherins were further purified by flowing over an anion exchange column MQ HR10/10 followed by size exclusion chromatography with a hiLoad 26/60 Superdex S75 (GE Healthcare). All proteins were in a final buffer of 150mM sodium chloride, 10mM Tris-Cl pH8.0, 3mM calcium chloride and for cadherins carrying the C-terminal CYS-tag 1mM TCEP was included in the buffer. Proteins were concentrated in 10K MWCO Amicon spin concentrators (Millipore) and 10µg of each protein analyzed by SDS-PAGE. Biotinylation of proteins was verified after transfer to nitrocellulose membranes by binding NeutrAvidin-HRP followed by chemiluminescent detection. All proteins were flash frozen in 15-100µL aliquots according to need to avoid multiple freeze-thaw cycles.

2.2 Biophysical Methods

2.2.1 Analytical ultracentrifugation

All equilibrium analytical ultracentrifugation experiments were performed together with Goran Ahlsen (Columbia University) using a Beckman XLA/I ultracentrifuge, with a Ti50An or Ti60An rotor. All proteins were diluted with buffer (150mM sodium chloride, 10mM Tris-Cl pH8.0, 3mM calcium chloride) and dialyzed for 16h at 4°C in 1L of the same buffer prior to each experiment. 120µL of proteins at three different concentrations 0.7mg/mL, 0.46mg/mL and 0.24mg/mL were loaded into six-channel equilibrium cells with parallel sides and sapphire windows. All experiments were performed at 25°C and data was collected at wavelengths of 280 nm (UV) and 660 nm (interference). Five-domain proteins (VE-cadherin EC1-5 and E-cadherin EC1-5) were spun for 20h at 8,800g and four scans (1 per hour) were collected, then speed was increased to 12,300g for 10h and four scans (1 per hour) were collected and speed was increased to highest speed of 16,400g for another 10h and four scans (1 per hour) were taken, which yielded 72 scans per sample. Three-domain proteins (VE-cadherin EC3-5, cadherin-8 EC1-3) were analyzed using the same protocol, except using speeds of initial 14,200g, followed by 23,500g and 35,200g as highest speed. For two-domain proteins (VE-cadherin EC1-2, EC3-4; type I cadherins E, N, P, T; type II cadherin-6, -8, -9, -10, -11; wild type, tagged and mutant proteins), speeds of 23,500g, 35,200g and 49,100g were used. Relative centrifugal forces are given at the measuring cell center at a radius of 65mm. Buffer density and protein ν -bars were calculated using the software SednTerp (Alliance Protein Laboratories), and retrieved data was analyzed using HeteroAnalysis 1.1.0.28 (<http://www.biotech.uconn.edu/auf>). We fitted data from all concentrations and speeds globally by nonlinear regression to either a monomer-dimer equilibrium model or an ideal monomer model. All experiments were performed at least in duplicate, except for C-terminally tagged bacterial cadherins, which were only measured once.

2.2.2 Analytical size exclusion chromatography

A volume of 150µL of purified proteins at a concentration of 6µM were flown over analytical superose 12 10/30 column (GE Healthcare) which was pre-equilibrated with 150mM sodium chloride, 100mM HEPES pH7.0, 3mM calcium chloride for at least two column volumes. Experiments were performed at 4°C using the AKTA FPLC-900 system operated by Unicorn and a steady flow of 300µL/min. Fractions of 500µL each were collected and UV-signal at 280nm recorded. Fractions of sufficient UV signal peaks were analyzed by SDS-PAGE and immunological detection with tetra His antibody (Qiagen), so every monitored peak was

validated to be the expected cadherin. Void volume of the column was determined to be 8mL using Blue Dextran (GE Healthcare).

2.2.3 Multi angle light scattering

Human VE-cadherin EC1-5 and EC3-5 and mouse E-cadherin mutant W2A K14E expressed in HEK 293 GNTI cells and purified as described above were used at a concentration of 1mg/mL for MALS experiments. Proteins were passed over a TSKgel Super SW3000 operated by an HPLC to separate different protein species from each other and then measured for absolute molecular weight and dispersity by the triple-angle MALS light scattering detector miniDAWN Treos (Wyatt Technology, Europe GmbH) at New York Structural Biology Center (New York, USA) using continuous flow detection. Data were analyzed and absolute molecular weights calculated with Astra V Software.

2.2.4 Liposome aggregation assays

2.2.4.1 Preparation of liposomes

1,2-dioleoyl-*sn*-glycero-3-phosphocholine (DOPC) and 1,2-dioleoyl-*sn*-glycero-3-[(N-(5-amino-1-carboxypentyl)iminodiacetic acid)-succinyl] nickel salt (DGS-NTA-(Ni)) were obtained from Avanti lipids and prepared according to the manufacturer's manual. Liposomes used for aggregation and cryo-EM studies were composed of a 9:1 ratio of DOPC and DGS-NTA(Ni), respectively, and were prepared using the hydration and extrusion method, in which liposomes were suspended in 25mM HEPES pH7.4, 0.1M potassium chloride, 10% (v/v) glycerol, 3mM calcium chloride (liposome aggregation buffer). To equalize size within liposomes they were extruded through a 100nm filter membrane following Avanti's instructions for the extruder. Liposomes were stored for 3 month at 4°C.

2.2.4.2 Liposome aggregation assays

Aggregation assays were conducted according to the method described by He et al (2009) and Harrison et al (2010b). Liposomes were first diluted in liposome buffer to a final concentration of ~5mg/mL and at the starting point of the experiment, hexa-His-tagged cadherin fragments were added to yield the final concentration of 6µM. Aggregation was monitored at OD of 650nm in 20sec intervals for a total of 2,500sec. For the reference

sample, protein was substituted with liposome aggregation buffer (negative control). Experiments were performed in triplicate for all human and chicken ectodomains and the negative control, and in duplicates for mouse E-cadherin ectodomains and human VE-cadherin EC3-5 fragments.

2.2.4.3 Cryo Electron microscopy studies

Liposome aggregation was performed with full ectodomains of human VE-cadherin and mouse E-cadherin, both expressed in HEK 293 F cells as described in the previous section. Liposomes were allowed to aggregate for 10min and were then transferred to 300 mesh copper TEM grids with R2/1 Quantifoil. Samples were vitrified by blotting and plunge-frozen into liquid nitrogen cooled ethane using the automated Vitrobot (FEI company, Hillsboro, Oregon; as described by Harrison *et al* 2010b). Grids were stored in liquid nitrogen until imaging was performed using a Tecnai Polara F30 TEM (FEI company, Hillsboro, Oregon) at the New York Structural Biology center (New York, New York) by Ruben Diaz (New York Structural Biology Consortium). Frozen grids were imaged at 300kV using a Tietz 4Kx4K CCD camera (Tietz video and Image Processing Systems GmbH, Gauting, Germany). Images were recorded under low-dose conditions at $\sim 10\mu\text{m}$ under focus using the serialEM software (Mastronarde, 2005) and processed with IMOD software (Kremer et al 1996) Microscope magnification was 39,000-59,000fold.

2.2.5 Atomic force microscopy imaging

AFM sample pucks were prepared as follows: 10mm diameter disks of Muscovite mica (Agar Scientific) were stamped out from the as-received sheets. Each sample puck was fixed to a 13mm steel puck (agar Scientific) with cyanoacrylate super-glue and allowed to dry for 16h. Poly-L-lysine (Sigma Aldrich) was diluted 1/100 into BPC-grade water (Sigma Aldrich) and 45 μL of this solution pipetted onto freshly-cleaved mica, given 30min incubation at 25°C, washed 10 times with 1mL BCP-grade water and dried under a gentle, steady stream of nitrogen.

Cadherin ectodomains used in AFM imaging studies were produced in HEK 293 F cells. VE-cadherin samples were diluted in 150mM sodium chloride, 20mM Tris-Cl pH8.0, 3mM

calcium chloride to a final concentration of $\sim 2\text{nM}$ and stored at 4°C which yielded workable and consistent surface concentrations of protein. E-cadherin samples were diluted using the same buffer, but to a higher concentration of E-cadherin, $\sim 8\mu\text{M}$, was needed to allow dimer formation to be observed. $45\mu\text{L}$ of sample was pipetted onto poly-L-lysine coated mica and incubated at room temperature for 10min, then washed 10x with 1mL of BPC-grade water and dried under a gentle and steady stream of dry nitrogen.

Imaging was performed at the Department of Pharmacology (Henderson Laboratory, Cambridge University, UK) with a Multimode atomic force microscope with attached Nanoscope IIIa controller (both Veeco) under ambient conditions in tapping mode, using OMCL0AC160TS single-crystal silicon probes (Olympus, Japan) with a resonant frequency of $\sim 300\text{kHz}$, a nominal spring constant of $\sim 42\text{Nm}$ and a radius of curvature $< 10\text{nm}$. We collected images at 3Hz with an integral gain of 0.2, a proportional gain of 0.35, a look-ahead gain of 0 and a set point of ~ 0.85 (to minimize vertical probe-induced sample deformation). Length determination of molecules was performed using SPIP (Scanning Probe Image Processor) version 3.3 from 3-dimensional AFM data using the full-width at half-maximal approach.

2.2.6 Protein crystallography

2.2.6.1 Screening trials

Sparse matrix screening and precipitant screening was performed in sitting drop assays at 20°C and 4°C using 100nL protein solution at concentrations of 6.8-8.6mg/mL and 100nL well solution in 96 well screening plates (Axygen). Crystal suites used for screening were Index (Hampton), Wizard I+II (Emerald), Classics, Classics II, PEGs, PEGs II, pH clear, pH clear II, JCSG⁺, Anions and Cations (Qiagen). $75\mu\text{L}$ of crystallization condition was transferred to each well of the 96 well plate using a twelve channel electronic pipette and the crystallization experiments were set up using the mosquito nanodrop crystallization robot. Plates were stored after set up either at 20°C or 4°C and checked after 12h, 24h and then daily for 14 days and again after 30 and 60 days with a microscope.

2.2.6.2 Crystal optimization

Crystal optimizations were performed using the hanging drop vapor diffusion method. 500 μ L of crystallization solution was prepared in reservoirs of 24 well screening plates (Hampton), of which the rims were greased prior to set up. For each crystallization condition three different protein: well solution ratios were used: 1 protein: 1 well solution, 1 protein: 2 well solution and 2 protein:1 well solution to increase the variation of crystallization conditions by varying initial and final precipitant and protein concentrations. Initial volumes of the mixed drops were 1.2 to 1.8 μ l. Protein and solution were pipetted on dust and lint free siliconized cover slips (Hampton) and placed above the well with the rim gently pushed onto the grease to seal the vapor diffusion chamber. Chicken VE-cadherin EC1-2 crystals grew within 18h at 20°C in 18% (w/v) PEG 8,000, 200mM calcium acetate and 100mM sodium cacodylate pH6.5. Crystals were harvested for crystallization by mounting with 200 μ m nylon loops mounted on metal bases (Hampton), then transferred and immersed in cryo protectant (well solution + 30% (w/v) glycerol) for 5-10sec and immediately flash frozen in liquid nitrogen. Crystals were stored in Hampton vials under liquid nitrogen, which were transported in canes.

2.2.6.3 Data collection

Diffraction data was collected on beam line X4C at the National Synchrotron Light Source, Brookhaven National Laboratory, USA. A data set of 180 frames with 1° oscillation per frame was collected on a single frozen crystal of chicken VE-cadherin EC1-2 at a wavelength of 0.979Å using an ADSC ccd Quantum 4 detector (Area Detector Systems Corporation) with 20sec exposure time.

2.2.6.4 Data processing

The collected images of the chicken VE-cadherin EC1-2 diffraction pattern were processed using the HKL suite (Otwinski and Minor 1997). The structure was solved by molecular replacement with the phaser program as part of the ccp4i suite using the crystal structure of mouse cadherin-11 EC1-2 (pdb ID code 2A4E) as template. Refinement of the obtained structure was carried out by alternating cycles of manual building in coot (Emsley, Cowlan 2004), followed by automated refinement in Refmac 5 (ccp4 suite, Bailey 1994). Data collection and refinement statistics are summarized in Table 11. Ramachandran plot statistics

for the final model of chicken VE-cadherin EC1-2 are 97.1% of residues in favored positions, 100% in allowed regions and no residues found in disallowed regions. The structure factors and pdb file have been submitted to the protein data bank and can be found under pdb accession ID 3PPE.

2.2.7 Surface plasmon resonance

All Surface plasmon resonance (SPR) binding experiments were conducted with a Biacore T100 biosensor (Biacore, Uppsala, Sweden) using a low charge series S CM4 sensor chip (Biacore). Reagents used for amine and thiol coupling were also purchased from Biacore.

2.2.7.1 Amine Coupling for affinity capture

Sensor chip surface carboxymethyl (CM) groups were activated by injection of 50mM N-hydroxysuccinimide (NHS) in presence of 200mM N-ethyl-N'-(3-dimethylaminopropyl) carbodiimide (EDC) over all four flow cells at 20 μ L per min for a total of 7min. Either Immunopure Neutravidin (Thermofisher), one of four different anti-FLAG antibodies, or a Rho1d4 (anti C9) antibody were dissolved in sodium acetate pH4.5 and flown over the activated surfaces for 7min with 20 μ L per min for coupling. Unoccupied activated carboxymethyl groups were quenched with a 7min injection of 1M ethanolamine-HCl pH8.5 at 20 μ L per min. Immobilization levels and summary of antibodies and Neutravidin immobilized by amine coupling is shown in Table 2. Running buffer was HEPES-buffered saline (HBS, 10mM HEPES pH7.4, 150mM sodium chloride) and immobilization was performed at 32°C.

Table 2: Immobilization levels of antibodies and NeutrAvidin used in SPR studies.

Name	Company	Immobilization level [RU]
Mouse mAB anti-FLAG M2 clone	Sigma cat# F3165	7,069
Mouse mAB anti-FLAG M2 clone ^a	Sigma cat# F1804	5,600
Rat mAB anti-DYKDDDDDK	Stratagene cat# 200473	5,684
Rat mAB anti-FLAG M2 6F7	Sigma cat# SAB4200071	4,203
Mouse Rho1d4 AB anti-C9	Flintbox	7,360
Immunopure Neutravidin	Thermo Fisher	9,000-13,000

^aAntibody was affinity purified.

C-terminally tagged cadherin captures and binding experiments were performed at 25°C in a running buffer composed of 150mM sodium chloride, 20mM Tris-Cl pH8.0, 3mM calcium chloride, 0.25mg/mL bovine serum albumin (Sigma) and 0.005% (v/v) Tween-20. In one experiment, cadherin-6-bio was captured over one flow cell and another was left with only immobilized NeutrAvidin which served as reference cell. In 10sec pulses cadherin-6-bio at a concentration of ~15µM was injected in 10sec pulses at a flow rate of 20µL/min until approximately 500RU were captured (Harrison et al., 2010a; Katsamba et al., 2009). The same approach was taken for cadherin-FLAG and -C9 captures and cadherin levels [RU] captured by antigen-antibody binding are shown in SPR traces in Figure 32a (FLAG) and 32b (C9) (Chapter 6).

2.2.7.2 Ligand thiol coupling

CYS-tagged proteins underwent a buffer change prior experiments as the proteins were kept in presence of 1mM TCEP. Zeba spin desalting columns (thermo fisher) were used by loading 30µL of protein-CYS onto a 10mM sodium acetate pH4.0 pre-equilibrated column. Spinning was performed according to the manufacturer's manual. Eluates were diluted ~10fold yielding final concentrations of 50µg/mL for N-cadherin-CYS and 300µg/mL for VE-cadherin-CYS and were tested in subsequent experiments for pre-concentration by ionic charge to the sensor chip surface (see Figure 33a, Chapter 6). For both proteins the highest binding response was achieved in sodium acetate pH4.0 buffer.

For covalent coupling of the thiol tagged proteins to the SPR sensor chip, carboxymethyl groups of the CM4 sensor chip were activated only in flow cells needed by injecting for 2min a mixture of 50mM NHS and 200mM EDC. In the next step reactive sulfur groups were introduced during a 4min pulse of 80mM PDEA pH8.5, which was freshly prepared immediately before the experiment by mixing 100µL of 120mM PDEA with 50µL 100mM sodium borate pH8.5. Desalted N- or VE-cadherin-CYS were injected to produce a binding response of 1570RU (60sec pulse) for N- and 4660 (12sec pulse, high concentration surface) and 1575 RU (20sec, 6sec, 7sec pulse with 50µg/mL diluted VE-cadherin-CYS, low concentration surface) for VE-cadherin. Remaining reactive disulfides were quenched by a 4min injection of 50mM L-cysteine (Sigma) in 1M sodium chloride, 100mM sodium acetate

pH4.0. Final immobilization levels were for N-cadherin-CYS 1542RU and for VE-cadherin-CYS 4643 and 1575RU. Immobilization profiles are shown in Figure 33b and 34b for N- and VE-cadherin, respectively. All immobilizations were performed at 25°C in HBS buffer and a flow rate of 20µL/min. To obtain a reference flow cell, the surface was treated exactly the same as described above, but CYS-tagged cadherin injection was omitted.

2.2.7.3 SPR binding experiments

For all binding experiments the same running buffer composed of 150mM sodium chloride, 20mM Tris-Cl pH8.0, 3mM calcium chloride, 0.25mg/mL bovine serum albumin (Sigma) and 0.005% (v/v) Tween-20 was used. Cadherins were immobilized on the sensor chip surface either by thiol coupling or affinity capture as described above. All analyte proteins were used at a concentration range of 40µM-78.1nM in a 2fold dilution series unless otherwise noted in the results section. Injections were performed in duplicates for 60sec at a flow rate of 50µL/min, which was followed by a 60sec dissociation phase and a buffer injection of 1min to minimize the contamination of the next sample by carryover. All binding experiments were conducted at 25°C except for a single experiment at 37°C with VE-cadherin.

A slight modification of the above method was used for the VE-cadherin kinetic experiment at 37°C and 25°C and the experiment with strand swap mutant W2A of N-cadherin at 25°C. These were performed at only one concentration of 40µM using a flow rate of 30µL/min. Running buffer composition, 60sec dissociation phase and buffer injections to minimize sample carryover remain the same.

2.3 Biochemical Methods

2.3.1 N-terminal sequencing

Purified mammalian proteins at a concentration of 1-2mg/mL were sent in solution to the Protein Core Facility (Columbia University, NY, USA) for N-terminal sequencing of the first five amino terminal residues using the Edman Sequencing technique.

2.3.2 Mass Spectrometry

For determination of absolute mass from proteins expressed and purified from mammalian cells including all posttranslational modifications, cadherins were brought in solution to the Protein Core Facility (Columbia University, NY, USA) at a concentration of 1-2mg/mL for mass spectrometry using MALDI-TOF (matrix-assisted laser desorption ionization time-of-flight). For determination of N-linked glycosylation sites, human VE-cadherin ectodomains produced in HEK 293 F cells and Endoglycosidase H treated ectodomains expressed in HEK 293 GNTI- cells were digested with trypsin in presence of EDTA and peptide masses determined using MALDI-TOF. N-linked glycosylation sites were determined by deviations in peptide mass between the two differently glycosylated proteins.

2.3.3 SDS-PAGE

10 μ g of protein were supplemented with 4x SDS loading buffer (Invitrogen) run on precast NuPAGE 4-12% BisTris Gel 1.00mmx15well (Invitrogen) in 1xMES buffer at 200V current using 4 μ L SDS SeeBlue(R) Plus prestained standard (Invitrogen).

2.3.3.1 Coomassie staining of proteins separated by SDS-PAGE

Protein bands were visualized by staining with Coomassie Brilliant Blue G-250 (0.2% (w/v) Coomassie, 7.5% (v/v) glacial acetic acid, 50% (v/v) ethanol) for 10minutes at 25°C and destained (0.75% (v/v) acetic acid, 10% ethanol) until gels were transparent and protein bands were clearly distinguishable from background. Gel images were taken by LAS 4000 Imaging system (Fujifilm).

2.3.3.2 Immunological detection of proteins separated by SDS-PAGE

Protein visualization using immunological methods was performed as follows. 13 μ l of conditioned media from transfected cells or 5 μ L of purified protein solution of 1mg/mL were separated using SDS-PAGE and proteins were transferred to nitrocellulose membranes activated for 20sec in 100% methanol (Fisher Scientific), by using a semi-dry blotting technique in Biorad transblot semi-dry transfer chambers according to the manufacturers manual. Whatman paper was equilibrated in Towbin buffer (25mM Tris-base, 192mM glycine, 10% (v/v) methanol) and a transfer-sandwich assembled as follows from bottom to top electrode: 2 whatman papers, activated nitrocellulose membrane, SDS-polyacrylamide gel, 2 whatman papers. Trapped air bubbles were gently removed by rolling over a 5mL glass pipette. Proteins were transferred from the gel to the membrane in 60minutes with current of 200mAmp. Following transfer, membranes were blocked either with TBS-Tween-20 0.025% and 5% milk when using 1:5,000 dilution of Tetra His Antibody (Qiagen) and secondary anti mouse-HRP coupled antibody (Peroxidase AffiniPure F(ab')₂ fragment donkey anti-mouse IgG (H+L) from Jackson ImmunoResearch) for detection of His tagged proteins or with 5% Bovine serum albumin, fraction V (Sigma, ~ 99% pure) for 1:2,000 dilution of Horse radish peroxidase conjugated NeutrAvidin (Thermo Scientific) for detection of biotinylated proteins. Blots were developed using ThermoFisher thing and developed by the LAS 4000 Imaging system (Fujifilm).

2.3.4 Removal of N-linked glycan with Endoglycosidase H

Mammalian proteins expressed in HEK 293 GNTI⁻ cells carry simplified N-linked glycans, which can be removed enzymatically by Endoglycosidase H to leave only a single mannose on Asn residues behind. N-linked glycosylation was removed from human and chicken VE-cadherin EC1-5 and EC3-5 expressed in these cells by using Endoglycosidase H (New England Biolabs) according to the company's instruction, with the exception, that the recommended reaction buffer was substituted with 150mM sodium chloride, 100mM HEPES pH7.0, 3mM calcium chloride and digest was carried out at 37°C. Subsequently, enzyme was removed by flowing proteins over size exclusion column Superdex S200 as described before.

2.3.5 Complex immunoprecipitation assays

For Co-immunoprecipitation (ip) experiments of homophilic and heterophilic cadherin complexes, experiments were conducted at 25°C using mixtures of purified, differently tagged cadherin EC1-2 fragments. For homophilic complex formation assays using N-cadherin-C9/N-cadherin-bio or VE-cadherin-C9/VE-cadherin-FLAG, 15µM of each protein were mixed, resulting in a total cadherin concentration of 30µM, which is well above the binding affinity of both proteins. The same concentration level of 15µM per tagged protein was also used for heterophilic Co-ip assays using mixtures of different cadherin subtypes. In negative controls the C9-tagged protein was replaced by immunoprecipitation buffer (150mM sodium chloride, 20mM Tris-Cl p8.0, 3mM calcium chloride, 1% Bovine serum albumin, 0.1% Tween-20) and in preliminary tests none of the proteins were found to nonspecifically bind to dynabeads protein G coated with antibody that were used in the full experiments for precipitation of the complex. In all cases, the mixtures of purified proteins were incubated with slow rotation at 25°C for 3h to allow equilibration between differently tagged cadherins. In the meantime, 40µL of dynabeads protein G (Invitrogen) were coated with Rho1d4 antibody prior each experiments at levels sufficient to provide equimolar binding sites for the total purified C9-tagged protein in the assay. Beads were washed with 3fold bead volume of ip buffer using a two sample dynabead magnet (Promega). Buffer was discarded and replaced with the Rho1d4 antibody solution. Beads were incubated rotating at 25°C for 15min to allow antibody immobilization and unbound antibody was then removed by three wash cycles with ip-buffer. The antibody coated beads were then added to the mixed protein solutions for precipitation of the C9-tagged cadherin along with any associated differently tagged cadherin. After 10min of incubation at 25°C on rotator, protein was removed, beads washed three times as described before, but this time with ice cold ip buffer. Finally, beads were resuspended in 1x SDS gel loading buffer (Invitrogen) and boiled at 98°C for 5min and immediately the precipitated proteins were separated by SDS PAGE. Proteins were detected either immunologically with anti FLAG antibody (affinity purified M₂mAB α-FLAG F1804, Sigma, see Table 2) and secondary anti mouse antibody or directly by Neutravidin-HRP, as described in Section 2.3.3.2 above.

Chapter 3:

Protein Production

3.1 Mammalian protein production in human embryonic kidney cells 293F and 293 GNTI

Previously published work showed that human VE-cadherin EC1-4 fragments formed hexamers to mediate adhesive binding (Hewat et al., 2007). Cryo EM data revealed that the hexamers are composed of two cell surface trimers which are formed by a *cis* interface located in EC4 (Section 1.8.3) and *trans* adhesion is mediated by EC1 domains between trimers on apposing cells. However, proteins used in these previously published studies did not include the membrane proximal domain EC5, and were produced in bacteria and purified from inclusion bodies, thus lacking post translational modifications like glycosylation. In order to study adhesive binding properties of VE-cadherin and investigate the proposed hexamer model in detail, we chose to work with soluble, native human and chicken VE-cadherin full ectodomains (residues Asp1-Asp542 for human and Asp1-Glu545 for chicken) expressed in mammalian cells to allow full post-translational modification. Each protein was expressed with a C-terminal hexa-histidine tag replacing the single transmembrane and cytoplasmic domains. Based on known characteristics of adhesive binding of other classical cadherins, we also wanted to test the importance of Trp2 and Trp4, key amino acids for type II cadherin homophilic binding, for VE-cadherin adhesive behavior. We therefore chose to introduce a double mutation, in which Trp2 and Trp4 side chains are both reduced to that of alanine into an additional human VE-cadherin EC1-5 construct (W2A W4A mutant). To address the biological relevance and biophysical behavior of the unique EC4-mediated *cis* interface suggested in the previously published studies of bacterially expressed VE-cadherin EC1-4 (Bibert et al., 2002; Hewat et al., 2007; Legrand et al., 2001), a further construct was prepared in which the N-terminal *trans* adhesive domains EC1-2 were omitted from human VE-cadherin ectodomains fragments to produce a fragment containing only membrane proximal domains EC3-5 (Ile204-Asp542).

In addition to VE-cadherin, ectodomains of wild type mouse E-cadherin (Section 2.1.1.1), an extensively studied, well characterized classical type I cadherin for which structural data is available (Harrison et al., 2010b), was used as reference protein in glycosylation studies (Section 3.2) and biophysical experiments described in Sections 4.2 and 4.7. We also conducted studies with monomeric W2A K14E mutants of E-cadherin (Harrison et al., 2010b), which are described in the Section 4.4 and 4.5.

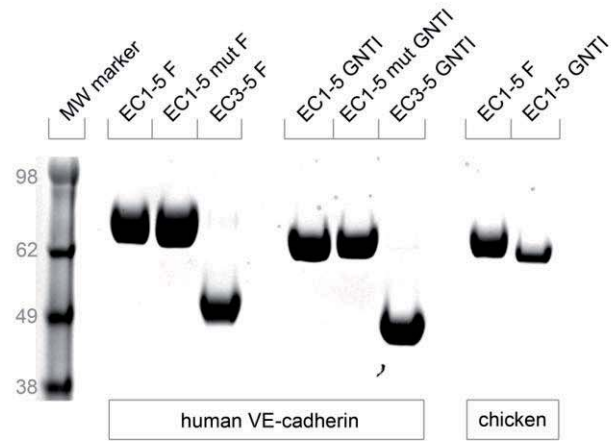


Figure 8: Mammalian expressed and purified human and chicken VE-cadherin at concentrations of 1mg/mL examined by SDS-PAGE and stained with coomassie brilliant blue. Human VE-cadherin EC1-5, strand swapping mutant EC1-5 and truncated fragment EC3-5 are shown on the left, chicken full ectodomains on the right. The set of human and chicken proteins produced in HEK 293F cells are approximately 5kDa larger than proteins expressed in HEK 293 GNTI(-) cells.

VE- and E-cadherin proteins were expressed in and secreted from two different mammalian cell lines: human embryonic kidney (HEK) 293F and 293 GNTI⁻ cells (Figure 8). The latter cell line lacks N-acetylglucosamine transferase I, an enzyme in the glycosylation pathway responsible for producing complex N-linked carbohydrate (Figure 9a). Proteins secreted from 293 GNTI⁻ cells have simple N-linked glycosylation in form of Man₅GlcNac₂ moieties that can be removed by endoglycosidases *in vitro*, producing proteins without N-linked sugars (Figure 9b). VE-cadherin proteins used in studies described here are therefore produced in either of three forms: glycosylated (from 293F cells), minimally glycosylated (from 293 GNTI⁻ cells) or, after treatment with Endoglycosidase H, without N-linked glycosylation. *In vivo*, cadherins are expressed with a prodomain preceding the first EC domain, which is removed on cell surfaces by furin proteases to produce mature cadherins (Koch et al., 2004). To ensure homogenous, mature N-termini and to avoid potentially inefficient removal of the prodomain during overexpression, we replaced the native signal sequence and prodomain of VE-cadherin with the signal sequence of CD33 (Section 2.1.1.1). All proteins were N-terminally sequenced to confirm native mature N-termini; which are listed in Table 3. The secreted proteins were purified from conditioned media as described in Section 2.1.1.5 and could be concentrated in glycosylated form to final concentrations of at least 10mg/mL. Minimally glycosylated and deglycosylated E-cadherin proteins also reached concentrations of at least 10mg/mL, but solubility of VE-cadherin was reduced to approximately 0.3mg/mL after removal of N-linked glycosylation. Solubility could not be improved significantly by increase or decrease of salt in the buffers, addition of 10% glycerol or by pH-change between pH8.0 and pH6.0. Concentrated proteins were examined by SDS poly acryl amid gel electrophoresis for purity and results show VE- and E-cadherin proteins used in this work are greater than 99% pure (Figure 8). Interestingly, VE-cadherin proteins have apparent molecular weights in SDS-PAGE that are approximately 10kDa higher than predicted molecular weights based on primary protein sequence, suggesting the presence of high levels of protein glycosylation. In contrast, E-cadherin proteins migrate at apparent molecular weights more similar to those predicted (Table 3).

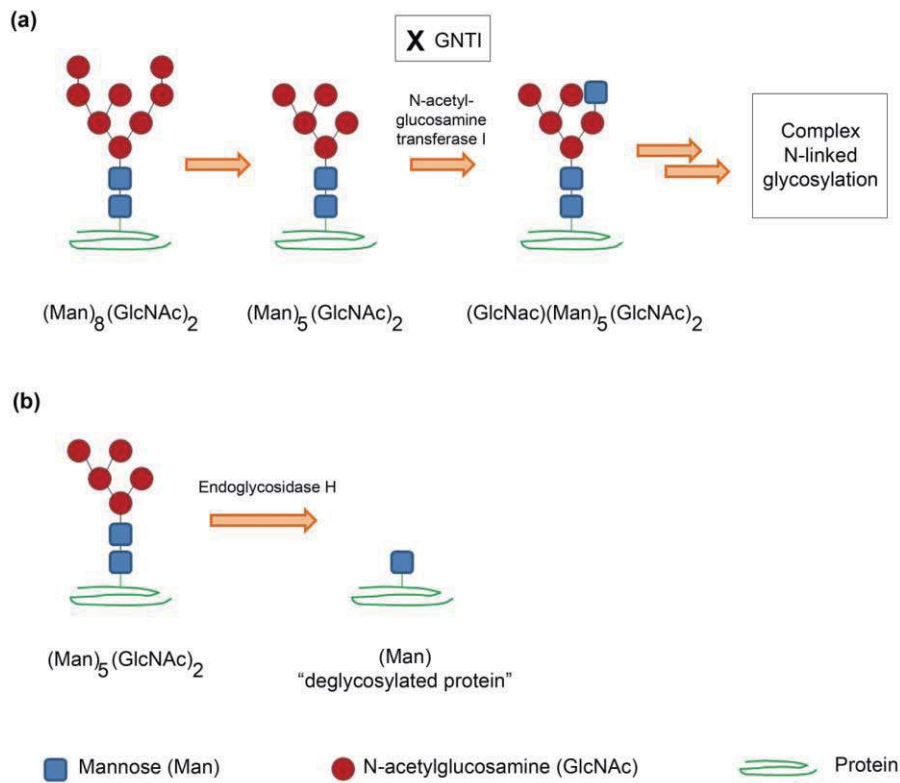


Figure 9: Schematic representation of alterations in N-linked glycosylation. (a) Complex N-linked glycosylation is added in the golgi apparatus of HEK 293 F cells. HEK 293 GNTI cells lack the enzyme N-acetylglucosamine transferase I (GNTI) which is responsible for mannose introduction as a requisite first step in the addition of complex N-linked carbohydrate. (b) (Man)₅(GlcNAc)₂ is a suitable substrate for Endoglycosidase H, which cleaves between the mannose sugars to remove all but the first mannose unit.

The human and chicken full VE-cadherin ectodomains and EC3-5 fragments described here were used to study the N-linked glycosylation pattern of VE-cadherin (Section 3.2) and for extensive biophysical experiments to investigate VE-cadherin mediated adhesion and to test the VE-cadherin hexamer model with native proteins (Chapter 4).

Table 3: Statistics of mammalian produced cadherins.

Protein	N-terminus	Predicted MW [Da]	293F MW [Da]
Chicken VE-cad EC1-5	DWIWN	62,088	71,591
Human VE-cad EC1-5	DWIWN	62,383	75,451
Human VE-cad EC3-5	INDNF	39,767	47,916
Human VE-cad EC1-5 W2AW4A	DAIAN	62,153	74,589
Mouse E-cad EC1-5	DWIVI	60,907	65,878
Mouse E-cad EC1-5 W2A K14E	DAIVI	60,084	65,069

3.2 VE-cadherin ectodomains are highly glycosylated

We found that mammalian expressed VE-cadherin proteins migrate with an apparent molecular weight in SDS PAGE approximately 10kDa higher than predictions based on primary sequence, indicating likely glycosylation (Figure 8 and Table 3, see above). Also, when comparing the migration of VE-cadherin proteins expressed in HEK 293F cells to those of minimally glycosylated proteins expressed in HEK 293 GNTI⁻ cells, we find that VE-cadherin proteins secreted by GNTI⁻ cells have significantly lower apparent molecular weights, suggesting the presence of complex N-linked glycans in the fully glycosylated protein (Lanes 1 and 2 in Figure 10). Removal of all N-linked sugars with Endoglycosidase H shifted the apparent molecular weights somewhat closer to the predicted molecular weights (Lane 3 in Figure 10). For comparison, E-cadherin, which migrates in SDS-PAGE closer to its predicted weight, was also included (Lanes 4, 5 and 6 in Figure 10). Endoglycosidase H treatment caused a small shift for E-cadherin consistent with the presence of N-linked glycans (Liwosz et al., 2006), Figure 9b). However, no significant difference in electrophoretic mobility was observed between fully and minimally glycosylated E-cadherin (Lanes 4-6 in Figure 10), suggesting that the N-linked glycans of E-cadherin are less complex than those of VE-cadherin.

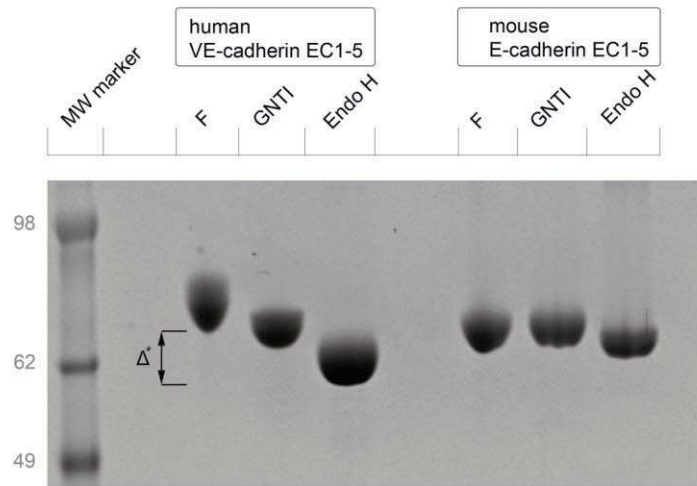


Figure 10: Mammalian expressed VE-cadherin carries substantial quantities of N-linked glycosylation in contrast to type I E-cadherin. In lanes 1, 2 and 3 is VE-cadherin EC1.5 and in lanes 4, 5 and 6 E-cadherin EC1-5 depicted. Lanes 1 and 5 show protein expressed in HEK 293 F cells (F). Lanes 2 and 5 show protein expressed in GNTI(-) cells (GNTI), which add only minimal N-linked glycan due to lack of N-acetyl glucosamine transferase I. Lanes 3 and 6 show VE- and E-cadherin, respectively, after treatment with Endoglycosidase H (Endo H) to remove N-linked carbohydrate. Note, that VE-cadherin apparent molecular weights differ substantially with approximately 13kDa depending on which cells expressed the protein, which suggests that this protein is highly glycosylated. In contrast, apparent molecular weights between E-cadherin expressed in 293F or GNTI (-) cells are closely similar and only a small shift can be observed after removal of N-linked glycan. Total mass of N- and O-linked glycan are summarized in Table XX. See text for further detail.

These findings led us to experimentally determine the precise molecular weight contributed by glycans for each protein by MALDI-TOF mass spectrometry analysis. First, fully glycosylated ectodomains of human and chicken VE-cadherin as well as mouse E-cadherin were analyzed, with comparison of experimentally determined masses with predicted molecular weights (Table 3). We determined a total glycan of 13,144Da for human VE-cadherin, 9,503Da for chicken VE-cadherin and 4,971Da for E-cadherin. Next, we wanted to elucidate the relative contributions of N- and O-linked glycosylation to the total glycan. Therefore VE-cadherin and E-cadherin, expressed in glycosylation deficient HEK 293 GNTI cells, were treated with Endoglycosidase H to specifically remove N-linked glycan, and we determined the molecular weight of protein without N-linked glycosylation by MALDI-TOF. Subtracting the molecular weight of the ‘deglycosylated’ protein from that of the fully glycosylated protein revealed the quantity of N-linked glycosylation (Table 4). O-glycosylation quantities could be calculated by subtraction of predicted molecular weight from the ‘deglycosylated’ weight. From this analysis we found that human VE-cadherin ectodomains carry 2,713Da of O-linked and 10,336Da of N-linked glycosylation and chicken VE-cadherin ectodomains 1,836Da of O-linked and 7,667Da of N-linked glycan. We repeated the experiment with truncated VE-cadherin EC3-5 and found that these three domains contribute 8,149Da (62%) to the total glycan, of which 6,570Da is N-linked and 1,579Da O-linked glycosylation. Using the same method as described above total glycan for E-cadherin was determined to be 4,971Da, composed of 1,793Da of O- and 3,178Da of N-linked sugar.

Table 4: Glycosylation quantities found on mammalian produced VE- and E-cadherin ectodomains.

Protein	Total glycan [Da]	N-linked glycan [Da]	O-linked glycan [Da]
Chicken VE-cad EC1-5	9,503	7,667	1,836
Human VE-cad EC1-5	13,144	10,336	2,713
Human VE-cad EC3-5	8,149	6,570	1,579
Mouse E-cad EC1-5	4,971	3,178	1,793

We also determined the locations of the N-linked glycosylation sites in VE-cadherin. Glycosylated and deglycosylated human VE-cadherin ectodomains were subjected to trypsin digest and the mass of the obtained peptides was determined by MALDI-TOF. Comparison of the two sets of peptides revealed five N-glycosylation sites: Asn14 and Asn64 in EC1, 62

Asn110 in EC2, Asn315 in EC3 and Asn395 in EC4. In EC5, the most membrane proximal domain, no glycosylation sites were found. O-glycosylation sites on VE-cadherin could not be determined, as the O-linked glycans have molecular weights too small to be detected reliably by our method.

To examine the positions of the N-linked glycosylation sites in regard of the whole ectodomain, we built a homology model of the ectodomain of human VE-cadherin using the Swissmodel server with C-cadherin (pdb-code: 1L3W) as template. Figure 11 shows the experimentally identified glycosylation sites mapped on to our homology model. Comparing glycosylation in VE-cadherin with that of E-cadherin determined from a recently published structure (Figure 11, (Harrison et al., 2010b) and from biochemical analyses (Liwosz et al., 2006) it is evident that several equivalent regions are glycosylated in both proteins (Figure 11-glycosylation). These are the concave face of EC3 and the concave face of EC4. However, at the sequence level, only one N-linked site is conserved between the two cadherins – Asn395 (VE-cadherin numbering) in EC4. Additionally, we included mouse type II cadherins -6, -8, -9, -10 and -11 in our analysis and, remarkably, we found that only the Asn395 consensus glycosylation site is also conserved in these cadherins.

Taken together, our results show that VE-cadherin ectodomains are highly glycosylated in comparison to type I E-cadherin and that approximately 62% of the N-linked glycosylation is located in domains EC3-4. Only one N-linked glycosylation site, which is located in EC4, is conserved within most classical cadherins. The importance of glycosylation for VE-cadherin function will be discussed in Section 4.8.

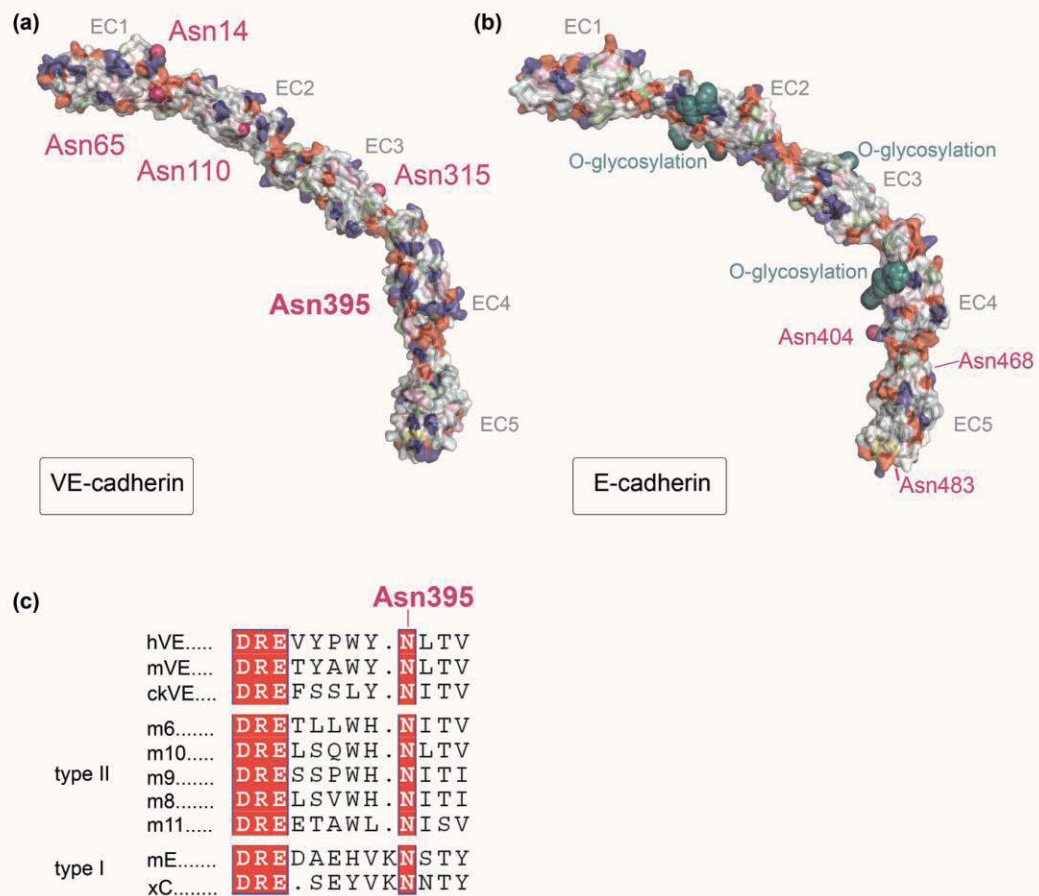


Figure 11: N-linked glycosylation sites in the VE-cadherin ectodomain. (a) The homology model of the VE-cadherin ectodomain is shown in molecular surface presentation colored by residues type: positively charged residues in blue, negatively charged in red, polar in light blue, semipolar in yellow, aromatic in rose and hydrophobic residues in grey. N-linked glycosylation sites were determined as described in the text and are depicted as magenta spheres on the ectodomain. (b) Molecular surface representation of the crystal structure of the E-cadherin ectodomain as representative for type I cadherins is shown with identical color code. N-linked glycosylation sites determined by Liwosj et al. (2006) are labelled as magenta spheres. Asn468 is located on the hidden side of EC5. Both E- and VE-cadherin share the N-linked glycosylation site found in domain EC4. O-glycosylation is demonstrated as teal colored spheres. Notably, E-cadherin carries O-linked glycosylation in closely similar regions, where N-linked glycosylation was found on VE-cadherin ectodomains. Highly similar glycosylation distribution is found in C- and N-cadherin (Harrison et al. 2010b). (c) Protein sequence alignments of VE-cadherin, with type I and II cadherins showing the conservation of the glycosylation site (N-x-S/T) at Asn395 in domain EC4. N-cadherin also has an N-linked glycosylation site in this area, which maps to the same region as those found in VE-, E- and C-cadherin, but is found to be shifted by three residues on sequence level.

3.3 Bacterial protein production in *Escherichia coli*

3.3.1 VE-cadherin protein fragments expressed in *E. coli*

To assess structural and biophysical features of VE-cadherin homophilic and heterophilic adhesive binding, we prepared adhesive fragments of human, chicken and mouse VE-cadherin spanning domains EC1-2. In addition, a single human domain EC1 and a fragment spanning only EC3-4 were prepared. These proteins were expressed at an average yield of 260µg per liter of Rosetta2 DE3 *E.coli* cells and could be purified by affinity chromatography, ion exchange and size exclusion chromatography as described in Section 2.1.2.3. All produced proteins by this method have native mature N-termini. To investigate the importance of strand swap binding for these fragments, two strand swap mutant proteins were also designed for mouse and chicken VE-cadherin domains EC1-2. In the first, indole side chains of Trp2 and Trp4 were both mutated to that of alanine (W2A W4A mutant), similar to the full length VE-cadherin ectodomain mutant described above. In the second, the N-terminus was extended by a single methionine for human and chicken VE-cadherin to disrupt a salt bridge involving the N-terminal amino group found to contribute to strand swap binding in other type I and II cadherins (Met-extension mutant). All wild-type and mutant fragments were successfully purified (Section 2.1.2.3) and could be concentrated to at least 7mg/mL. Figure 12 shows the result of SDS-poly acryl amide gel electrophoresis of the purified proteins, indicating all proteins to be greater than 99% pure. Molecular weights observed on the gel correspond to predicted molecular weights based on primary protein sequences.

Structural studies using these VE-cadherin adhesive fragments are described in Section 5.2-5.5 and biophysical characterization of the wild-type and mutant fragments are described in Section 5.1.

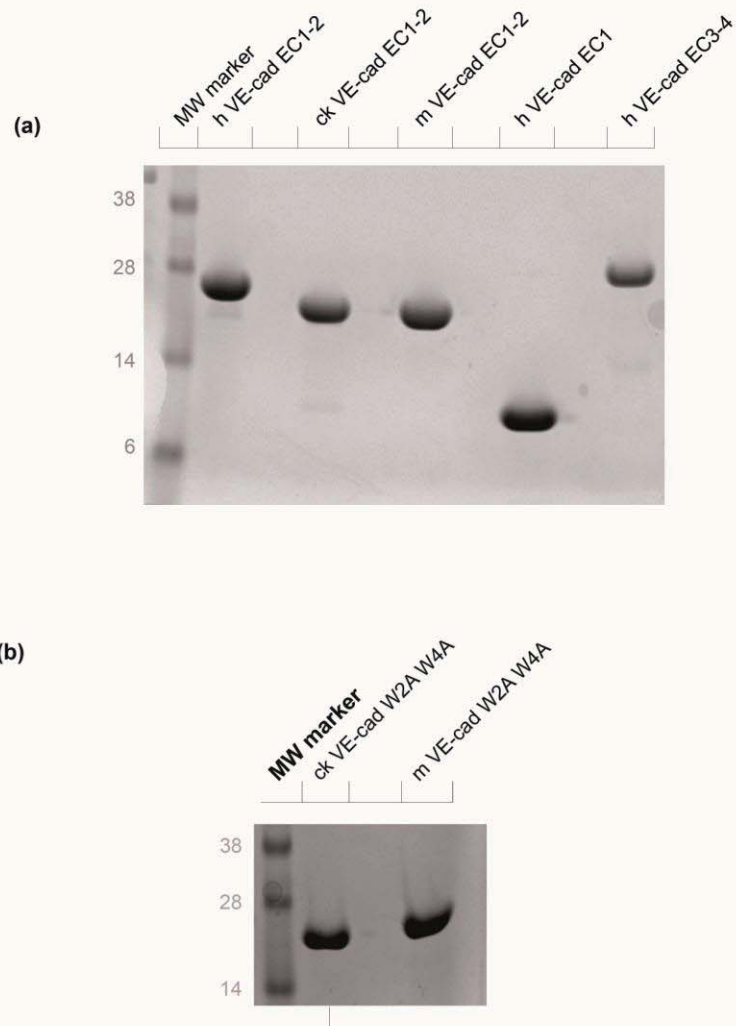


Figure 12: SDS-PAGE of purified VE-cadherin fragments of three different species. (a) Wild type human (h), chicken (ck) and mouse (m) VE-cadherin EC1-2 have an apparent molecular weight of ~27kDa. Human domain EC1 alone is of approximately 10kDa size and human VE-cadherin EC3-4 ~28kDa. (b) Purified strand swap mutants (W2A W4A) of chicken and mouse VE-cadherin, size of the protein is similar to wild type VE-cadherins (see panel (a)). All proteins are stable, no degradation due to proteolysis occurred. 13 μ g of each protein were loaded into each well. Cadherin abbreviated as 'cad'.

3.3.2 Classical cadherin fragments expressed in *E. coli*

In addition to VE-cadherin we also wanted to characterize the binding properties of other type I and type II cadherins and the outlier T-cadherin, as well as to perform homophilic and heterophilic binding experiments to elucidate specificity in cadherins.

A set of six wild type untagged type II cadherins was prepared (Section 2.1.2.3): mouse type II cadherins-6, -8, -9, -10, and 11 encompassing domains EC1-2 and additionally chicken cadherin-6b EC12. The EC1-2 fragment of cadherin-8 failed to dimerize and remained monomeric in gel filtration and equilibrium AUC experiments, therefore we extended the cadherin-8 construct by domain EC3. Cadherin-8 EC1-3 was able to form dimers in solution (see Section 5.1 for AUC results and Table 14 for K_D). All proteins were expressed in *E. coli* and purified as described above for VE-cadherin fragments. Protein expression levels of type II cadherins were at an average of approximately 260 $\mu\text{g/L}$ bacterial culture and all proteins yielded had mature native N-termini. Figure 13a shows that proteins were greater than 98% pure. All type II cadherins were soluble to concentrations of at least 7mg/mL and only cadherin-11 showed minimal signs of degradation by proteolysis in some preparations. SDS-PAGE of purified proteins is shown in Figure 13a.

We also prepared the type I cadherins E-cadherin and N-cadherin as well as the outlier T-cadherin as EC1-2 adhesive fragments from mouse using the same expression system. P-cadherin protein, produced in the same way, was kindly provided by Fabiana Bahna. Yield for all type I proteins was at an average of approximately 1.3mg/L bacterial culture and all had native mature N-termini. E- and P-cadherin were soluble to concentrations of at least 7mg/mL, but solubility of N-cadherin was limited to 1mg/mL.

The type I and type II cadherin fragments were used for analytical ultracentrifugation studies of homophilic binding (Sections 5.1 and 6.1) and for surface plasmon resonance studies of homophilic and heterophilic binding (Sections 6.2 and 6.3).

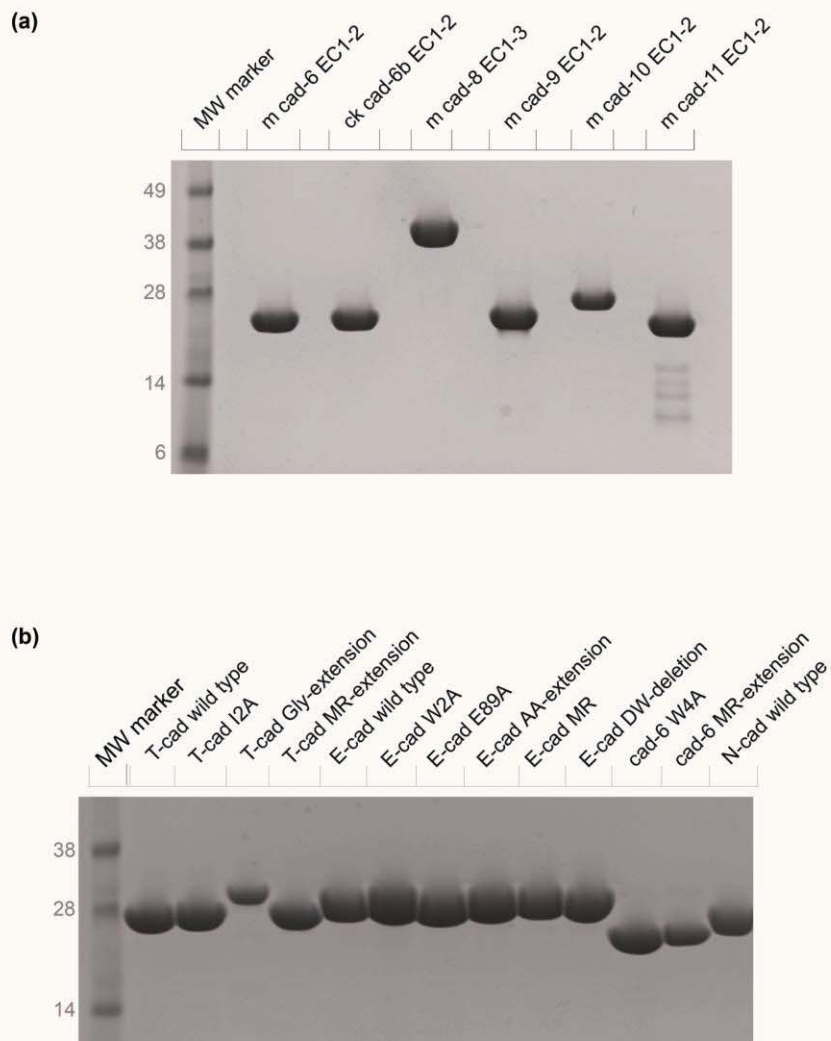


Figure 13: SDS PAGE of purified EC1-2 and EC1-3 fragments of classical type I and type II cadherin. (a) Wild type fragments of type II cadherins chicken (ck) 6b and mouse (m) cadherin-6, -9, -10 and -11 domains EC1-2 have apparent molecular weights of approximately 24kDa; mouse cadherin-8 EC1-3 ~42kDa. Note that cadherin -11 has evidence of minor degradation due to proteolysis. (b) Mouse two domain wild type and strand swapping mutants I2A, Gly-extension, MR-extension of T-cadherin (left four lanes) and type I E-cadherin wild type and strand swap mutants W2A, E89A, AA- extension, MR-extension, DW-deletion (middle lanes) and on the right type II cadherin-6 W4A and MR-extension mutant are shown. N-cadherin wild type in outmost right lane. Wild type cadherin-6 shown in panel (a). Atypical T-cadherin and classical type I cadherins have approximate apparent molecular weight of 28kDa, and cadherin-6 has lower apparent molecular weight of ~24kDa. 13µg of each protein loaded per well; 'cad' for cadherin.

Table 5: Summary of bacterial produced cadherins.

Protein	Description
VE-cadherin	
Human VE-cadherin EC1-2	Wild type
Chicken VE-cadherin EC1-2	Wild type
Mouse VE-cadherin EC1-2 ^a	Wild type
Human VE-cadherin EC1	Wild type
Human VE-cadherin EC3-4	Wild type
Chicken VE-cadherin EC1-2 W2A W4A	Strand swapping mutant
Mouse VE-cadherin EC1-2 W2A W4A	Strand swapping mutant
Chicken VE-cadherin EC1-2 Met-extension	Strand swapping mutant
Human VE-cadherin EC1-2 Met-extension	Strand swapping mutant
Type II cadherins	
	Wild type
Mouse cadherin-6 EC1-2 ^a	Wild type
Mouse cadherin-6 EC1-2 W4A	Strand swapping mutant
Chicken cadherin-6b EC1-2	Wild type
Mouse cadherin-8 EC1-2	Wild type
Mouse cadherin-8 EC1-3	Wild type
Mouse cadherin-9 EC1-2	Wild type
Mouse cadherin-10 EC1-2	Wild type
Mouse cadherin-11 EC1-2 ^a	Wild type
Type I cadherins	
Mouse E-cadherin EC1-2	Wild type
Mouse E-cadherin EC1-2 W2A	Strand swapping mutant
Mouse E-cadherin EC1-2 E89A	Strand swapping mutant
Mouse E-cadherin EC1-2 Ala-Ala-extension	Strand swapping mutant
Mouse E-cadherin EC1-2 Met-Arg-extension	Strand swapping mutant
Mouse E-cadherin EC1-2 Asp-Trp-deletion	Strand swapping mutant
Mouse N-cadherin EC1-2 ^a	Wild type
Mouse N-cadherin EC1-2 Ala-Ala-extension	Strand swapping mutant
Mouse P-cadherin EC1-2 ^b	Wild type
Mouse T-cadherin EC1-2 ^c	Wild type
Mouse T-cadherin EC1-2 I2A	Strand swapping mutant
Mouse T-cadherin EC1-2 Gly-extension	Strand swapping mutant
Mouse T-cadherin EC1-2 Met-Arg-extension	Strand swapping mutant

^a tagged versions of these proteins are listed separately in table 16;

^b P-cadherin protein: courtesy of Fabiana Bahna.

Type I and type II cadherin EC1-2 fragments containing mutations targeting the strand swap binding interface were prepared for binding experiments reported in Chapter 7. Mutations were introduced into E-, T- and cadherin-6 as described in Section 2.1.2.1. Strand swap mutant proteins W2A, E89A, Ala-Ala extension, Met-Arg-extension for E-cadherin; I2A, a Gly-extension and Met-Arg extension mutant for T-cadherin and W4A for cadherin-6 were expressed and purified in the same way as the corresponding wild type proteins. In a second cadherin-6 EC1-2 mutant we extended the N-terminus by residues Met and Arg, however, this protein was unstable in solution resulting in precipitation and was thus omitted from the final studies. See section 7.2 for full description of the mutations. Yield for all mutant proteins was similar to wild type and proteins were successfully purified and had native mature N-termini unless specifically altered. SDS-PAGE of all mentioned proteins shown in Figure 13b.

3.3.3 Preparation of C-terminally tagged classical cadherins

For SPR and co- immunoprecipitation (IP) experiments, proteins needed to be tethered to sensor chips or beads, respectively, by suitable engineered tags. Due to their adhesive mechanism cadherins require native N-termini and need to be positioned such that their adhesive N-termini are accessible for binding as they would be *in vivo* on cell membranes. Therefore, only C-terminal tags were tested. These were introduced into type I N-cadherin and type II cadherins-6, -11 and VE-cadherin, as is summarized in Table 6. Common tags like the biotinylated Avi-tag (GGGLNDIFEAQKIEWHE), FLAG- (DYKDDDDK) and C9- tag (GGGTETSQVAPA) were used for this purpose and additionally, we designed a novel tag consisting of a single cysteine after three glycine residues as spacer, which will be referred to as “CYS-tag” (GGGC). This tag allows the use of thiol coupling in order to covalently bind CYS-tagged proteins to surfaces. Approximate molecular weight was assessed by SDS-PAGE for the C-terminally tagged proteins and they were found to be pure (Figure 14a and b).

The entire set of Avi*bio-, FLAG-, C9- and CYS-tagged proteins was used in SPR experiments described in chapter 6 and reported in Ciatto et al. (2010) and Harrison et al. (2010) and the subset of C9-, FLAG- and biotinylated VE- and N-cadherin proteins were used in IP-experiments (Section 6.4).

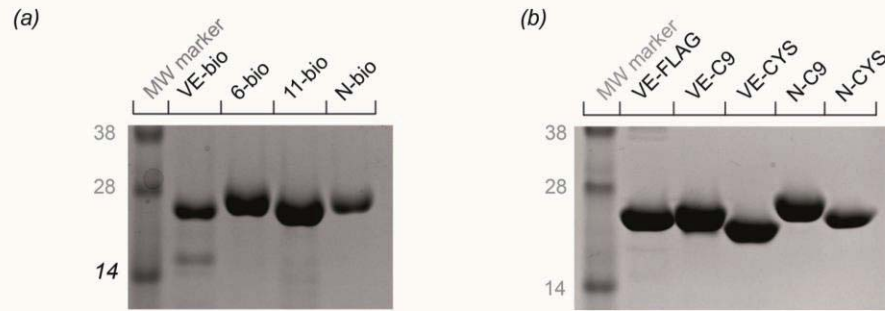


Figure 14: SDS-PAGE of two domain C-terminally tagged wild type cadherins. (a) Biotinylated mouse VE-cadherin, cadherin-6,-11 and N-cadherin. Biotinylation introduced by Avi-tag (see text for detail). Apparent molecular weight for all proteins similarly ~26kDa. Cadherin-11 has evidence of degradation by proteolysis similarly to that of the wild type protein. VE-cadherin-Avi*bio also shows a degradation product of approximately 15kDa weight. (b) Mouse VE-cadherin with C-terminal FLAG-tag, C9-tag and CYS-tag and N-cadherin with C9 and CYS-tag. Note that CYS-tagged proteins reflect the shorter tag by lower apparent molecular weights. 13 μ g of each protein loaded per lane.

Table 6: Summary of C-terminally tagged classical mouse cadherins and associated experiments.

Cadherin	Tag	Experiment	Section
VE-cadherin	Avi*bio	AUC	6.2
VE-cadherin	FLAG	AUC, SPR, IP	6.2, 6.4
VE-cadherin	C9	AUC, SPR, IP	6.2, 6.4
VE-cadherin	CYS	AUC, SPR	6.2
N-cadherin	Avi*bio	AUC, SPR, IP	6.2, 6.4
N-cadherin	C9	AUC, SPR, IP	6.2, 6.4
N-cadherin	CYS	AUC, SPR	6.2
Cadherin-6	Avi*bio	AUC, SPR	6.2 ^a
Cadherin-11	Avi*bio	AUC	6.2

^a This protein has been used successfully in SPR studies in Harrison *et al* (2010) and Katsamba and Carrol *et al* (2009)

Chapter 4:
Full length VE-cadherin ectodomains
form dimers similar to those of classical cadherins

4.1 Biophysical studies of the adhesive binding mechanism of native VE-cadherin ectodomains

Previously published binding studies conducted on bacterially produced VE-cadherin EC1-4 domain fragments (Bibert et al., 2002; Hewat et al., 2007; Legrand et al., 2001; Taveau et al., 2008) suggest a novel and unique binding mechanism for VE-cadherin in the context of the adhesive mechanism known for other classical cadherins. In this proposed model VE-cadherin molecules associate laterally on the same cell surface, via a strong *cis* interface involving domain EC4. Trimers then adhere to a second trimer extending from the opposing cell to assemble a hexamer via *trans* interactions in EC1 domains (Hewat et al., 2007). By contrast, for other classical type I and II cadherins it is known that they mediate adhesive binding by a 3D-domain swapping mechanism between opposing monomers, resulting in strand swapped adhesive cadherin dimers and not higher order multimers. For type I cadherins it was recently found using structural analysis, cryo EM of artificial adherens junctions and assays of cell adherens junction formation, that an additional *cis* interface is necessary in order to form junctions, involving the EC1 domain of one protomer and EC2 of the following protomer (Boggon et al., 2002; Harrison et al., 2010b). However, unlike the *cis* interactions determined for bacterially expressed VE-cadherin, these type I cadherin *cis* interactions are very weak and only *trans* dimerization can be detected in solution equilibrium AUC experiments.

We took an extensive biophysical approach to analyze the degree of multimerization and adhesive behavior of soluble VE-cadherin ectodomains and to test the unique binding model described above. Since we found that VE-cadherin ectodomains are substantially glycosylated (see previous section), we used only glycosylated full ectodomains of human and chicken VE-cadherin, in addition to the W2A W4A strand swap binding mutant and a truncated VE-cadherin EC3-5 that includes the putative trimerizing domain EC4. Their binding behavior was assessed by sedimentation equilibrium analytical ultracentrifugation, analytical size-exclusion chromatography, multi angle light scattering and liposome aggregation assays.

4.2 Biophysical behavior of VE-cadherin in sedimentation equilibrium analytical ultracentrifugation

Sedimentation equilibrium analytical ultracentrifugation (AUC) analysis was used to determine the oligomerization state of VE-cadherin. We chose to investigate the association behavior of full VE-cadherin ectodomains, expected to produce hexamers according to the

hexamer model of VE-cadherin binding; a strand swap mutant, which was expected to trimerize via domain EC4 and truncated VE-cadherin EC3-5, also expected to associate into trimers. Equilibrium AUC allows determination of an exact molecular mass independently from molecule shape and, in addition, data can be fit to dimeric or multimeric binding models to yield dissociation constants (K_D) in equilibrium as a measure of adhesive binding affinity. Interestingly, glycosylated wild type human and chicken VE-cadherin both were found to reach a monomer/dimer equilibrium in all conducted experiments without evidence for the presence of any higher order multimers (Figure 15 AUC). Human and chicken VE-cadherin ectodomains exhibit strong binding affinities with determined K_D values of $1.14\mu\text{M}$ and $1.03\mu\text{M}$, respectively, which are an order of magnitude stronger than K_D s determined previously for hexamer association. The residual values for fitting of the data to monomer-dimer equilibrium models were uniformly close to zero, indicating a reliable fit (Figure 15).

After we found that a remarkably strong affinity is associated with VE-cadherin homodimerization, we wished to compare it to published affinities of other cadherins. A binding affinity for C-cadherin EC1-5 and for two domain EC1-2 fragments of type I E- and N-cadherin were available. To test, if a comparison of affinities between mammalian expressed full length cadherins with those of bacterially produced two domain fragments is feasible, we performed an equilibrium AUC experiment with our mammalian expressed mouse E-cadherin EC1-5. A monomer/dimer equilibrium could be confirmed for this type I cadherin with a K_D of $109\mu\text{M}$ (Table 7) matching previously published K_D s for EC1-2 fragments of the same protein ($96.5\mu\text{M}$, (Harrison et al., 2010a; Katsamba et al., 2009)). This suggests that it is permissible to compare the determined VE-cadherin K_D to previously published K_D s for type I cadherins. Mouse N-cadherin EC1-2 associates with a K_D value of $25.8\mu\text{M}$ (Katsamba et al., 2009) and C-cadherin full ectodomains with a K_D of $64\mu\text{M}$ (Chappuis-Flament et al., 2001), which leads to a range of approximately $26\mu\text{M}$ - $109\mu\text{M}$ for type I cadherin affinities. Thus, VE-cadherin adhesive binding in the range of $1\mu\text{M}$ is considerably stronger than type I E-, N- and C-cadherin by between 20 to 110 fold.

To reduce or ablate strand swap mediated cadherin binding we mutated docking tryptophans Trp2 and Trp4 to alanine in VE-cadherin. The double mutant protein was subjected to equilibrium AUC experiments and we found that the dimerization affinity is diminished approximately 120 fold (Figure 15c).

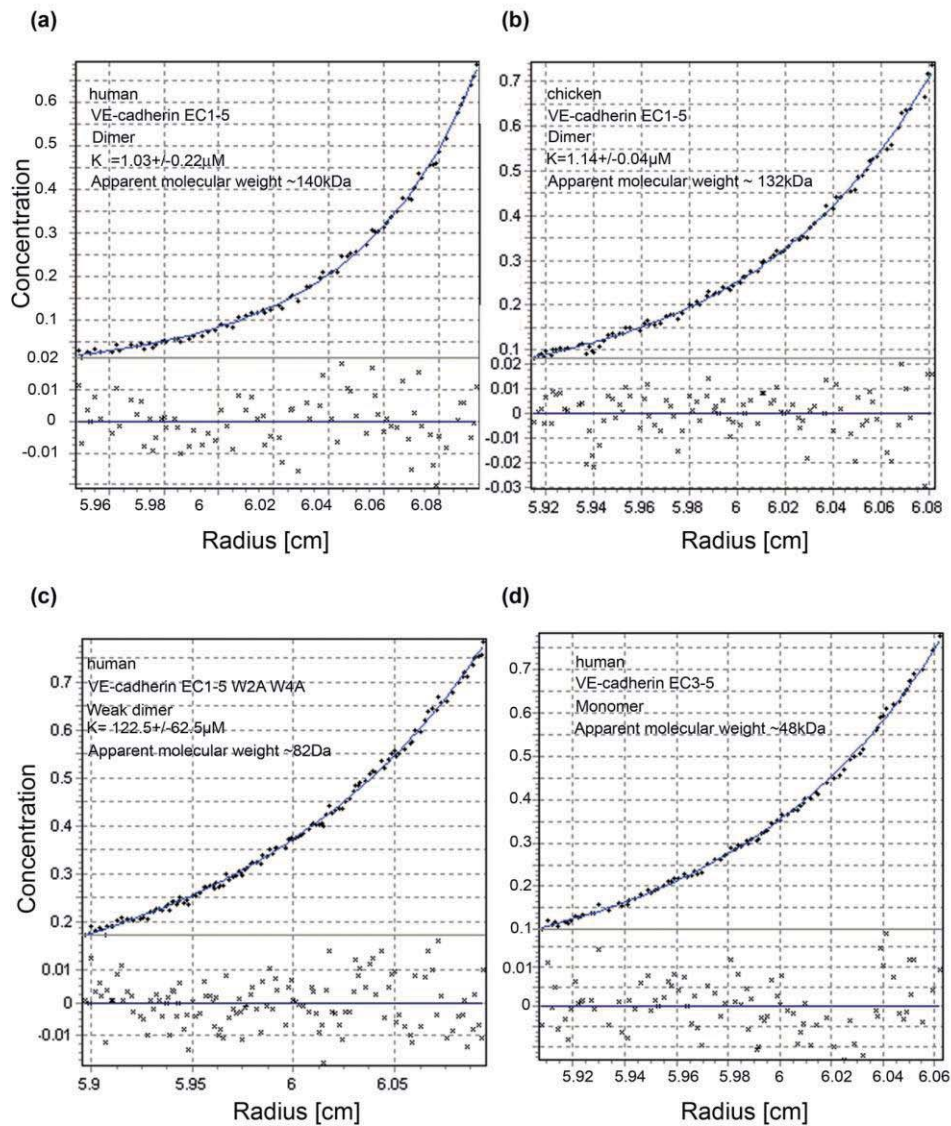


Figure 15: Sedimentation equilibrium analytical ultracentrifugation experiments showing similar profiles of different VE-cadherin ectodomains. (a) human and (b) chicken wild type ectodomains homodimerize, fitting for dimer model ($A+A=2A$) shown in blue, residuals shown at the bottom. No evidence for higher order multimers was found. (c) Strand swap mutant VE-cadherin W2A W4A exhibits weak dimerization behavior. AUC profile is fitted to a dimer model ($A+A=2A$). (d) human VE-cadherin EC3-5 is a monomer in solution with apparent molecular weight of approximately $\sim 48\text{kDa}$ which is identical to MALDI-TOF determined weight. Curve (blue) represents fitting to a monomeric model. See text for detailed description.

The dimerization of this mutant, though extremely weak compared to wild-type, may suggest a second binding mechanism deviating from strand swap binding, similar to behavior of strand swap mutants of other cadherins (Ciatto et al., 2010; Harrison et al., 2010a), discussed in Chapter 7). Because we could not exclude, that the observed binding might arise from EC4 triggered *cis* interactions, we also conducted AUC experiments with truncated glycosylated VE-cadherin EC3-5 to investigate the adhesive contribution of domain EC4. The results reveal that EC3-5 fragments fail to dimerize or trimerize and are monomers in solution (Figure 15d).

Table 7: Dissociation constants (K_D) for homodimerization of mammalian produced VE-cadherin and E-cadherin.

Protein	Description	K_D [μ M]
Human VE-cadherin EC1-5	Wild type	1.03±0.22
Chicken VE-cadherin EC1-5	Wild type	1.14±0.04
Mouse E-cadherin EC1-5	Wild type	109±9
Human VE-cadherin EC1-5 W2A W4A	Strand Swapping mutant	122.5±62.5
Human VE-cadherin EC3-5	Wild type	Monomer

Overall, AUC experiments show that VE-cadherin ectodomains do not associate into hexamers and instead, adopt a monomer/dimer equilibrium similar to other classical cadherins, though with a substantially higher affinity. VE-cadherin binding was markedly reduced when residues Trp2 and Trp4 important for strand swap mediated adhesion were mutated to alanines. In addition, no association of EC3-5 fragments could be observed in our experiments, supporting the assumption that VE-cadherin follows a classical cadherin 3D domain swapping mechanism. Thus, only domains EC1-2 of VE-cadherins appear to function directly in adhesion, indicating that the putative hexamer model may be artifactual.

4.3 Analytical size-exclusion chromatography

In a different approach to further biophysically study VE-cadherin binding behavior, we performed analytical size-exclusion experiments, which allow different molecular species to be resolved according to their hydrodynamic radii. Glycosylated VE-cadherin EC1-5 was

passed over an analytical Superose 6 column at a concentration of 7 μ M, which is well above its K_D for dimerization (see previous section). Figure 16 shows the elution profile of wild type VE-cadherin, which elutes in a two peak distribution: one major peak at higher molecular size and a minor peak at lower molecular size. The strand swap targeted mutant W2A W4A has an inverse peak distribution with a minimal high molecular size peak and a major lower molecular weight peak (Figure 16, green trace), which both overlap with those of the wild type protein (Figure 16, blue trace). These findings suggest in combination with our AUC data that the two observed peaks represent a dimer - monomer distribution and that the increased abundance of the lower molecular size peak in the mutant reflects its low affinity dimerization observed in AUC. In contrast, truncated VE-cadherin ectodomain fragments spanning domains EC3-5 eluted at substantially higher volume in only one peak (Figure 16, orange trace), suggesting it to be smaller than the five domain strand swap proteins and thus monomeric.

The size-exclusion chromatography data are in agreement with our AUC results. VE-cadherin full ectodomains form homodimers and monomers; strand swap ablated cadherin elutes predominantly as monomer and truncated VE-cadherin lacking adhesive domains EC1-2 resolve as only one species in size-exclusion experiments, which is most likely monomeric. No evidence of trimers or hexamers could be found in these experiments. Notably, VE-cadherin EC1-5 does not elute as one species representing a dynamic mixture of monomer and dimer in rapid exchange as seen for E-cadherin ((Harrison et al., 2010a): Figure 5c); it elutes as two distinct peaks, which might indicate in comparison to other classical cadherins a slowed kinetic rate as we have observed in studies of E-cadherin X-dimer interface mutants (Harrison et al., 2010a).

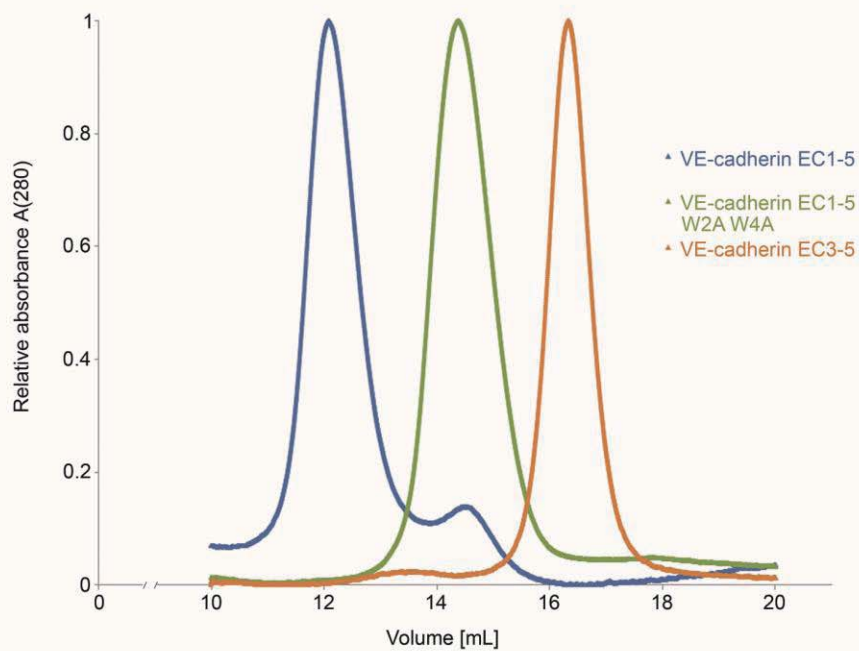


Figure 16: Comparison of elution profiles from analytical size-exclusion experiments with human VE-cadherin EC1-5 (blue), double tryptophan mutant W2A W4A (green) and EC3-5 (orange). Each protein injected at a concentration of $7\mu\text{M}$. VE-cadherin EC1-5 elutes in two peaks: a major peak of higher molecular size and a minor peak representing a smaller species. Only one peak is observed for the strand swap mutant W2A W4A. Notably, the peak overlaps with the lower molecular weight peak of the wild type elution profile (blue). The EC3-5 fragment elutes as single peak with the smallest molecular size of the three proteins. Void volume of the column is approximately 8mL.

4.4 Multi angle light scattering

Our biophysical data derived from AUC measurements and analytical size-exclusion chromatography strongly favor a monomer/dimer interaction for VE-cadherin. Analytical size exclusion chromatography as a technique separates different protein species dependent on molecule shape and size, hence it confirmed that VE-cadherin adheres as homodimer, but cannot provide accurate molecular masses to unambiguously identify each molecular species. Multi angle light scattering (MALS) preceded by an analytical size exclusion column allows the assessment of accurate masses of each chromatographic peak and provides additional information about dispersity found in the peak. We passed VE-cadherin EC1-5 and EC3-5 and additionally as a control monomeric mutant E-cadherin W2A K14E all expressed in HEK 293 GNTI cells over a TSKgel Super SW3000 size exclusion column at concentrations of 1mg/mL and their molecular mass and dispersity was determined by MALS (Table 8). All three proteins were monodisperse, with only one species of protein present in each chromatographic peak. E-cadherin EC1-5 W2A K14E mutant showed a mass of 66.5kDa corresponding to its monomeric weight. The mass of full length VE-cadherin EC1-5 was found to be 137 Da corresponding to the molecular weight of two cadherin molecules and the EC3-5 fragment revealed a mass of 52kDa showing it to be monomeric.

Table 8: Molecular weight for human VE-cadherin EC1-5 and EC3-5 and mouse E-cadherin W2A K14E determined by MALS.

Protein	MALS MW [Da]	Oligomerization state
Human VE-cad EC1-5	137,400	Dimer
Human VE-cad EC3-5	51,970	Monomer
Mouse E-cad EC1-5 W2A K14E	66,500	Monomer

The results of this experiment confirm data of AUC and analytical size-exclusion experiments supporting the conclusion that VE-cadherin forms adhesive dimers via adhesive domains EC1-2 and not higher order multimers.

4.5 Liposome aggregation assays with cadherin ectodomains

VE-cadherin is crucial for the angiogenesis and maintenance of the integrity of the vascular endothelium, enabling formation of cell-cell adhesion junctions between endothelial cells (Uehara, 2006) Introduction 1.8). To mimic VE-cadherin adhesion at endothelial junctions and to study VE-cadherin interactions in an assay system more closely approximating cellular conditions, we used cadherin coated liposomes serving as ‘artificial cells’. Liposomes 100nm diameter lipid bilayer micelles composed of a 9:1 ratio of DOPC and Nickel chelating DGS-NTA (Ni), were coated with cadherin ectodomains for aggregation experiments. C-terminally His-tagged VE- and E-cadherin ectodomains can be affinity bound to the liposome via their His-tag to Nickel (II) ions presented on the liposome surface (Figure 17, left panel). Thus, cadherins are oriented on liposomes with their N-terminal EC1 domains exposed. A lipid bilayer also has the beneficial property that it is not a static surface, but is instead fluid and allows proteins to diffuse similar to a cell membrane environment. Therefore, it is possible after initial cadherin-mediated contact between two liposomes has occurred for artificial junctions to assemble by recruitment of mobile cadherin on the surface. In the experiment, liposomes are incubated with the purified cadherin ectodomains to allow aggregation (Figure 17, right panel). Multi liposome aggregates scatter more light than a suspension of single liposomes, thus scattering of light can be used to monitor cadherin-mediated liposome aggregation. Optical density (OD) at a wavelength of 650nm was measured over a time period of 2,500 seconds in 20 second intervals after addition of cadherin proteins to liposomes to initiate aggregation.

First, we performed liposome aggregation assays with wild type E-cadherin ectodomains. E-cadherin has been shown in many independent assay systems to mediate adhesion, including in cryo EM studies of adherens junctions (Farquhar and Palade, 1963; Harrison et al., 2010b; McNutt and Weinstein, 1973) and cell-cell aggregation assays (Katsamba et al., 2009; Patel et al., 2006; Shimoyama et al., 2000). Therefore, we used E-cadherin to test that liposome aggregation assays are applicable to cadherin adhesion. Figure 17b (right panel) shows the result of E-cadherin mediated liposome aggregation, as a plot of monitored OD against aggregation time. It can be observed that optical density increased steadily suggesting occurrence of liposome aggregation, which reached a ‘steady state’ at approximately 750sec, indicating an equilibrium in which rates of liposome association and dissociation are balanced. To test if aggregation is a general property of liposomes in solution or if it is a property inherent only to cadherin coated liposomes, we monitored uncoated liposomes for

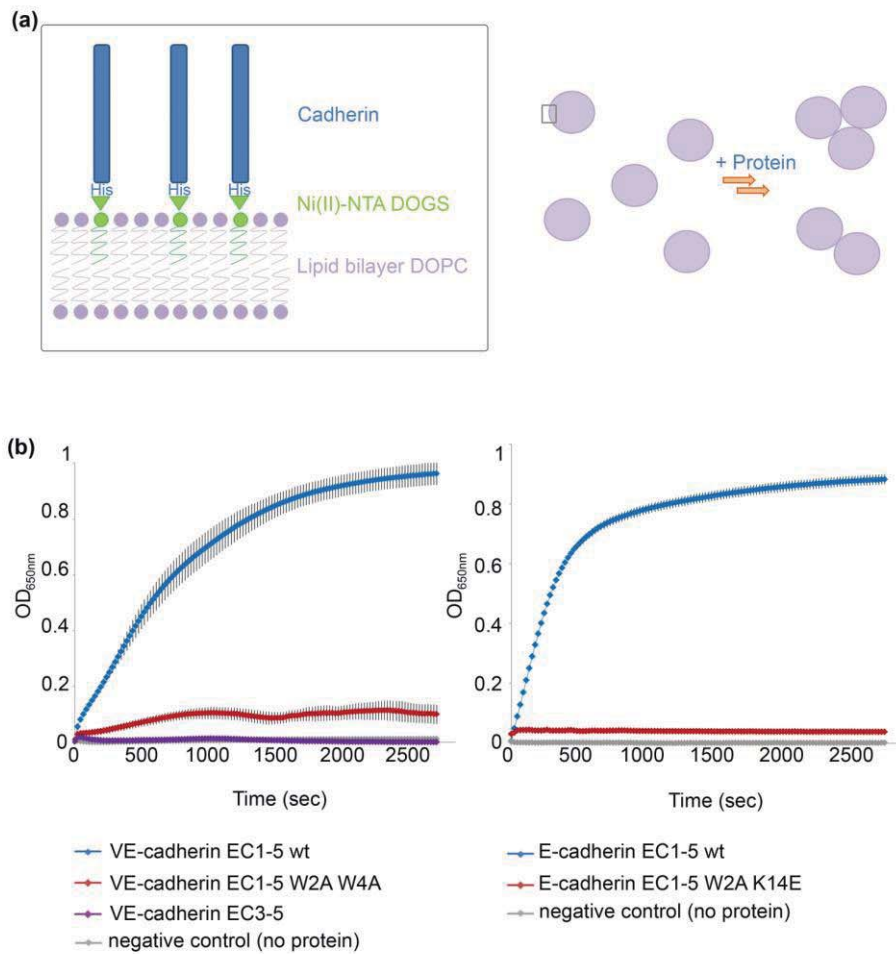


Figure 17: Liposome aggregation by VE- and E-cadherin ectodomains. (a) Schematic representation of cadherin ectodomain arrangement on solvent exposed liposome surface. Cadherins are depicted as blue rectangulars bound via their C-terminal hexa-histidine tag (His) by affinity to Nickel (II) NTA-lipids (green), which represent 10% of lipids in the lipid bilayer (inset). Liposomes are monodispers and after addition of protein, liposomes aggregate due to protein-protein interactions, which can be measured by absorbance at 650nm. (b) Liposome aggregation profiles of VE-cadherin (left panel) and E-cadherin (right panel). Wild type VE-cadherin and E-cadherin (blue trace) aggregate liposomes. Introduction of the strand swap mutation W2A W4A in VE-cadherin and the strand swap (W2A) and X dimer (K14E) mutation in E-cadherin strongly diminishes the ability to aggregate liposomes (red traces). VE-cadherin encompassing EC3-5 fails to aggregate liposomes (purple trace). Uncoated liposomes served as negative control (grey traces).

the same period of time. No notable change in optical density could be detected during the course of the experiment, which clearly shows that no spontaneous liposome aggregation occurs in the absence of cadherin (Figure 17b).

In addition, we tested the aggregation ability of E-cadherin mutants W2A K14E, in which mutations disrupt the strand swap and X-dimer interfaces leaving it with no adhesive properties (Harrison et al., 2010a). Liposomes were not aggregated by the double interface E-cadherin mutants (Figure 17b, right panel). Thus, aggregation observed in the liposome assays is induced by specific E-cadherin strand swap interactions mimicking the extracellular process of cell adhesion and making liposome aggregation suitable to measure *trans* homophilic binding of cadherins.

We tested wild type full ectodomains of human VE-cadherin EC1-5 in this assay system at concentrations of 8 μ M. VE-cadherin aggregated liposomes efficiently and the aggregation profile had a closely similar shape to that of type I E-cadherin-mediated aggregation with the difference that equilibrium was reached slightly later at around 1,500s (Figure 17b, left panel). We also conducted liposome aggregation experiments with the VE-cadherin strand swap mutant W2A W4A and the EC3-5 fragment. Introduction of the W2A W4A mutation into VE-cadherin reduced the ability to aggregate liposome significantly to only minimal levels in comparison to wild type VE-cadherin (Figure 17b, left panel, red trace). These data suggest that ablation strand swap mediated *trans* adhesion is sufficient to impair liposome aggregation, but at the same time, it was not able to abolish homophilic binding entirely. These findings closely agree with our AUC experiments showing residual binding for the VE-cadherin strand swap mutant (see above). In contrast, the double interface mutant of E-cadherin (W2A K14E) ablated E-cadherin adhesive binding almost entirely. Given that this mutant is designed to disrupt the strand swap binding and X-dimer interface in E-cadherin, one could assume, that the residual observed binding between strand swap VE-cadherin mutants might be due to X-dimer formation. To examine if VE-cadherins *trans* adhesive properties are localized solely in EC1-2 like in other type I and type II cadherins or if domains EC3-5 also participate in aggregation of liposomes, we tested truncated EC3-5 fragments. No change in absorbance could be detected during the course of the experiment above negative controls with liposomes alone (Figure 17b, left panel). Lack of any liposome aggregation indicates that VE-cadherin domains EC3-5 are not able to exhibit *trans* adhesive binding, which suggests in turn that residual binding observed for the VE-cadherin strand swap mutant

is likely to be mediated by EC1-2 domains, which could be speculated to arise from X-dimer formation (Harrison et al., 2010b).

The liposome experiments show that wild type VE-cadherin can efficiently aggregate liposomes by protein inherent *trans* adhesive properties similar to those of E-cadherin. Further, these data suggest, that for initial VE- and E-cadherin mediated adhesive contact between lipid membranes the cadherin transmembrane and cytoplasmic domains and intracellular interactions appear to be dispensable.

4.6 Electron microscopy studies of *in vitro* VE-cadherin junctions

Electron micrographs of VE-cadherin junctions in the endothelium show that apposed plasma membranes are almost parallel to each other with an enrichment of protein density in the intercellular space and that extracellular adhesion is stabilized by linking of the cytoplasmic cadherin domain via intracellular proteins to actin filaments that concentrate at junctional sites (Uehara, 2006). In addition, Taveau et al. (2008) published cryo EM micrographs of artificial junctions formed by bacterially produced VE-cadherin EC1-4. These liposomes showed a double layered midline in between liposomes, which could be fitted with the VE-cadherin hexamer proposed by Hewat et. Al. (2007). Our laboratory also performed cryo EM studies on E-cadherin coated liposomes revealing artificial junctions different from those published for VE-cadherin EC1-4, but similar to cryo EM data of adhesive junctions (Harrison et al., 2010b). Our studies of glycosylated, native full VE-cadherin ectodomains all suggest uniformly that VE-cadherin behaves as a classical cadherin dimer and does not associate into higher order multimers such as those reported for the bacterially produced EC1-4 fragments. Therefore, we wanted to visualize artificial adherens junctions assembled by our glycosylated VE-cadherin in order to compare these to junctions assembled by type I E-cadherin and to previously published data for bacterial VE-cadherin junction assembly.

Liposomes, which were also used in liposome aggregation assays described in Section 4.5, were coated with C-terminally tagged wild type human VE –cadherin and incubated until liposome aggregation reached equilibrium. Aggregates were then transferred to holey copper carbon EM grids and flash frozen for imaging by cryo-EM. Figure 18a shows an electron micrograph of two single liposomes in the hole of the carbon grid in which buffer and

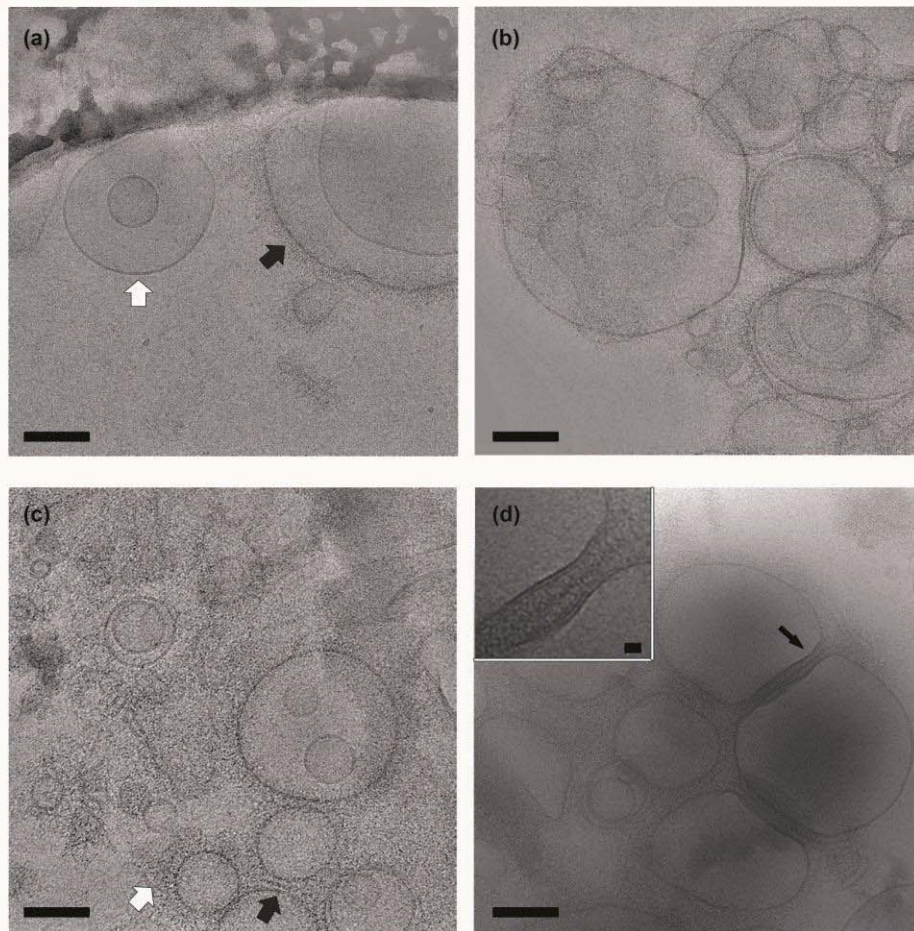


Figure 18: Electron micrographs of VE-cadherin on liposomes. (a) Depicted are two liposomes (arrows) located in one of the holes in the carbon grid. The lipid bilayer is represented as dark, crisp double line. One of the liposomes is surrounded by dark, fuzzy matter, indicating VE-cadherin coated surface (black arrow). The other has a smooth surface showing no evidence for protein (white arrow). (b) Representative electron micrograph of a 3D liposome aggregate. Several layers of liposomes are on top of each other. (c) A typical two dimensional aggregate of cadherin coated liposomes can be observed. VE-cadherin is found to be enriched at contact sites between liposomes (black arrow). Notably, VE-cadherin in solution is able to organize cadherins bound to the liposome surface (white arrow) similarly to cadherin organization found at contact sites between liposomes. (d) Two well defined artificial adherens junctions are depicted in this micrograph. Almost all cadherin on the liposome surface migrated into the junctions, in which the lipid bilayers of apposing liposomes are parallel to each other and approximately 4nm apart. A dark, protein-rich midline can be observed in both artificial junctions. The inset shows a 3fold amplification of the area indicated by the black arrow. See text for detailed description. Scale bar in all images represents 100nm; scale bar for inset represents 20nm.

liposomes become trapped keeping the sample hydrated during freezing. Liposomes are easily determined in micrographs by two crisp dark bands around their edge, which represent the two leaflets of the lipid bilayer. Most of the liposomes visualized in these experiments have a mantle of dense, grainy, unorganized matter evenly distributed over the surface, representing a coating of cadherin ectodomains (Figure 18a, black arrow). These are easily distinguishable from liposomes that are uncoated or minimally coated on which there is no diffuse density attached to the surface and only the lipid bilayer is seen (Figure 18a, white arrow).

Liposome aggregation occurs in three dimensions in suspension and the large clusters are then transferred to flat grids for freezing, so that mostly multilayered aggregates appear on the grids as Figure 18b shows.

This sample thickness complicates intensive study as there is too much electron density for clear visualization of individual contacts. Nonetheless, single layers of ‘two dimensional’ contact forming liposomes were observed, as are shown in Figure 18c and d. These liposomes show examples of artificial adherens junctions, which have the following features: a) straightening of the lipid bilayer at the contact site in comparison to usual rather rounded shape of liposomes, b) membranes of apposing liposomes involved in junction formation are approximately in parallel and c) enrichment of electron density between the apposing liposomes (Figure 18c, black arrow). Another phenomenon we frequently observed is shown in Figure 18 (white arrow) in which soluble, ‘free’ cadherin, which is not affinity bound to a liposome surface, binds to cadherin ectodomains coated on liposomes.

Figure 18d shows an electron micrograph of an aggregate of three liposomes including two large contact sites which show the characteristic features of artificial adherens junctions and an intermembrane spacing of approximately 40nm. It appears that almost all cadherin bound to the middle liposome was recruited into the junctions, as there is almost no apparent cadherin density on the liposome surface outside the junction. VE-cadherin ectodomains located in the junction appear to be densely concentrated and well ordered and show a thin, more electron-dense “midline”, which is parallel to and evenly spaced from both liposome lipid bilayers. The midline could be caused by overlapping cadherin EC1 domains in strand swap dimer conformation. The occurrence of a midline is reminiscent of junctions observed in desmosomes, which are assembled by desmocolins and desmogleins, also members of the cadherin superfamily (Al-Amoudi and Frangakis, 2008; He et al., 2003). Additionally, in EM

micrographs of E-cadherin coated liposomes which also formed artificial adherens junctions, a similar phenomenon was observed (Harrison et al., 2010b). Previously published cryo EM of liposome junctions assembled by bacterially produced VE-cadherin EC1-4 lacked this feature and had a more even distribution of density between apposed lipid layers, indicating a very different arrangement of cadherin from that observed here (Bibert et al., 2002; Taveau et al., 2008).

In conclusion, artificial adherens junctions assembled by mammalian produced VE-cadherin have a dense “midline”, which suggests an arrangement of ectodomains different from that in previously reported artificial junctions formed by bacterially produced proteins. Our native VE-cadherin artificial junctions are more similar to those of type I E-cadherin (Figure 6, (Harrison et al., 2010b)), supporting in conjunction with our biophysical studies described in Section 4.1-4.3 and 4.4, a classical cadherin binding mechanism for VE-cadherin involving *trans* adhesion between monomers, possibly accompanied by weak *cis* interactions. Notably, VE-cadherin ectodomains are capable to form adherens junction like structures in liposomes without transmembrane and intracellular domains. This suggests that initial intermembrane contact and junction assembly are triggered by VE-cadherin ectodomains alone, although for strengthening of initial junctions into mature adherens junctions *in vivo*, the transmembrane and cytoplasmic domains as well as intracellular binding partners may be necessary.

4.7 Atomic force microscopy imaging studies of VE-cadherin ectodomains

Experiments conducted with glycosylated VE-cadherin involving equilibrium AUC (Section 4.2), analytical size exclusion (Section 4.3), MALS (Section 4.4), liposome aggregation assays (Section 4.5) and cryo EM studies of artificial adherens junctions described in the previous section, strongly suggest, that natively glycosylated VE-cadherin adopts adhesive behavior closely similar to that of other classical cadherins. We wanted to obtain data on an atomic level about the binding mechanism of VE-cadherin, but attempts to obtain diffracting crystals of glycosylated full-length human and chicken VE-cadherin ectodomains were in vain. Therefore, we chose atomic force microscopy (AFM) imaging as an alternative to shed light on the overall arrangement of VE-cadherin dimers and those of E-cadherin for comparison. Full cadherin ectodomains were tethered to poly-L-lysine coated mica surfaces at a concentration of 2nM (8 μ M for E-cadherin) and subsequent imaging of the samples was performed in tapping mode (see Section 2.2.5).

Three dimensional AFM imaging data could be successfully derived from VE-cadherin and E-cadherin samples. Two distinct shapes reappeared in the resulting images for each protein (Figure 19a and b, c left and right panel). One of these can be described as a crescent shaped form and has a length of $28\pm 2\text{nm}$ for VE-cadherin and $21.1\pm 0.2\text{nm}$ for E-cadherin (19a, c left panel). They are markedly reminiscent in curvature and shape of individual protomers in the published C-cadherin crystal structure (Figure 19, (Boggon et al., 2002), pdb:1L3W). The other recurring form identified in the AFM images is approximately $48\pm 9\text{nm}$ long for VE- (Figure 19b) and $33.2\pm 1.3\text{nm}$ for E-cadherin (Figure 19c, right panel) and appears to be composed of two of the aforementioned crescent shaped forms, overlapped at their N-termini with a resulting increase in measured sample thickness in this region (Figure 19b and c, right panel). The overall arrangement of E- and VE-cadherin complexes is strikingly similar to the crystallographically determined C-cadherin strand swapped *trans* dimer and to dimers of E- and N-cadherin reported recently (Boggon et al., 2002; Harrison et al., 2010b). These data suggest that VE-cadherin ectodomains form complexes shaped like classical cadherin dimers, including a clear increase in sample thickness due to the overlap of EC1 domains, and a corresponding dimer length that is slightly less than twice the monomer length. Overall, it appears that the strand swap mechanism common to other classical cadherins also underlies VE-cadherin homophilic binding. Cigar shaped objects like the previously reported hexamers which were abundant and readily identifiable in cryo EM studies of bacterially produced VE-cadherin EC1-4 (Hewat et al., 2007) could not be identified in any of the AFM images.

Notably, in comparison to VE-cadherin images, in those for E-cadherin fewer dimeric forms and a larger number of single protomers were found. The different distinct distribution of monomers and dimers might arise due to a difference in affinities for homodimerization, because E-cadherin affinity is approximately two orders of magnitude lower than that of VE-cadherin. At the low protein concentrations required for the imaging experiments, VE-cadherin therefore has more dimers present than the lower affinity E-cadherin.

This data supports our previous findings that native full VE-cadherin ectodomains form strand swapped dimers like other classical cadherins, which appear similar in arrangement to those of type I cadherins.

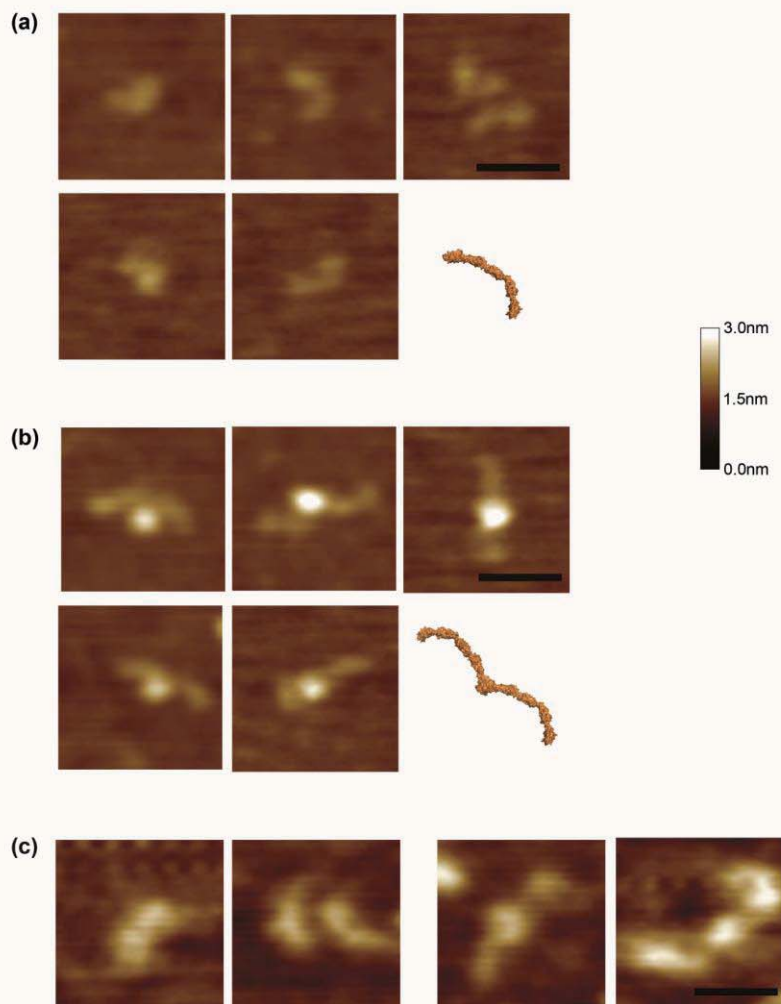


Figure 19: AFM-imaging of full ectodomains of VE-cadherin deposited on poly-L-lysine mica reveals monomer and dimer forms. (a) Recurring crescent forms with a length of approximately 28nm. These resemble C-cadherin ectodomain protomers in crystal structures (PDB 1L3W), depicted in orange surface representation (bottom right panel). (b) Other frequently observed form in which two crescent shaped forms overlap at their tips with an overall length of approximately 48nm. These forms are reminiscent of trans dimer structures observed in the crystal structure of C-cadherin (orange surface model, bottom right panel). Scale bar for all images is 35nm. (c) AFM-images of E-cadherin deposited on poly-L-lysine mica. Left two panels show E-cadherin protomers alone. In the right panel are E-cadherin forms depicted, which appear as protomers with overlapping N-termini, suggesting dimers. Both shapes are closely similar to those observed for VE-cadherin. Scale bar is 20nm. Color scale indicates sample thickness above the mica surface for all images.

4.8 VE-cadherin EC4 domain enables multimerization only when glycosylation is absent

Despite previously published evidence for a hexamer as the minimal adhesive unit, which was found for bacterially produced VE-cadherin EC1-4 fragments (Bibert et al., 2002; Hewat et al., 2007; Legrand et al., 2001), native, glycosylated VE-cadherin behaved as a classical cadherin dimer in all of our biophysical experiments (see Sections 4.2-4.7). Additionally, VE-cadherin exhibited behavior similar to that of type I E-cadherin in liposome aggregation assays (Section 4.5), cryo EM studies of artificial adherens junctions (Section 4.6) and shares the overall dimer configuration with those of type I cadherins, as AFM imaging experiments revealed (see previous section). These findings question the biological relevance of the putative hexamer model for VE-cadherin mediated homophilic adhesion involving a strong *cis* trimer interface located in EC4.

Between the published work in which hexamers are observed (Bibert et al., 2002; Hewat et al., 2007; Legrand et al., 2001) and our own studies, two striking differences in the protein used are evident. The differences are the presence glycosylation, which is present in our proteins but absent from the bacterially expressed proteins and the inclusion of domain EC5, which is again present only in our constructs. To investigate what effect glycosylation and domain EC5 have on VE-cadherin adhesive behavior, we initially produced a truncated VE-cadherin EC3-4 fragment in bacteria lacking both glycosylation and domain EC5, in addition to lacking the N-terminal adhesive domains EC1-2 such that association of the EC3-4 domains could be specifically studied.

First, we tested the bacterially produced human VE-cadherin EC3-4 fragments in equilibrium AUC experiments. Surprisingly, we found it to behave as a strong dimer with a K_D of $1.93 \pm 0.26 \mu\text{M}$, which is approximately in the same range as the described K_{DS} for full length VE-cadherin ectodomains (Table 7). Additionally, in some of these experiments, EC3-4 domains associated via an isodemic mechanism, in which the dissociation constants for every addition of monomer are considered the same, which leads to multimerization. Although curves could not be fitted to an explicit trimer model, the data suggest that higher order complexes were formed, which is possibly triggered by non-specific hydrophobic protein interactions (Weis et al., 1991). These data are in direct contrast to the biophysical evaluation of mammalian produced glycosylated VE-cadherin EC3-5 proteins, which did not associate and consistently remained monomeric in all experiments (Section 4.2-4.5).

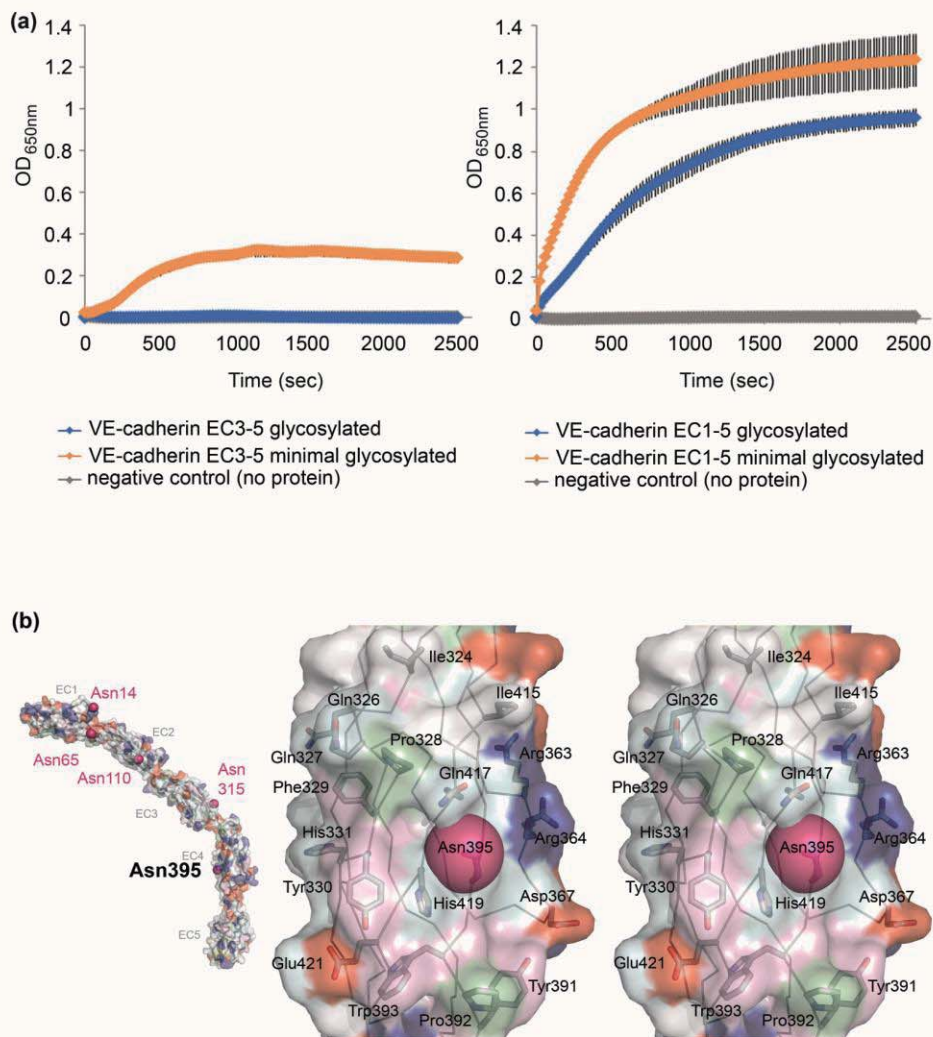


Figure 20: VE-cadherin behaves differently with and without complex N-linked glycosylation. (a) Liposome aggregation assays conducted with VE-cadherin EC3-5 fragments (left panel) and full length ectodomains (right panel). Domains EC3-5 with complex glycosylation fail to aggregate liposomes (blue trace). Identical protein fragments with reduced N-linked glycosylation due to expression in glycosylation deficient HEK 293 GNTI (-) cells are able to aggregate liposomes (orange trace). VE-cadherin EC1-5 aggregates liposomes (blue trace, right panel). When N-linked glycosylation is reduced, aggregation of liposomes is enhanced above wild type protein. (b) Conserved glycosylation site Asn395 in domain EC4 as trigger for artifactual protein-protein interactions. Homology model of VE-cadherin EC1-5 (left) with sugar sites depicted as magenta spheres. Close up stereo image of domain EC4 reveals that N-linked glycosylation site Asn395 is located within a region with hydrophobic and aromatic surface residues. Residue side chains with solvent exposed surface area greater than 20% are shown as sticks. Surface is colored as described in Figure 11.

The results suggested that high affinity multimeric association of the bacterial protein might be directly due to absence of glycosylation in EC4, or to absence of the EC5 domain. To test this hypothesis, we studied association behavior of a human VE-cadherin EC3-5 fragment produced in glycosylation deficient HEK 293 GNTI cells (Section 3.1) in equilibrium AUC experiments. Results showed that, unlike equivalent fully glycosylated fragments, minimally glycosylated EC3-5 proteins formed isodesmic aggregates or weak dimers with K_D values in the range of $221\mu\text{M}$, which is closely similar to the behavior of the bacterial EC3-4 fragment (Table 9). When N-glycosylation was fully removed from the protein by treatment with Endoglycosidase H, we obtained similar results as for the minimally glycosylated protein. Also, we found that this association happens independently from the presence of calcium (II) ions (not shown). The lower affinity in comparison to that found for bacterially expressed EC3-4 fragments might be due to the presence of O-glycosylation or to the presence of the EC5 domain, which had to be included in the mammalian constructs due to lack of expression in EC3-4 trials. Nonetheless, the experiments establish a clear role for N-linked glycosylation in preventing non-specific aggregation of EC3-4 domains. We wanted to identify if the non-specific interaction in minimally glycosylated proteins is specific to *cis* interactions or if these proteins can also mediate *trans* adhesion in liposome aggregation assays. Natively glycosylated EC3-5 fragments failed to aggregate liposomes as described in Section 4.5. When glycosylation was only minimal, EC3-5 fragments gained the ability to aggregate liposomes (Figure 20a, left panel). This suggested that lack of complex glycosylation leads to non-specific protein associations in *cis* or *trans*.

In liposome aggregation assays using full length ectodomains, minimally glycosylated VE-cadherin EC1-5 behaves similar to the glycosylated protein, with the exception that equilibrium is reached in shorter time and the degree of aggregation appears to be higher (Figure 20a, right panel). In addition, we conducted equilibrium AUC experiments, which showed that minimally glycosylated or deglycosylated VE-cadherin EC1-5 formed isodesmic aggregates in presence or absence of calcium (II) ions with reproducible isodesmic $K_{D(i)}$ of approximately $7.8\mu\text{M}$ and $3.4\mu\text{M}$, respectively. Despite the fact that cadherin homophilic interactions are calcium dependent (Harrison et al., 2010b; Takeichi, 1991), isodesmic aggregation was found to be independent from calcium, which strongly suggests the observed interactions to be artifactual. Interestingly, the ideal number of protomers in isodesmic polymerizing systems is $n=6$ (Frieden and Goddette, 1983), coinciding with the number of protomers in bacterially produced VE-cadherin multimers detected previously (Hewat et al.,

2007). When N-linked glycosylation was fully removed from VE-cadherin EC1-5 by Endoglycosidase H the protein became unstable and prone to aggregate, resulting in heavy precipitation and precluding testing in functional assays.

Table 10: Different glycosylation pattern of human VE-cadherin protein fragments results in different behavior in equilibrium AUC experiments.

Protein	Glycosylation	Isodesmic behavior	
		observed?	Dimerization K_D [μ M]
VE-cadherin EC3-4	None (produced in bacteria)	Yes	1.93±0.26
VE-cadherin EC3-5	Native	No	NA ^a
VE-cadherin EC3-5	Minimal	Yes	178±43
VE-cadherin EC3-5	Deglycosylated	Yes	299
VE-cadherin EC1-5	Native	No	1.03±0.22
VE-cadherin EC1-5	Minimal	Yes	65±19 ^b
VE-cadherin EC1-5	Deglycosylated	Yes	NA ^c

^a Protein is found to be monomeric; see Section 4.2 for detail.

^b Affinity value has a high error due to protein aggregation and precipitation during the experiment.

^c Deglycosylated VE-cadherin EC1-5 could only be fitted to an isodesmic model, not to an equilibrium dimer model. Heavy precipitation due to aggregation occurred during experiments.

How does glycosylation affect association of EC3-4 domains? Our findings in concert with the fact that the *cis* interface found in putative hexameric structures is located in domain EC4, prompted us to look more closely at the N-linked glycosylation site Asn395 located in this domain, (Figure 20b). This site is conserved within most of the type I and II cadherins as described in Section 3.2. A close up view of the region of domain EC4 in which the glycan is positioned was generated based on the human VE-cadherin homology model (Figure 20b). The N-linked site appears to be nested in an environment of predominantly non-charged and hydrophobic surface residues, which an attached sugar moiety would shield from non specific contact (Figure 20b). Thus, this area might be responsible for the unspecific interactions prompting the observed multimers in VE-cadherin fragments without glycosylation.

Overall, data derived from different biophysical studies involving full length and truncated VE-cadherin fragments in various glycosylation states, suggest strongly that the trimeric *cis* association triggered by EC4 that forms the basis for hexamer formation previously reported in bacterially produced VE-cadherin EC1-4 fragments represent an artifact due to lack of glycosylation. Removal of N-linked glycosylation appears to expose protein regions which are normally shielded by sugar moieties in the native protein, allowing non-specific and non-biologically relevant interactions which may result in artifactual multimers. These data support the hypothesis that domain EC4 is only able to form higher order multimers when glycosylation is absent.

Chapter 5:
Structure of the homophilic binding interface
of a VE-cadherin EC1-2 adhesive fragment

5.1 EC1-2 domains are responsible for strand swap mediated homodimerization

We showed in biophysical experiments described in sections 4.1-4.8 that full length VE-cadherin EC1-5 homodimerizes, whereas truncated EC3-5 domain fragments lack this ability and do not associate. These data suggest that domains EC1 and 2 are crucial for VE-cadherin to mediate *trans* adhesive binding. This is in agreement with published data from crystal structures (Boggon et al., 2002; Patel et al., 2006), biophysical experiments such as equilibrium AUC (Harrison et al., 2010a; Katsamba et al., 2009), cell-cell adhesion and domain shuffling experiments (Patel et al., 2006) showing that the *trans*-adhesive properties of all typical classical cadherins, map to N-terminal domains EC1-2 (Harrison et al., 2010a; Shan et al., 2004). The strand swapped mature adhesive interface itself involves residues in EC1 and in particular residue Trp2 for type I cadherins or Trp2 and Trp4 for type II cadherins (Patel et al., 2006; Shapiro et al., 1995). Further studies identified the X-dimer interface as a binding intermediate in E-cadherin and cadherin-6 adhesion and revealed, that EC1 and 2 are both required for this interface and for proper adhesive function, especially EC1 and EC2 residues in and around the Ca²⁺ binding interdomain linker region (Ciatto et al., 2010; Harrison et al., 2010a) and Chapter 7). The detailed binding mechanism for VE-cadherin mediated adhesion has not been determined at the atomic level, but previous antibody binding studies targeting the A strand containing residues Trp2 and Trp4 (May et al., 2005) and our experiments with full length ectodomains and truncated VE-cadherin fragments (Section 4.1-4.5, 4.8) strongly suggest that VE-cadherin employs a similar binding mode to other classical cadherins and domains EC1-2 are crucial for adhesion.

To test if VE-cadherin EC1-2 domains are also sufficient for full *trans* binding activity, human, chicken and mouse VE-cadherin fragments spanning putative adhesive domains EC1-2 were produced in bacteria as described in Section 2.1.2.3. The multimerization behavior was analyzed by equilibrium analytical ultracentrifugation and we found, that all three VE-cadherin formed dimers in solution which is in agreement with results we obtained for full length human and chicken ectodomains (Table 7). The K_{DS} for dimerization were determined to be 1.63μM for chicken, 2.22μM for mouse and 4.38μM for human VE-cadherin (Table 10), values in the same range to the corresponding full length proteins (Table 7), suggesting EC1-2 domains are sufficient for full activity and that absence of any glycosylation in EC1-2 does not have any influence on adhesive binding and affinities of two domain fragments. This is in contrast to full length proteins, which are strongly dependent on native glycosylation in

domains EC3-5 (See Section 4.8). These data suggest that EC1-2 domain proteins are appropriate for studies focused on the VE-cadherin binding mechanism.

Table 10: Dissociation constants (K_D) for homodimerization of VE-cadherin EC1 and EC1-2 fragments.

Protein	Description	K_D [μ M]
h VE-cadherin EC1-2	Wild type	4.38±1.2
m VE-cadherin EC1-2	Wild type	2.22±0.11
ck VE-cadherin EC1-2	Wild type	1.63±0.19
h VE-cadherin EC1	Wild type	NA ^a
m VE-cadherin EC1-2 W2A W4A	Strand swapping mutant	NA ^a
ck VE-cadherin EC1-2 W2A W4A	Strand swapping mutant	NA ^a
h VE-cadherin EC1-2 Met-extension	Strand swapping mutant	231±78 ^b
m VE-cadherin EC1-2 Met-extension	Strand swapping mutant	70±100 ^b

^a Protein is found to be monomeric in equilibrium AUC experiments.

^b Due to instability of mutant proteins heavy precipitation occurred during the experiments resulting in errors.

Classical cadherins bind by exchanging, or “swapping”, N-terminal A*-strands with each other to form strand swapped dimers, in which either Trp2 for type I cadherins or Trp2 and additionally Trp4 for type II cadherins are docked into a hydrophobic pocket in the partner EC1 domain. The adhesive properties of type I and type II cadherins are impaired and homodimerization involving the strand swap mechanism is prevented when indole side chains of tryptophan residues are mutated those of alanine (Harrison et al., 2010b; Kitagawa et al., 2000; May et al., 2005; Tamura et al., 1998). We wanted to test if Trp2 and Trp4 in VE-cadherin are needed for adhesive binding of our EC1-2 fragments, so Trp2 and Trp4 in human, mouse and chicken VE-cadherin were mutated to alanines and proteins used in equilibrium AUC experiments. Human mutant proteins had very low expression levels and could not be purified in sufficient amounts for AUC experiments. Data for mouse and chicken mutant VE-cadherin revealed that the mutant proteins fail to dimerize and remain monomeric after introduction of the strand swap mutation W2A W4A (Table 10). Human and mouse VE-cadherin mutants, in which the N-terminus is extended by a single methionine, showed

reduced adhesive behavior (Table 10) These data strongly support the idea that VE-cadherin utilizes the strand swap mechanism common to classical cadherins.

For E-cadherin and cadherin-6 it can be demonstrated, that after ablation of strand swap binding, some weak residual binding remains, which can be attributed to a different interface referred to as the X dimer, involving regions of both EC1 and EC2 (Chapter 7, Harrison 2010). VE-cadherin EC1-2 W2A W4A mutants did not show residual binding within AUC detection limits ($\sim 1\text{mM } K_D$). Thus, we removed the entire domain EC2 and expressed domain EC1 alone for equilibrium AUC experiments. Results showed that VE-cadherin EC1 domain cannot homodimerize and remained monomeric in solution, suggesting that VE-cadherin also requires EC2 and therefore possibly an X dimer intermediate.

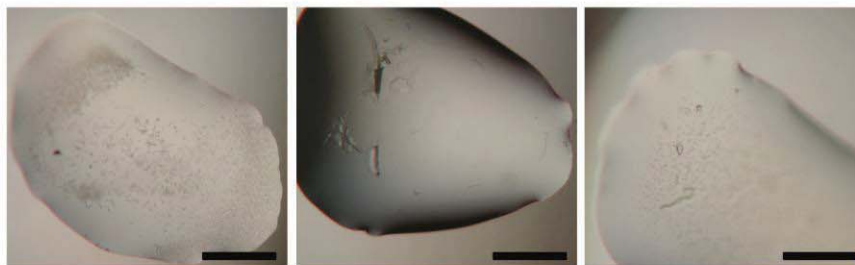
Taken together, our data show that VE-cadherin EC1-2 forms homodimers in solution and appears to utilize a strand swap mechanism common to classical cadherins. Both domains are necessary to mediate adhesive binding. Notably, dimerization of two domain VE-cadherin fragments was independent of glycosylation state. Therefore, VE-cadherin EC1-2 fragments expressed in bacteria are suitable for structural studies of the adhesive binding interface.

5.2 Screening and optimization of crystals of VE-cadherin EC1-2

While our experiments with full length native VE-cadherin ectodomains and with smaller adhesive fragments show that VE-cadherin is likely to bind via a strand swapped dimer mechanism with a similar overall configuration to other classical cadherins, details of the adhesive interface on a molecular level remain elusive. In order to determine details of the adhesive interface on atomic level we wanted to study the minimal EC1-2 binding unit of VE-cadherin using protein crystallography.

Chicken two domain fragments of VE-cadherin crystallized at 8.6mg/mL in sitting drop experiments of initial sparse matrix screens in three different conditions, all with high molecular weight PEG as precipitant (Figure 21a). Crystals found in the condition containing 0.2M calcium acetate, 0.1M sodium cacodylate, pH6.5 and 16% (w/v) PEG 8,000 were small, non birefringent, single crystals with sharp edges (Figure 21a, left panel). The other drop contained two sharp edged very birefringent hexagonal crystal plates found in precipitate

(a)



0.2M Calcium acetate
0.1M Sodium cacodylate pH6.5
18% (w/v) PEG 8,000

0.2M Magnesium chloride
0.1M Bis-Tris pH6.5
25% (w/v) PEG 3,350

0.2M Lithium sulfate
0.1M Tris pH8.5
25% (w/v) PEG 3,350

(b)



0.2M Calcium acetate
0.1M Sodium cacodylate pH6.5
20% (w/v) PEG 8,000

0.2M Calcium acetate
0.1M Sodium cacodylate pH6.5
18% (w/v) PEG 8,000

0.2M Calcium acetate
0.1M Sodium cacodylate pH6.5
16% (w/v) PEG 8,000

Figure 21: Chicken VE-cadherin EC1-2 crystals. (a) Sparse matrix screening hits, sitting drops of 100nL+100nL. Crystals shown on the left are small, extend in three dimensions and no precipitation, but microcrystals occurred. Crystals depicted in the middle occurred without and crystals in the right image appeared within precipitation. Middle image shows hexagonal and rectangular, very thin plates and right image shows a group of rectangular soft shaped crystals. (b) Chicken VE-cadherin crystals after optimization. Crystals grown in hanging drop assays with 600nL protein and 1200nL mother liquor to reduce precipitant concentration. Crystals are cuboidal, sharp edged and were used for data collection. Scale bar for all images 500mm.

(crystallization condition listed in Figure 21a, middle panel) and the last drop (composition shown in Figure 21a, right panel) contained soft edged, very birefringent rectangular boxes surrounded by precipitate (Figure 21a right panel).

Crystals shown in the left panel of Figure 21a, were chosen for optimization as they had sharp edges and no protein precipitate was found in the drop. A large number of small crystals is usually caused by high nucleation rates, which indicate a precipitant concentration and/or protein concentration that are too high. We changed for optimization to hanging drop assays and reduced the precipitant concentration in the crystallization solution. At the same time we shifted the protein:crystallant ratio from initial 1:1 to a 2:1 ratio with 2fold protein in comparison to mother liquor, lowering the initial precipitant concentration while increasing total protein concentration in the drop (Figure 21b, optimization). We found significantly improved crystals in the altered condition which were larger in all three dimensions, cuboidal and birefringent (Figure 21b). Crystals grew up to approximately 300-400 μm size (Figure 21b), which were sufficiently sized to test for X-ray scattering behavior. We mounted crystals in Hampton nylon loops of 200 μm size, immersed crystal prior to freezing in cryo-protectant composed of the crystallization solution with an additional 30% glycerol and flash froze the crystals in liquid nitrogen. Diffraction data was collected at the National Synchrotron Light Source, Brookhaven National Laboratories using beam line X4C. Crystals diffracted to 2.1 \AA resolution and a full data set 180 frames could be collected from a single VE-cadherin crystal with one degree rotation per image. One of the recorded diffraction images is shown in Figure 22 depicting a representative diffraction pattern with sharp diffraction spots, indicating low mosaicity (0.57 $^\circ$). Data was processed to a resolution of 2.1 \AA with Denzo and Scalepack and unit cell dimensions were $a=b=99.973\text{\AA}$ and $c=105.987\text{\AA}$. With $\alpha=\beta=\gamma=90^\circ$. Examination of systematic absences in the data, identified the space group as either $P4_32_12$ or $P4_12_12$; of these two possibilities, $P43212$ was determined to be correct during molecular replacement.

Matthews coefficient analysis indicated that two molecules were present in the crystallographic asymmetric unit, with a solvent content of approximately 56% ($V_m=2.8\text{\AA}^3/\text{Da}$). The structure could be solved with molecular replacement using the crystal structure of cadherin-11 EC1-2 (pdb code 2A4E) as search model. We built the structure in alternating cycles of molecular building in Coot and refinement in Refmac (ccp4i suite) to a final R-factor of 18.29% and R_{free} – factor of 24.18. Detailed data collection and refinement statistics

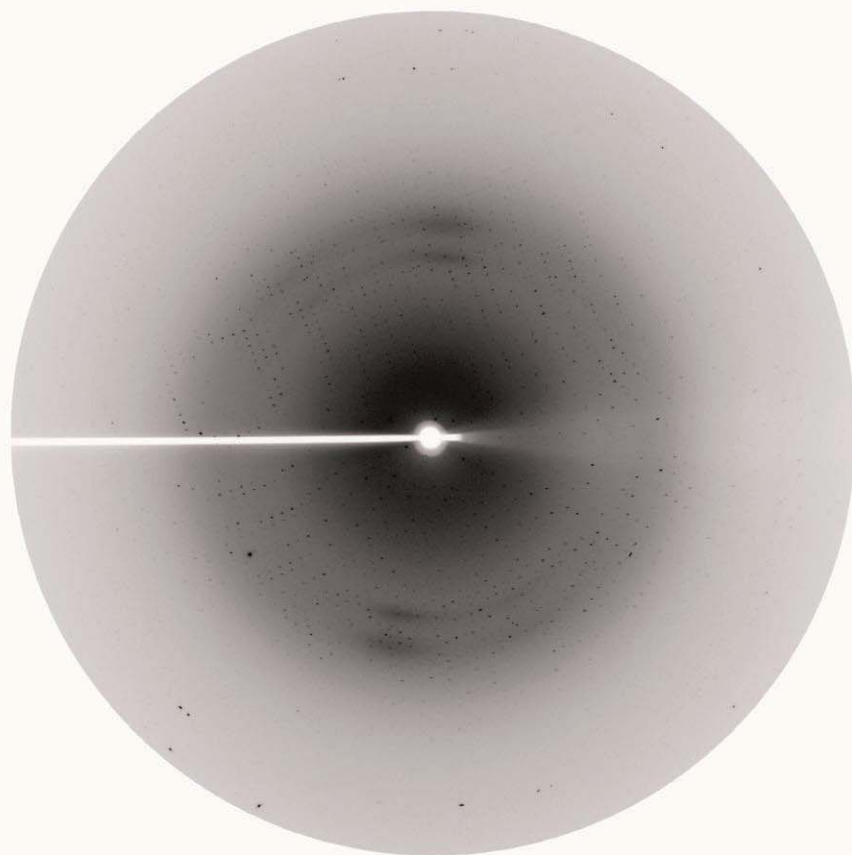


Figure 22: Diffraction pattern from chicken VE-cadherin EC1-2 crystal in space group $P4(3)2(1)2$ with unit cell dimensions of $a=b=99.973$, $c=105.987$ and $\alpha=\beta=\gamma=90$. The data set was collected with an image plate detector (MAR scanner 345mm plate) at beam line X4C at the National Synchrotron Light Source at Brookhaven National Laboratories. Resolution limit for diffraction is 2.1 Angstrom. Crystal to detector distance was 150mm and oscillation range was 1 degree per frame. Total of 180 frames collected.

are summarized in Table 11. The Ramachandran plot of the refined structure revealed 97.1% of the residues were in favorable regions and no structural outliers are present. The structure of chicken VE-cadherin EC1-2 is described in Section 5.3.

In addition to chicken VE-cadherin, we also screened human and mouse VE-cadherin EC1-2 fragments at 4°C and 20°C for crystallization in over 800 different conditions each in sparse matrix crystal screening suites. Human VE-cadherin formed clear, non birefringent spherulites in one condition, (composition listed in Figure 23a), and mouse VE-cadherin yielded non birefringent needle clusters in a condition composed of 0.1M Imidazole pH8.0 and 10% (w/v) PEG 8,000 (Figure 23a, right panel). However, despite extensive optimization efforts including changes of precipitant concentrations, precipitant type, pH-variation and 96 different additives, we could not improve the initially obtained spherulites during optimization trials. Mouse VE-cadherin crystals could be improved as the size of the blades in needle clusters could be enlarged and the number of clusters in comparison to the initial hit reduced (Figure 23b). However, despite extensive efforts, crystal blades remained too thin in the third dimension and were consequently highly fragile (Figure 23b, right panel, note the crystal cracking).

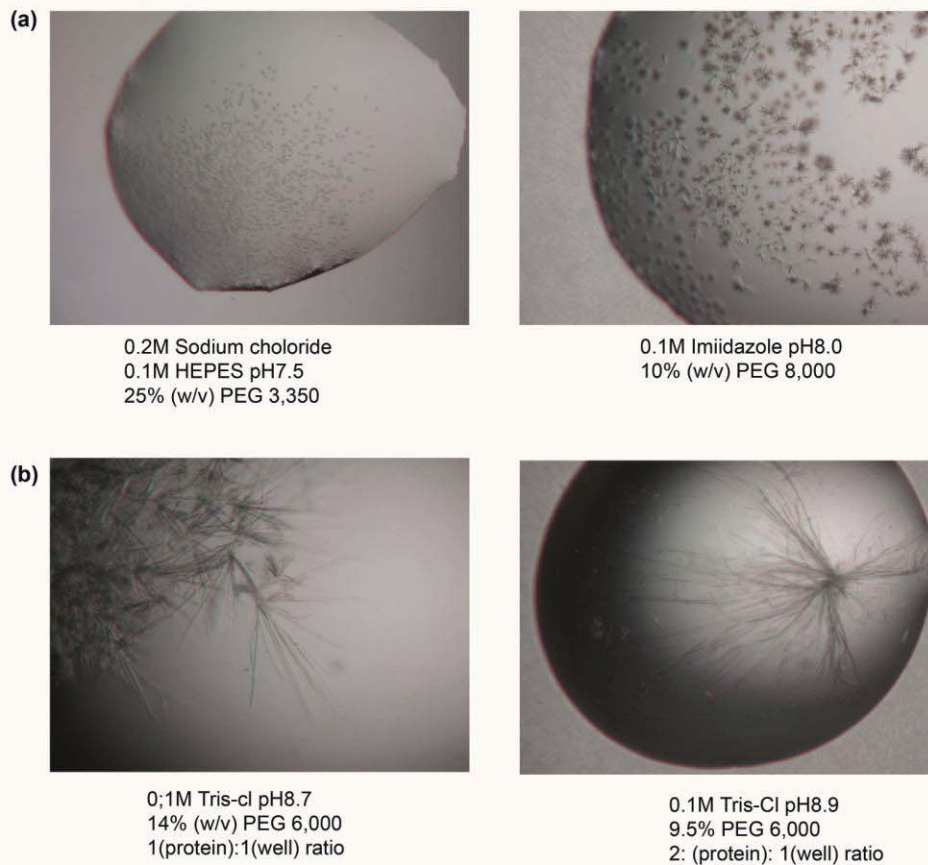


Figure 23: Images of crystals of human and mouse chicken VE-cadherin EC1-2. (a) Initial sparse matrix screening in sitting drop assays (100nL:100nL) yielded crystals for human and mouse VE-cadherin (left and right panel, respectively). Crystallization conditions are given below the images. Crystals of human protein were small and rounded lacking sharp edges (left panel) and those for mouse VE-cadherin were composed of small needle clusters of predominantly brown color. (b) Images of crystals resulting from optimization trials for mouse VE-cadherin EC1-2. Precipitant was changed to lower molecular weight and buffer reagents, but same protein: crystallization solution ratio (left panel) lowered nucleation rate and improved size of needles. Elevated pH, lower precipitant concentration and change of protein:well solution ratio from initially 1:1 to 2:1 (600nL:1200nL) yielded low nucleation rates. Blades in needle clusters grew substantially, but however, remained thin and thus fragile (right panel). Optimization assays performed in sitting drop set-up.

5.3 Crystal structure of chicken VE-cadherin EC1-2 reveals a strand swapped dimer

We crystallized chicken VE-cadherin EC1-2 and obtained high resolution diffraction data up to 2.1Å from which a structure could be solved as described in the previous section. Data collection and refinement statistics are summarized in Table 11.

Table 11: Crystallographic data and refinement statistics.

Data collection	
Space group	<i>P4₃2₁2</i>
Cell dimensions a, b, c (Å); α , β , γ (°)	99.97, 99.97, 105.99; 90, 90, 90
Resolution (Å)	80-2.1
R_{merge}	13.7 (41.8)
$I/\sigma I$	1,395.2/64.4 (339.1/48.2)
Completeness	100(100)
Redundancy	14.1
Observed reflections	450,866
Unique reflections	31,991
Refinement	
Resolution (Å)	72.7-2.1
Number of reflections	31,937
R_{work}	18.29
R_{free}	24.18
Number of atoms	3,841
Protein	3,247
Ion	6
water	588
R. m. s. deviations	
Bond length (Å)	0.016
Bond angles (°)	1.592
Mean B factors (Å²)	
Protein	19.38
Ion	13.58
water	32.06
Ramachandran plot	
Outliers (%)	0

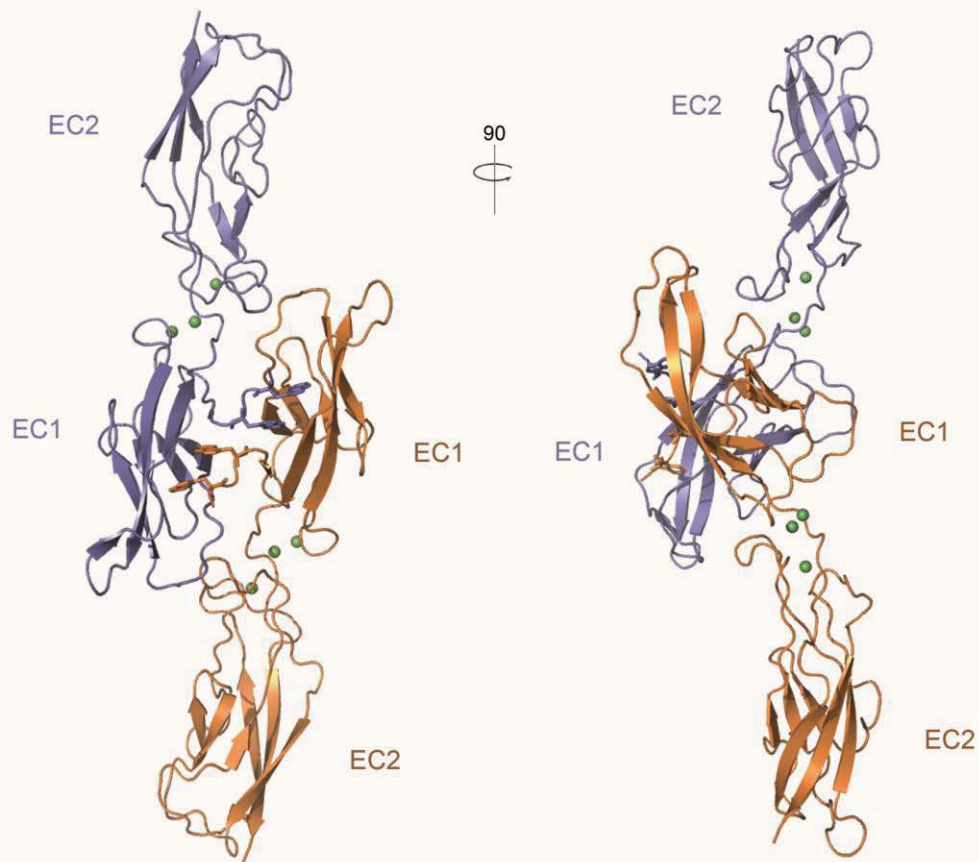


Figure 24: Crystal structure of the EC1-2 domain of chicken VE-cadherin showing a strand swapped cadherin dimer. Ribbon diagram in two rotations showing the symmetrical strand swapped dimer found in the crystallographic asymmetric unit. Each of the two EC domains per protomer adopt cadherin typical seven stranded β -barrel fold. Trp2 and Trp4 residues on intermolecular exchanged A*-strands are depicted as sticks. One VE-cadherin protomer is shown in blue, the other in orange. Each protomer coordinates three Ca^{2+} ions in the interdomain linker region (green spheres). Notably, EC1 domains are arranged almost perpendicular to each other in the strand swapped dimer, the overall dimer arrangement appears approximately linear.

In the crystallographic asymmetric unit two molecules are present, which are both closely similar to each other (Figure 24). The protomers have an elongated, slightly curved overall shape reminiscent of that of previously published classical cadherin structures. Each molecule consists of two extracellular cadherin (EC) domains, which are each composed of a seven stranded β -barrel fold and are characteristic for cadherins. EC domains are connected with each other through a short interdomain linker (Figure 25a) in which three divalent calcium ions are coordinated (Figure 25a, inset) as observed in all previously reported type I and II cadherin structures. Predominantly, acidic residue side chains and backbone carbonyl groups of EC1, the interdomain linker and EC2, in addition to a single solvent water molecule, contribute to the calcium coordination (Figure 25a). Specifically, domain EC1 provides the calcium coordinating residues Glu11, Glu12, Asp 62 and Glu64, which are conserved within all type II cadherins. In type I subfamily members Glu12 is replaced with asparagine that does not directly coordinate calcium (II) and remains solvent exposed, but they otherwise share the same calcium (II) coordination pattern. Side chains of residues Asp96, Asn98 and Asp99 in the linker region and Asp132 and Asp184 of domain EC2 and in addition, back bone carbonyl groups of residues Ile97, Asn100 and His139 also coordinate calcium (II). This calcium binding linker region thus forms a continuous network of bonds between the successive domains and is likely to limit flexibility of the two EC domains relative to each other, and to rigidify VE-cadherins overall shape, precisely as suggested by other classical cadherins structures consistent with other experimental data (Ahrens et al., 2003; Sotomayor and Schulten, 2008).

The two VE-cadherin protomers observed in the crystallographic asymmetric unit form a strand swapped dimer, which shares the essential features with those of other classical cadherins (Figure 24). Both N-terminal EC1 domains are arranged approximately perpendicular to each other forming a symmetrical adhesive dimer interface, in which the N-terminal segments of the respective A-strand, the A*-strand, are exchanged between protomers (Figure 24, 25b). Protomers are arranged in a *trans* orientation in the dimer as if extending from opposing cell surfaces. On the molecular level, tryptophan side chains at positions two and four are central to this 'strand swap' dimer. Trp2 and Trp4 are located on the A*-strand and are reciprocally docked into a hydrophobic cavity, the 'acceptor pocket', of the partnering molecule. This intermolecular docking is stabilized by three types of interactions (Figure 25b, inset). Both ϵ 1 nitrogen atoms of Trp2 and Trp4 indole rings engage

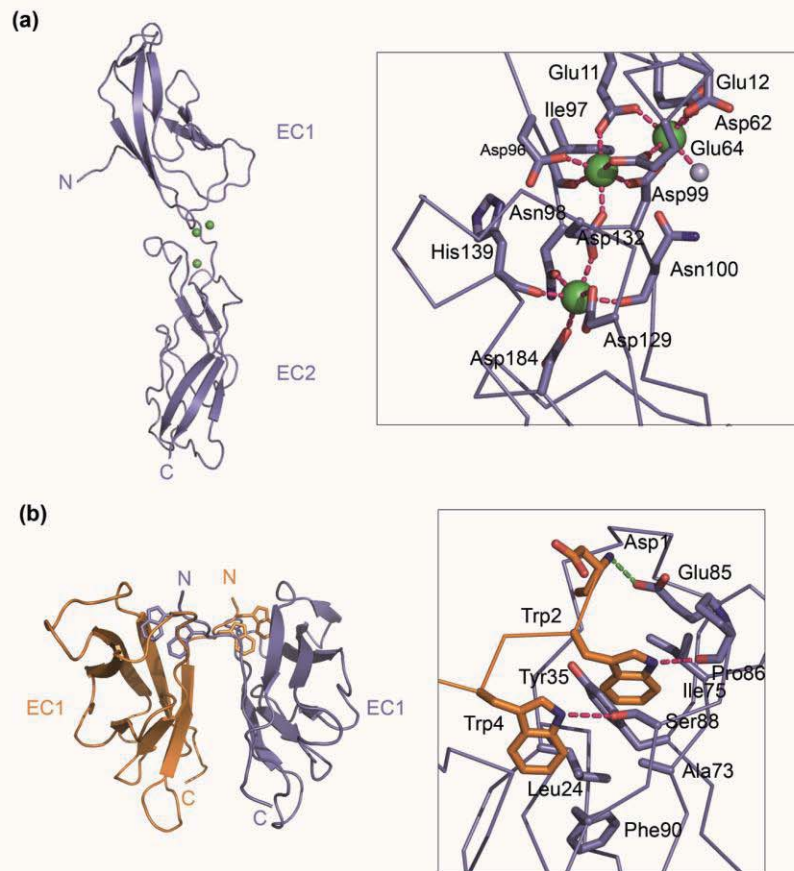


Figure 25: Chicken VE-cadherin calcium coordination and detailed view of interactions in the strand swapped dimer. (a) Single protomer of VE-cadherin EC1-2 shown as ribbon diagram with calcium ions located between EC1 and EC2 shown as green spheres. Inset is a detailed view of calcium coordination in this linker region. Three Ca^{2+} ions are coordinated by side chains of Asp, Glu or Asn and by backbone carbonyl-groups, shown in stick representation in addition to one water molecule (grey sphere). Coordination interactions between protein, ions and water are shown as magenta dotted lines. (b) Detailed view of the strand dimer interface. Interactions found in the dimer are restricted to EC1 domains. Boxed is a detailed view of the intermolecular interface. Pocket of one protomer is shown in blue, A-strand of the partnering molecule is represented in orange. Only residues partaking in strand swapping are shown as sticks. Docking of the A-strand into the pocket is mediated by: van der Waals interactions between the tryptophan side chains and residues Leu24, Tyr35, Ala73, Ile75, Phe90 of the acceptor pocket; two hydrogen bonds (magenta dotted lines) between the ϵ nitrogen of Trp2 and Trp4 and the backbone carbonyl of Pro86 and the hydroxyl-group of Ser88, respectively, and a saltbridge between the N-terminal amine group of Asp1 and the carboxylate side chain of Glu85 (green dotted lines).

in intermolecular hydrogen bonds with the backbone carbonyl group of Pro86 and the side chain oxygen of Ser88, respectively. The interaction between Trp2 and Pro86 is also found in other structures of classical cadherins, whereas the latter hydrogen bond is unique to the VE-cadherin dimer. In other type II cadherins, the Trp4 side chain forms instead an indirect hydrogen bond via a water molecule with the residue equivalent to Ser88.

Additionally, Trp2 and Trp4 side chains partake in hydrophobic van der Waals interactions with residues lining the hydrophobic acceptor pocket. Residues Leu24, Ala73 and Phe90 are positioned at the “base” and Tyr35 and Ile75 towards the “top” of the hydrophobic pocket. The last of the observed pocket interactions is a salt bridge formed by the carboxyl group of Glu85, which holds the N-terminal amino group of Asp1 in place through an ionic interaction as if locking the exchanged strands. This salt bridge is conserved within classical cadherins and along with Trp related interactions is crucial for proper cadherin mediated binding (Harrison et al., 2005) explaining the necessity of native N-termini for strand swapping cadherins, since an extended N-terminus, would lead to a shift of the salt bridge position. In addition to the pocket related interactions, two more intermolecular hydrogen bonds can be observed near the periphery of the pocket region. The back bone carbonyl group of Asp1 and amide group of Ile3, both located on the donor A-strand of one protomer, engage in hydrogen bonds with the back bone amide and carbonyl group of B-strand residues Ser27 and Thr25, respectively, from the other protomer.

5.4 The VE-cadherin strand swapped interface is unique

The specific molecular interactions between the donor strand and acceptor pocket in the strand swapped dimer of VE-cadherin described above are closely similar to those observed in structures of type II cadherins -8, -11 and MN- (Patel et al., 2006). However, sequence identity analysis suggests an outlier position for VE-cadherin within the type II cadherins and indeed the crystal structure revealed features that are unique to the adhesive interface of VE-cadherin, which will be elucidated below.

5.4.1 VE-cadherin uses a different set of residues for *trans* dimerization than other classical cadherins

We examined the adhesive interface of VE-cadherin in comparison to those of type I and II subfamily members in detail and first determined how much solvent accessible surface area is buried in the respective interfaces using the program PISA. Resulting buried surface area (BSA) values are summarized in Table 12. We found that EC1 domains contribute almost all of the interface residues in the adhesive strand swapped dimer and thus focused our detailed comparison on EC1 domains. In type I subfamily members E-, N- and C-cadherin BSA values average approximately to 850Å² per protomer (Table 12) and in type II cadherin-8, -11, and MN the adhesive interface buries a markedly larger region of 1,225-1,265Å² per protomer (Table 12, (Patel et al., 2006)). In comparison, VE-cadherin buries an interface of 1067Å² per protomer (Table 12), which is almost exactly intermediate between the areas buried in type I and II cadherins.

Table 12: Buried accessible surface area (BSA) for type I and type II cadherin interfaces, BSA value for one protomer given.

Protein	BSA [Å²]^a	pdb ID
EC1-domain		
ck VE-cadherin	913.0	3PPE
m cadherin-8	1264.2	1ZXK
m cadherin-11	1225.8	2A4C
ck MN-cadherin	1254.9	1ZVN
m E-cadherin	817.3	2QVF
m N-cadherin	875.8	2QVI
x C-cadherin	847.6	1L3W
EC12-domains		
ck VE-cadherin	1066.2	3PPE
m cadherin-8	1271.9	2A62
m cadherin-11	1529.2	2S4E
m E-cadherin	817.3	2QVF
m N-cadherin	875.8	2QVI
x C-cadherin	847.6	1L3W

^a In case of two molecules per asymmetric unit, values given for chain A.

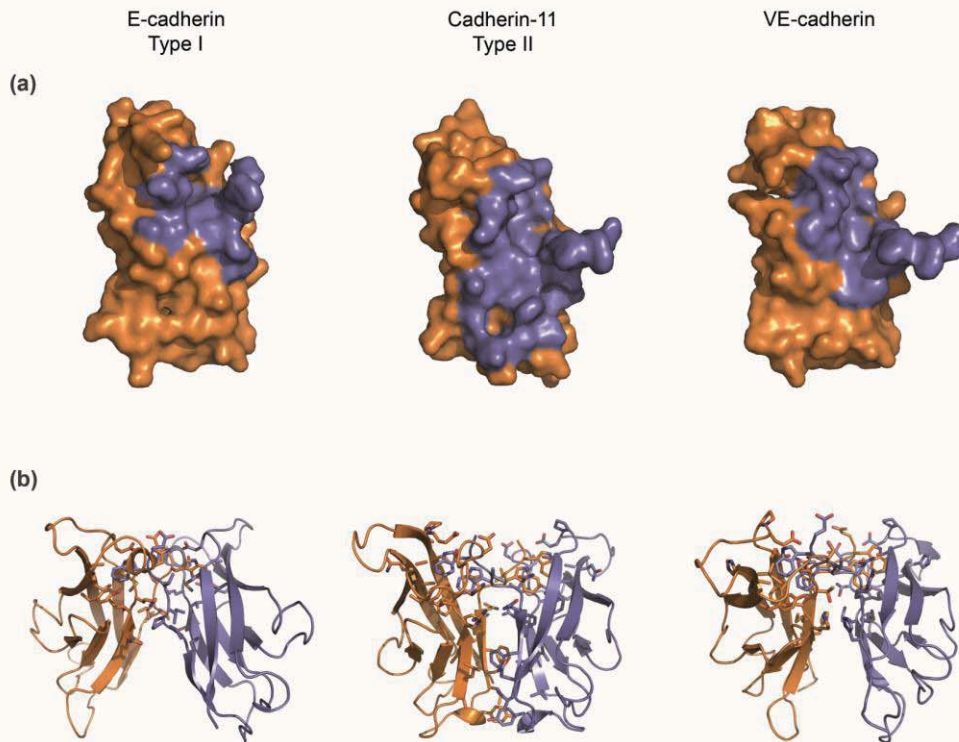


Figure 26: Comparison of the strand swapped dimer interface of VE-cadherin with those of type I and type II cadherins. (a) EC1 domains of single protomers of E-cadherin (left panel, PDB: 2QVF), cadherin-11 (middle panel, PDB: 2A4C) and VE-cadherin (right panel, PDB: 3PPE) are displayed as a molecular surface (orange). The “footprint” of the partnering molecule in the strand swapped dimer, determined as regions with a per residue buried surface area in the dimer greater than 10\AA^2 , is highlighted blue on the surface. The interface for type I cadherins (left panel) and VE-cadherin (right panel) is restricted to a smaller region than in type II cadherins (middle panel), in which the interface is not only localized around the A-strand but extends toward the base of the EC1 domain. (b) Ribbon diagrams of EC1 domains of the same dimers as in panel (a), with residues involved in the interface ($\text{BSA} > 10\text{\AA}^2$) represented as sticks. One protomer is colored orange, the other blue. Note that the adhesive interface of VE-cadherin shares features of both subfamilies of classical cadherins.

To visualize the molecular surface area that is buried in the strand swap interface, EC1-domains of VE-cadherin and representatives of the type I (E-cadherin) and type II (cadherin-11) subfamilies are shown in Figure 26a as molecular surface representation with the surface region buried in the dimer interface shown in blue as the ‘footprint’ of the partner protomer. The ‘footprint’ for E-cadherin is relatively small (Figure 26a, left panel) and located around the ‘upper’ half of the EC1 domain, corresponding to the region in which the swapped A*-strand is docked into the acceptor pocket of the partnering molecule (Figure 26b, left panel). In type II cadherins residues Trp2, as in type I cadherins, and in addition Trp4 are anchored in a proportionally larger hydrophobic acceptor pocket (Figure 26, middle panel).

However, the dimer interface in type II cadherins is extended along the ‘face’ of the entire domain EC1 towards the base (Figure 26, middle panel), This is in contrast to the buried surface area found in type I cadherins, where the interface is restricted to the ‘upper half’ of the domain (Figure 26a and b, left and middle panel) and, together with the larger swapped element, explains the higher BSA values for type II cadherin dimers. In VE-cadherin is the adhesive region limited to the “upper” half of domain EC1 (Figure 26a, right panel) corresponding to the A*-strand and hydrophobic acceptor pocket (Figure 26b, middle panel), like in type I cadherins. Strikingly, despite VE-cadherin having close similarity in the strand swap region, the extended non-swapped region present in type II cadherins is absent from the adhesive interface of VE-cadherin leaving this particular region solvent exposed.

The non-swapped hydrophobic region contributing to the adhesive dimer that is characteristic to type II cadherins is formed by hydrophobic residues 8, 10, 13 and 20 contributed from both protomers (Figure 27a and b). These residues interact via van der Waals interactions and stack closely against each other in the swapped dimer (Figure 26b, middle panel, (Patel et al., 2006)). These residues are conserved in character at the sequence level in typical type II cadherins, but not in VE-cadherin, which has mostly hydrophilic residues at these positions similar to type I cadherins (Figure 27a). These residues in VE-cadherin are not found to engage in intermolecular protein-protein interactions of any kind in this region (Figure 27b, Figure 26, right panel), leading to an overall dimer arrangement more reminiscent of that of type I cadherins than type II cadherins (Figure 26). Although VE-cadherin lacks the extended non-swapped hydrophobic region of type II cadherins, it shares most residues required for interactions between the swapped strand and the acceptor pocket closely with those of type II cadherins (Figure 27b).

The structure of the adhesive VE-cadherin dimer reveals a unique adhesive interface, in that the VE-cadherin interface resembles that of type I cadherins, whereas the strand-swap interactions between A*-strand and acceptor pocket are almost completely conserved between VE-cadherin and type II subfamily members. This strongly suggests that VE-cadherin represents an outlier among the type II classical cadherins.

5.4.2 Analysis of structural superpositions of VE-cadherin with type I and II cadherins

To identify the impact of divergence at the sequence and binding interface level on general arrangement of the VE-cadherin protomer and dimer, we superposed VE-cadherin protomers with those available from type I and type II cadherin structures.

The overall structures of EC1-2 single protomers appear quite similar to each other in respect of relative orientation of EC domains and the overall EC domain fold (Figure 28a, left panel, superpositions). Root mean square (r. m. s.) deviations were also determined for superposed cadherin pairs (Table 13).

VE- and type II cadherin-11 have an r.m.s value of 1.85Å over 194 aligned C_α-atoms, whereas VE-cadherin and type I E-cadherin compare to 1.51Å over 187 C_α-atoms. In comparison, E-cadherin and cadherin-11 have a higher r. m. s deviation of 2.3Å over 183 C_α-atoms. Evaluated over EC1-2 structures, VE-cadherin superpositions suggest that the structure is similarly different from type I and II cadherins. In comparison type I subfamily members E-, C- and N-cadherin superposed with each other yield in r. m. s. d. values in the range of 0.99-1.13Å, indicating closely similar structural arrangement.

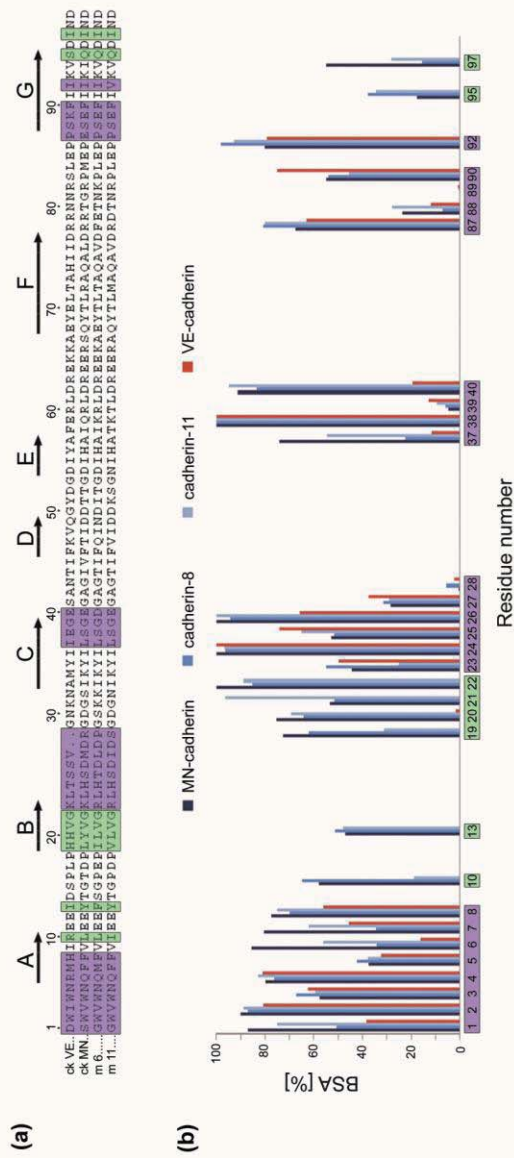


Figure 27: VE-cadherin uses a different set of residues for *trans*-dimerization than type II cadherins. (a) Sequence alignment of the EC1-domain of chicken VE- and MN-cadherin (1PPE and 1ZVN, respectively) and mouse cadherin-8 (1ZXX) and -11 (2A4C), for which strand swapped dimer structures have been determined. Residues buried in the adhesive interface (>5% buried) in all structures are boxed in purple. Residues comprising the type II cadherin specific hydrophobic interface are buried in dimers of cadherin-8, -11 and MN-cadherin, but remain solvent exposed in VE-cadherin (residues are boxed in green). (b) Comparison of BSA values for EC1 domain residues in the strand swapped dimer interfaces of VE-cadherin and other type II cadherins, as a percentage of the residue surface area. VE-cadherin shares the buried A-strand and acceptor pocket residues with type II cadherins (purple boxes), but residues in the type II cadherin hydrophobic interface, positions 10, 13, 19, 20 and 22, are greater than 95% solvent exposed in the VE-cadherin dimer.

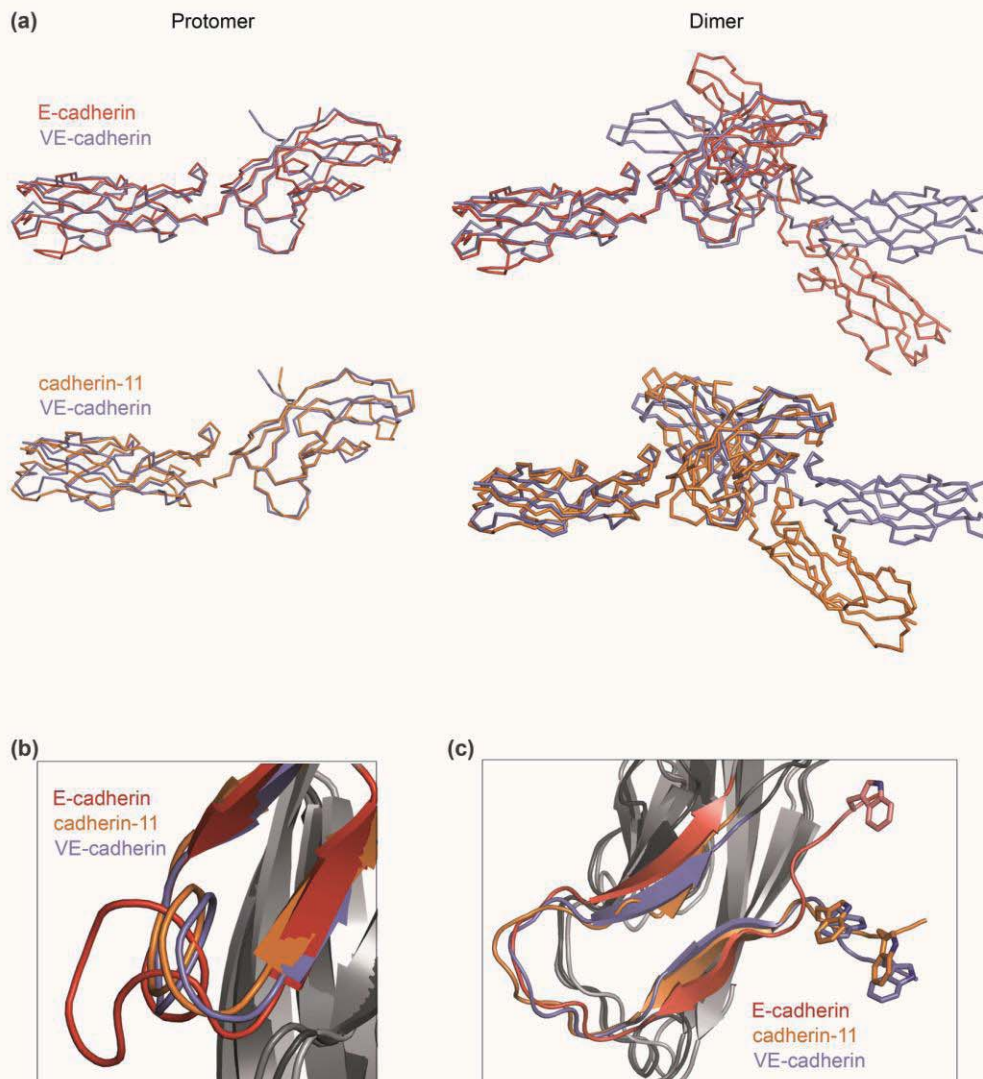


Figure 28: Superposed α -carbon traces from crystal structures of VE-cadherin and type I and type II classical cadherins. (a) Single protomer (left panel) and dimer (right panel) superpositions of chicken VE-cadherin EC1-2 (slate) with E-cadherin, a type I cadherin (red, upper panel, PDB:2QVF) and cadherin-11, a type II cadherin (orange, lower panel, PDB:2A4E). The structures are represented as α -carbon traces. Note that overall structure and interdomain angles are closely similar between the three different classical cadherins, but relative orientation of EC2 domains in the VE-cadherin dimer differs remarkably from that in dimers of the other cadherins. Angle enclosed between long axis of EC2 domains is for VE-cadherin 168° , compared to 129° for E-cadherin and 143° for cadherin-11. (b) Close up view of the pseudo β -helix between the C- and D-strand, unique to type I cadherins (red), not found in VE-cadherin or cadherin-11. (c) Detailed view of A-strand and B-strand positions in domain EC1. Note that A- and B-strands are closely similar within all three classical cadherins, but A*-strand arrangement in the dimer is strikingly different between type I E-cadherin and type II cadherins VE and -11. Close up domain views depicted as ribbon diagrams in different shades of grey (dark: VE-cadherin, middle: cadherin-11 and light for E-cadherin) with important features presented in same color code as in panel (a); tryptophan side chains shown as sticks.

Table 13: Root mean square deviations between superposed EC1 (yellow), EC2 (red) and EC12 (blue) domains of type I and type II cadherins.

	EC1							
	EC2	VE	11	8	MN	E	N	C
EC12								
VE		-	1.16 ^a	1.15	1.31	1.52	1.66	1.84
			1.02	1.16	NA ^b	1.09	1.17	1.27
11		1.86	-	0.78	0.55	1.42	1.67	1.67
				0.96	NA	1.01	1.04	1.18
8		1.46	1.65	-	0.80	1.34	1.63	1.62
					NA	1.35	1.35	1.30
MN		NA	NA	NA	-	1.49	1.75	1.75
						NA	NA	NA
E		1.52	2.31	1.87	NA	-	0.94	0.86
							0.73	0.69
N		1.70	2.13	1.83	NA	0.94	-	1.01
								0.80
C		2.01	2.36	2.40	NA	1.14	1.21	-

^a In case of two molecules present in the crystallographic asymmetric unit, values retrieved by superpositions of chain A only.

^b Structural data only available for domain EC1.

Although, domains EC1-2 are required for *trans* adhesion, specificity appears to arise from differences in domain EC1 to which the mature swapped interface maps (Patel et al., 2006). Therefore, we also superposed single EC1 domains of selected strand-swapped cadherin structures separately with VE-cadherin and each other (Table 13, lavender for EC1, purple for EC2 domain r. m. d. values, respectively). When calculations are restricted to EC1 domains alone, VE-cadherin is more similar to type II cadherins with r. m. s. deviations in the range of 1.11-1.16Å in comparison to values in the range of 1.53-1.84Å for comparisons with type I cadherins. This difference can be explained by the fact, that type II cadherins lack a structural feature of a quasi β -helix between A- and B-strands which is specific to type I cadherins (Figure 28b). Also, presence of two tryptophan residues in all type II cadherins, which require a larger acceptor pocket than type I cadherins, might contribute to the lower r. m. s. deviations

between VE-cadherins and type II subfamily members. Additionally, swapping A* strands of type II cadherins and VE-cadherin align closely in an orientation different from that in type I cadherins, which likely arises from the differences in the adhesive dimer interface between the two subfamilies (See Section 5.4, Figure 28a and c). Notably, however, type II cadherins MN, 8 and 11 are almost identical to each other as suggested by r. m. s. deviations in the range of 0.53-0.68Å (Table 13). These analyses suggest that VE-cadherin is to some extent a structural outlier within type II cadherins.

Next, dimer superpositions were investigated. The overall arrangement of type I and II cadherin dimers was compared by superposing based on one of the protomers of the dimer with that of the other dimer (Figure 28a, right panel). Results reveal that VE-cadherin has a markedly divergent dimer arrangement in comparison to type I and II cadherin dimers as the relative orientation of the long axes of EC2 domains appears to be almost linear. We determined the angles between protomers in swapped dimers of VE-cadherin, E-cadherin as representative of type I cadherins and type II cadherin-11 using PyMol to determine angles between partner EC2 longitudinal axes. The angle of the VE-cadherin dimer was found to be 168°. Type I E-cadherin and type II cadherin-11 have much smaller angles of 129° and 143°, respectively, which suggests that VE-cadherin adopts a different arrangement in the adhesive interface in comparison to those of other classical cadherins that is likely to arise from the unique features of the swapped interface described above.

5.5 Investigation of other interfaces in the VE-cadherin crystal structure

Recent crystal structures of E-, N- and C-cadherin revealed a potential *cis* interface between cadherins oriented as if originating from the same cell surface (Boggon et al., 2002; Harrison et al., 2010b). The interface occurs between the face of EC1 opposite the strand swap interface and the base of EC2 of a partner molecule. The interface was observed in EC1-2 as well as EC1-5 domain fragments of E- and N-cadherin (pdb-code 2QVF and 2QVI and E- and N-cadherin EC1) and the full ectodomain of C-cadherin (pdb-code 1L3W). Mutations that disrupt this interface were found to prevent the ordered assembly of these cadherins in artificial junctions between liposomes and to destabilize cellular junctions between cadherin transfected cells. These results suggest that the combination of *cis* and *trans* interactions in cadherin ectodomains are responsible for initial junction formation. VE-cadherin also forms adherens junctions (see Introduction 1.8.2 and Section 4.6) suggesting the possibility that a

similar set of *cis* and *trans* interactions is involved. We therefore set out to examine other crystal contacts of the chicken VE-cadherin structure that might function in assembly of the cadherin at junctions in addition to the swapped *trans* interface. In order to determine contacts of interest we evaluated the crystal packing by buried surface area in contact regions with PISA. There are four crystal contacts that bury a surface area over 300Å² per protomer. The largest buried surface area, 1068.9Å² per protomer, corresponds to the *trans* dimer described in the previous section (Figure 25 (overall dimer) in Section 5.4). The second largest buried area (716.8Å²) is found for a contact between EC1 domains of VE-cadherin protomers on the face opposite the strand swap interface (Figure 29a). The remaining two interfaces are found to bury 440.9-458.5Å² of the solvent accessible surface area of a protomer. The same interfaces are found independently for both protomers present in the crystallographic asymmetric unit and have a highly similar arrangement, in which the molecules are oriented approximately perpendicular to each other with the contact region below the strand swap interface at the top of EC2 of one protomer and the side of EC1 for the other (Figure 29b). In principle, either of the interfaces observed in addition to the swapped *trans* interface could contribute to assembly of VE-cadherin in junctions. However, we have no evidence for biological relevance of these additional crystal contacts at this point. Notably, there is no indication of crystal contacts similar to the reported type I cadherin *cis* interface in the VE-cadherin structure. The interface is also absent from previously reported type II cadherin -6, -8 and 11 structures (pdb-codes 3LND, 2A62 and 2A4E, respectively). Nonetheless, there is evidence from cryo EM studies and other experiments (Kiener et al., 2006; Uehara, 2006) that VE-cadherin and other type II cadherins form adherens junctions. This assembly is likely to require an additional *cis* interaction enabling lateral junction formation that is different to that of E-, N- and C-cadherins, especially as it was shown that a passive ‘diffusion trap’ is not sufficient for junction formation in the absence of such interactions (Wu et al., 2010). Clearly, further studies of type II cadherins are needed to understand how their ectodomains assemble into adherens junctions.

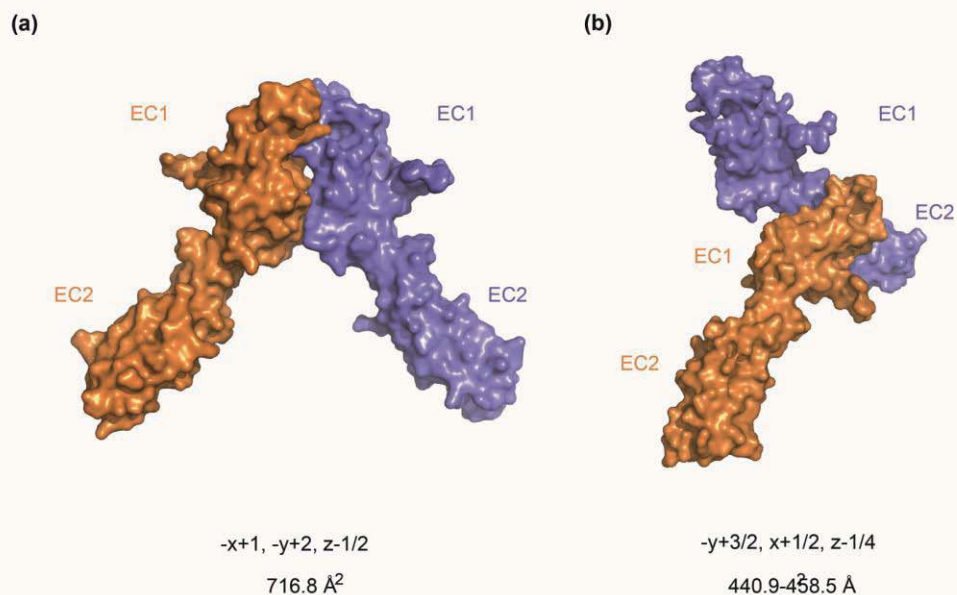


Figure 29: Molecular surface presentation of crystal contacts found in the crystallographic asymmetric unit of chicken VE-cadherin. (a) Crystall contact involving the face of EC1 domains opposite the strand swap interface. (b) Interface is found between symmetry mates in the crystallographic asymmetric unit, in which two molecules are oriented almost perpendicular in each other in up-right position. Contact site is between the side of EC1 approximate to the strand swap interface for one protomer (orange) and below the dimer interface on EC2 in the other (blue). This interface is found for both protomers and their symmetry mates and buries a closely similar interface. Symmetry operation for protomer arrangement and accessible surface area buried in the interface given per protomer.

Chapter 6:
Binding affinities and adhesive specificity in
the type II cadherin subfamily

6.1 Comparison of VE-cadherin and type II cadherin homophilic binding affinities in analytical ultracentrifugation experiments

Given the differences in the strand swapped adhesive interfaces of VE- and type I and II cadherins identified in our structure of VE-cadherin EC1-2 (see Section 5.3), we wanted to compare VE-cadherin binding affinities with those of other classical cadherins.

VE-cadherin binding affinities for the full length ectodomain as well as the two domain fragments were reported in Sections 4.2 (mammalian) and 5.1 (bacteria) and bind tightly with affinities in the low micromolar range (Table 7 (mammalian VE-cadherin) and 10 (bacterial VE-cadherin), Section 4.2 and 5.1, respectively). Despite a similar overall binding interface between VE-cadherin and type I cadherins, reported type I cadherin binding affinities of human E-, N- and frog C-cadherin, 156 μ M, 24.6 μ M and 64 μ M, respectively, are overall at least one order of magnitude weaker than those of VE-cadherin (Table 7 and 10, (Chappuis-Flament et al., 2001; Katsamba et al., 2009). The only affinity measurement reported for type II cadherins at the time this work was conducted was for a two domain fragment of mouse cadherin-6 (Harrison et al., 2010a; Katsamba et al., 2009), which shows tight adhesive binding (K_D 3.13 μ M) within the same range of that of VE-cadherin. Based on K_D values found for these two type II cadherins, it appears that binding affinity in the low micromolar range may be a general property of this subfamily. To test this hypothesis a set of adhesive EC1-2 fragments of mouse type II cadherins -9, -10 and -11 and chicken cadherin-6b and in addition cadherin-8 EC1-3 were designed and produced in *E. coli* (Section 2.1.2.3). We performed sedimentation equilibrium AUC experiments for each of these proteins to determine their K_D values for homodimerization. Surprisingly, type II cadherin affinities were found to stretch over a wide range from 9.2 μ M for cadherin-6b to 42.2 μ M for cadherin-10 (Table 14). These data unambiguously show that not all type II cadherins share a dimerization affinity as strong as that of VE-cadherin and cadherin-6 and that significant variation in homodimerization affinity exists in the type II cadherin subfamily. Despite the large range of adhesive binding affinities, overall the tested type II cadherins showed stronger binding than type I subfamily members.

In total, we determined affinities for five type II cadherins in addition to VE-cadherin and cadherin-6 and found a high degree of variation in homodimerization strength. Within this range, these data suggest that one of the strongest binding affinities yet determined belongs to

VE-cadherin. This is surprising based on our finding that the VE-cadherin strand swapped dimer buries a lesser surface area than in other type II cadherins (Section 5.4).

Table 14: Dissociation constants (K_D) for homodimerization of wild type classical type II cadherins.

Protein	Description	K_D [μ M]
ck cadherin-6b EC1-2	Wild type	9.2±0.6
m cadherin-6 EC1-2	Wild type	3.13±0.1 ^a
m cadherin-8 EC1-3	Wild type	15±0.4
m cadherin-9 EC1-2	Wild type	17±1.1
m cadherin-10 EC1-2	Wild type	42±2.7
m cadherin-11 EC1-2	Wild type	33.8±0.2
m VE-cadherin EC1-2	Wild type	2.22±0.11 ^b

^a K_D also reported by Katsamba and Carrol et al. (2009) and Harrison et al. (2010a).

^b K_D also reported in Section 5.1.

6.2 Adhesive specificity of type II cadherins in surface plasmon resonance assays

Type II cadherins were reported previously to heterophilically interact promiscuously but in a specific pattern in cell-cell aggregation experiments involving a set of eight different proteins (Shimoyama et al., 2000). The results revealed that certain cadherin pairs: cadherin-6 and -9; cadherin-7 and -14; cadherin -8 and -11 and cadherin-9 and -10 form fully intermixed cell aggregates similar to those formed between cell lines expressing the same cadherins, suggesting that each pair has matched binding specificities. However, for cells expressing other combinations: cadherin-6 and -7, cadherin-6 and -10, cadherin-7 and -9, cadherin-7 and -12, cadherin -9 and -14 and cadherin-12 and -14 partial intermixing is observed in that cells expressing each cadherin form separate aggregates, which interact with each other to some extent. This type of aggregate was also found in cell aggregation assays of N- and E-cadherin transfected cells and was explained to arise from a heterophilic interaction with intermediate strength between both homophilic protein-protein binding strengths (Katsamba et al., 2009). Other combinations of type II cadherins, such as cadherin-6 and -8 and cadherin-9 and -11, showed no tendency to coaggregate in the study conducted by Shimoyama et al. (2000).

Interestingly, we found that specificities reported in Shimoyama et al. (2000) mirror the pattern of sequence identity in the type II cadherin subfamily and heterophilically adhering cadherins can be grouped by position in the phylogenetic tree (Figure 30). For example, cadherins -6, -9 and -10 form a group that are related at the sequence level and exhibit full or partial intermixing in all combinations (Shimoyama et al., 2000). This suggested a potential rational basis for patterns of specificity in the subfamily that remained to be fully tested.

Table 15: Sequence identities given in per cent between EC1 (lavender) and EC1-2 (light blue) domains of all strand swapping classical cadherins used in our studies.

	EC1	VE	11	8	10	9	6	N	E
EC12									
VE		100	45	45	38	41	39	/	26
11		47	100	72	64	62	62	35	28
8		45	76	100	59	59	60	35	29
10		43	71	66	100	78	84	32	28
9		45	68	65	82	100	79	32	27
6		43	69	67	84	82	100	34	29
N		34	40	40	38	38	39	100	58
E		31	33	33	33	32	34	/	100

The published cell aggregation study is not comprehensive as not all of the thirteen presently known type II cadherins, including VE-cadherin, were studied. Based on substantial differences on sequence level between VE-cadherin and other type II cadherins (Table 15) which were found to translate into a unique strand swapped adhesive interface (Section 5.4), the question arises if VE-cadherin can exhibit heterophilic binding to other type II or even to type I cadherins. Furthermore, although cell aggregation assays are a powerful tool to elucidate binding specificities of cell-cell adhesion proteins (Shimoyama et al., 2000), they are only semi-quantitative being strongly dependent on equal expression levels and are time consuming to conduct, limiting the suitability of the assay for large sets of proteins. We therefore set out to establish an assay system omitting these problems, where heterophilic binding within the type II cadherin subfamily can be quantitated. In studies our group conducted previously, surface plasmon resonance (SPR) was used as method for homophilic

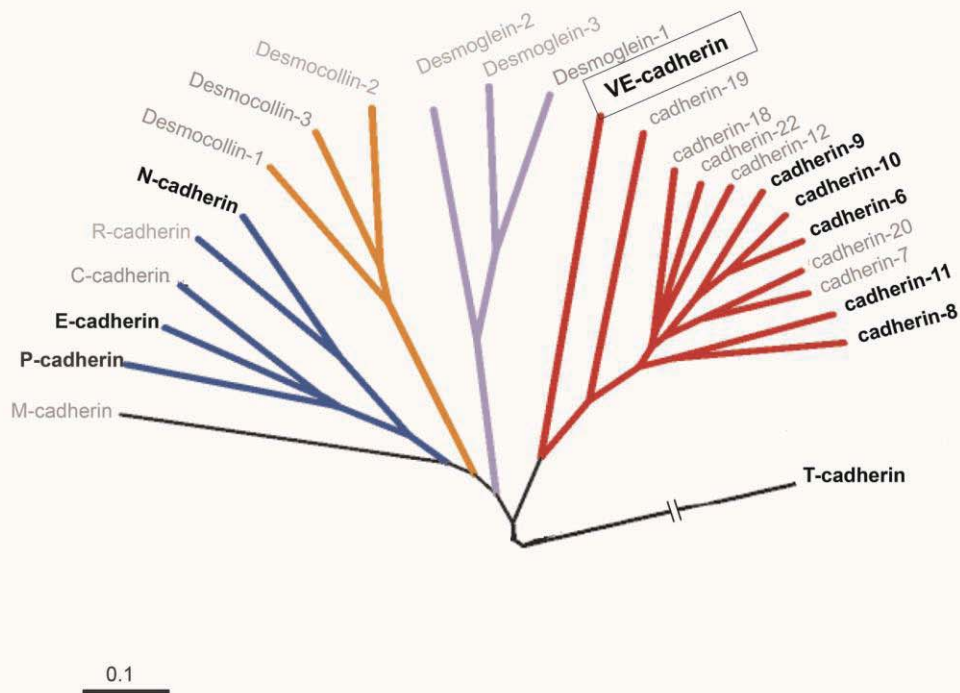


Figure 30: Phylogenetic tree branch of strand swap cadherins on the basis domain EC1 adapted from Nollet (2000). Classical type I cadherins are depicted on the left (blue branch), classical type II cadherins on the right (red branch), Desmocollins (orange) and Desmogleins (lavender) are found in the middle. Scale bar represents the substitution rate of one amino acid per ten amino acid residues. Note that VE-cadherin represents an outlier within the type II cadherin family. Cadherins used for homophilic and heterophilic binding experiments are highlighted bold. Length of branch indicated for T-cadherin is for schematic purposes only, indicated by strand break.

binding studies including E-, N-, T- cadherin and cadherin-6 (Ciatto et al., 2010; Harrison et al., 2010a; Katsamba et al., 2009) and also to assess relative heterophilic binding specificity of type I E- and N-cadherins with each other and type II cadherin-6 (Katsamba et al., 2009). We wanted to test if this method can be used to thoroughly and quantitatively study homo- and heterophilic binding characteristics of purified cadherin proteins on molecular level and additionally, if our findings on molecular level correlate to cadherin behavior demonstrated on cellular level.

6.2.1 Identification of a suitable tag for immobilization of VE-cadherin for SPR

Surface Plasmon Resonance (SPR) as technique can assess relative binding between cadherins. One cadherin is immobilized on the sensor chip surface and the other, the ‘analyte’, is passed over in solution, (Figure 31). In case of protein-protein interactions total mass on the surface changes which is detected by change of reflection angles of a laser focused on the opposite side of the sensor surface chip (Figure 31). In order to conduct homophilic and heterophilic binding studies with VE-cadherin and other classical cadherins, a suitable tag for immobilization on the sensor chip surface needed to be determined. Previous studies of binding behavior of type I E-, N- and outlier T-cadherin as well as type II cadherin-6 were conducted with soluble native EC1-2 domain cadherins as the analytes and C-terminally Avi-tagged biotinylated equivalents (cadherin-Avi*bio), which were captured on the sensor chip surface by immobilized NeutrAvidin, a high affinity biotin binding protein approximately with a binding affinity in the femtomolar range (Ciatto et al., 2010; Harrison et al., 2010a; Katsamba et al., 2009). The captured ‘cadherin-Avi*bio’ proteins are positioned upright resulting in proteins with free adhesive domains pointing away from the sensor chip surface, which can be used for homo- and heterophilic binding studies (Figure 31). This technique and experimental set up was suitable for binding experiments with type I N-, E- and atypical T- cadherin and type II cadherin-6 (Ciatto et al., 2010; Harrison et al., 2010a; Katsamba et al., 2009). However, limitations were discovered for detecting ‘slow’ kinetic binding behavior because molecules have a small limited time to engage in protein-protein interactions in the course of the experiment (Harrison et al., 2010a).

Based on these data we prepared VE-cadherin and type II cadherin-11 both with C-terminal biotinylated Avi-tags (Section 3.3.3 and 2.1.2.3). However, we found that in equilibrium

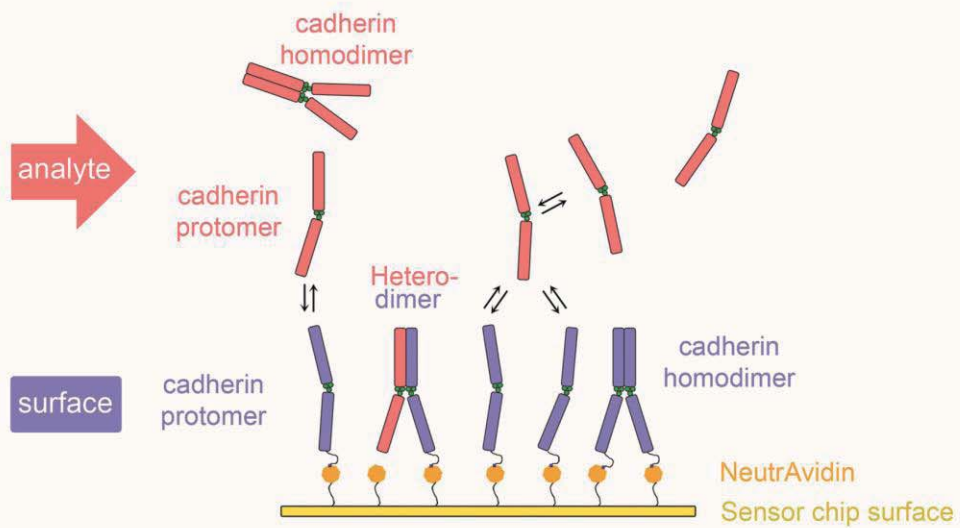


Figure 31: Surface Plasmon Resonance experiments with cadherins. One cadherin species is captured via its C-terminal Avi*bio tag (blue) by immobilized NeutrAvidin on the sensor chip surface. Untagged cadherin (red), the 'analyte' is injected over the surfaces. Due to the nature of cadherins, homodimers form both, in solution and on the surface. When cadherin protomers of the analyte phase bind to cadherins tethered to the surface, the overall mass on the surface changes, a binding signal is produced. Schematic adapted from Katsamba et al. (2009). EC domains are depicted as rectangular, calcium(II) by green circles.

AUC experiments homodimerization is ablated and the cadherins remained monomeric despite free unaltered N-termini (Table 16 (K_D of C-terminally tagged cadherins). Abrogation of binding might arise from the hydrophobic nature of the Avi-tag (GGGLNDIFEAQKIEWHE; biotinylation on Lys), which may interfere with protein folding or association. Thus, this tag was found to be unsuitable for these particular cadherins and a new approach was taken, in which proteins are tethered to the chip-surface by an antibody-antigen interaction. An eight amino acid FLAG- tag (DYKDDDDK) was chosen to replace the Avi*bio-tag on the VE-cadherin C-terminus. Purified VE-cadherin-FLAG (Section 2.1.2.3 and 3.3.3), was subjected to equilibrium AUC experiments to test for proper homodimerization and was found to dimerize with a K_D of $25.6 \pm 2 \mu\text{M}$, which a little weaker than that of the wild type protein but nonetheless indicative of binding (Table 16 and Table 10).

FLAG-antibodies were linked to the surface of the sensor chip by amine coupling and VE-cadherin-FLAG was captured on the surface by antigen - antibody recognition. However, VE-cadherin-FLAG proteins dissociated continuously from the surface after capture resulting in unreliable measurements (Figure 32a). Subsequently, three more FLAG-antibodies (Figure 32a, Table 2) with different specifications were tested which all resulted in a highly unstable surface. This problem might be due to a weak affinity of antibody-FLAG binding. Therefore, an alternative antigen-antibody pair, the C9-tag and the Rho 1d4 antibody, were tried for VE-cadherin and additionally for N-cadherin, a protein for which SPR studies can be conducted as a positive control. This tag has, like the FLAG tag, mostly hydrophilic residues and is composed of nine residues with the sequence TETSQVAPA (Table 16). AUC experiments of N-cadherin-C9 and VE-cadherin-C9 confirmed that homodimerization is not impaired and K_D s are in the same range as those of wild type proteins (Table 16). In the same experimental set-up as for the FLAG-experiment, 1d4 antibodies were amine coupled to the CM4 sensor chip and either N-cadherin-C9 or VE-cadherin-C9 captured on the surfaces by the C9-1d4 interaction. The diffusion of C9-tagged protein off the chip was monitored and found to be highly similar to that of the FLAG-tagged protein (Figure 32b, the C9 diffusion), so the C9-tag is also unsuitable for the desired experiments.

Table 16: Dissociation constants (K_D) for homodimerization of C-terminally tagged classical type I and II cadherins EC1-2 from mouse. Standard Error is reported.

Protein	Description	K_D [μM]
VE-cadherin-Avi*bio	GGGLNDIFEAQKIEWHE ^a	Monomer
Cadherin-11-Avi*bio	GGGLNDIFEAQKIEWHE ^a	Monomer
Cadherin-6-Avi*bio	GGGLNDIFEAQKIEWHE ^a	2.9±0.3
N-cadherin-Avi*bio	GGGLNDIFEAQKIEWHE	9.2±1.3
VE-cadherin-FLAG	DYKDDDDK	25.6±2.0
VE-cadherin-C9	TETSQVAPA	42.4±3.8
N-cadherin-C9	TETSQVAPA	24.2±0.73
VE-cadherin-CYS	GGGC	5.17±0.25
N-cadherin-CYS	GGGC	9.50±0.76 ^b

^a Biotin is added to lysine. ^b K_D also reported in Section 5.1.

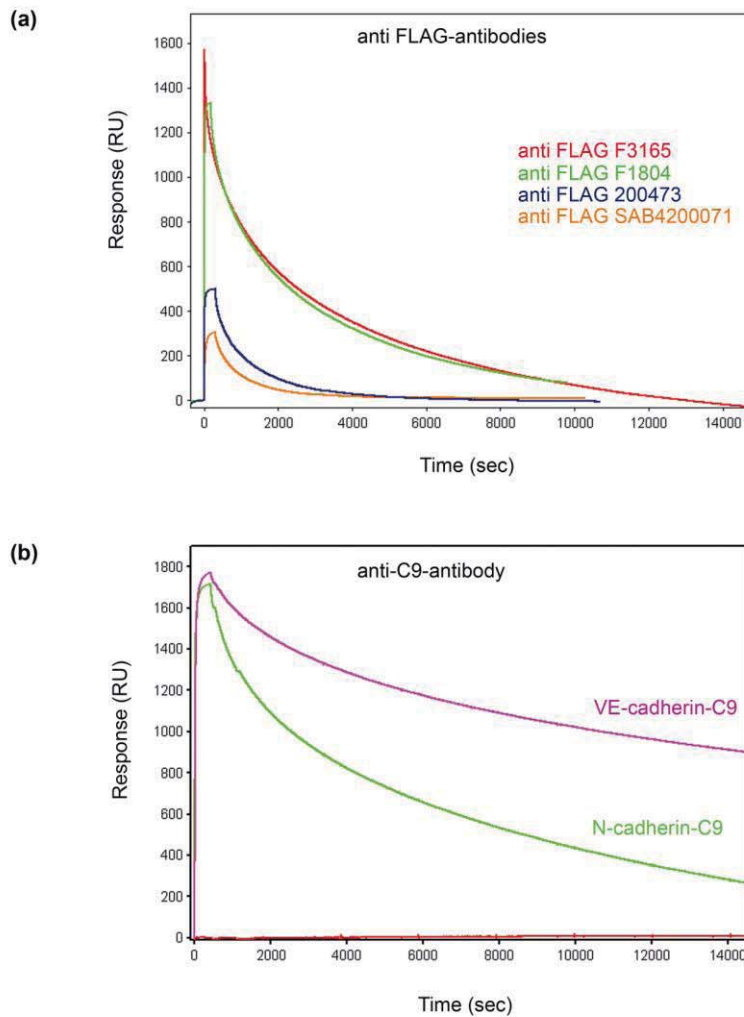


Figure 32: Stability of antibody captured VE-cadherin-FLAG and VE- and N-cadherin-C9 surfaces. (a) Profile shows surface stability of VE-cadherin-FLAG captured by four different anti-FLAG antibodies (see Table 2), names of antibodies indicated on diagram. None of the anti-FLAG-antibodies provides a stable VE-cadherin-FLAG surface, resulting in decreasing cadherin quantities on the sensor chip surface during each experiment. (b) Depicted is the stability of the C9-1d4 antigen-antibody pair for VE-cadherin-C9 (purple) and N-cadherin-C9 (green). Similarly to panel (a), surfaces are highly unstable, cadherin-C9 constantly diffuses off the surface. None of the antibody captures is sufficiently stable for quantitative relative binding experiments required for our studies (see text for detail).

For studies centered on the comparison of relative binding, a stable surface is a necessity, so a different approach was needed. Covalent amine coupling of cadherin proteins to the surface is not suitable as these proteins need to have free, unaltered N-termini and need to be positioned ‘upright’ on the chip. A milder covalent coupling method targets free thiol groups from cysteine side chains instead of free amine groups on lysine side chains or N-terminal amino groups. This method was considered suitable for VE-cadherin as there is no cysteine group in the native EC1-2 protein. A single amino acid-tag, the CYS-tag (GGGC) was designed and added to the C-terminus of N- and VE-cadherin (Section 3.3.3). AUC experiments of VE- and N-cadherin-CYS confirmed functionality of the proteins as they homodimerize with affinities in the same range of those of wild type proteins (Table 16). To see if the CYS-tag is adequate for the desired experiments, we first conducted cadherin binding studies with N-cadherin-CYS and native wild type N-cadherin at different concentrations, because binding profiles for comparative reasons using N-cadherin-Avi**bio* were available (Katsamba et al., 2009).

In order to couple the proteins chemically to the sensor chip surface, they first needed to be bound via ionic interactions to the negatively charged CM-dextran surface. In solution pH lower than the pI of the protein surface, proteins are positively charged and can be pre-concentrated in the CM-dextran moiety of the chip. To find the optimal pH in which most protein accumulates on the surface, N-cadherin-CYS is diluted into different solution pHs in the range of 3.5-5.0 and flown over the sensor chip. Figure 33a shows that proteins at pH4.0 yielded the highest binding response in comparison to other solution pH, which was then used to pre-concentrate N-cadherin-CYS on the chip prior immobilization. As described in more detail in methods Section 2.2.7.2, the carboxyl groups on CM-dextran were activated with NHS/EDC (Figure 33b (1)) and prepared with PDEA to introduce reactive disulfide groups (Figure 33b (2)). After chip surface activation, N-cadherin-CYS is coupled to the chip (Figure 33b (3)) and the remaining free thiol groups were blocked by L-cysteine (Figure 33b (4)). A total of 1,542 RU of N-cadherin-CYS was covalently bound to the surface (Figure 33b) and the surface was found to be stable with no dissociation like in antibody-antigen experiments observed (Figure 32a (FLAG-tagged cadherin), 32b (C9-tagged cadherin)).

We conducted a homophilic binding N-cadherin experiment with a 3-fold dilution series of concentrations in the range of 40-0.49 μ M of wild type N-cadherin as analyte. The binding profile is depicted in Figure 33c and shows concentration dependent binding behavior highly

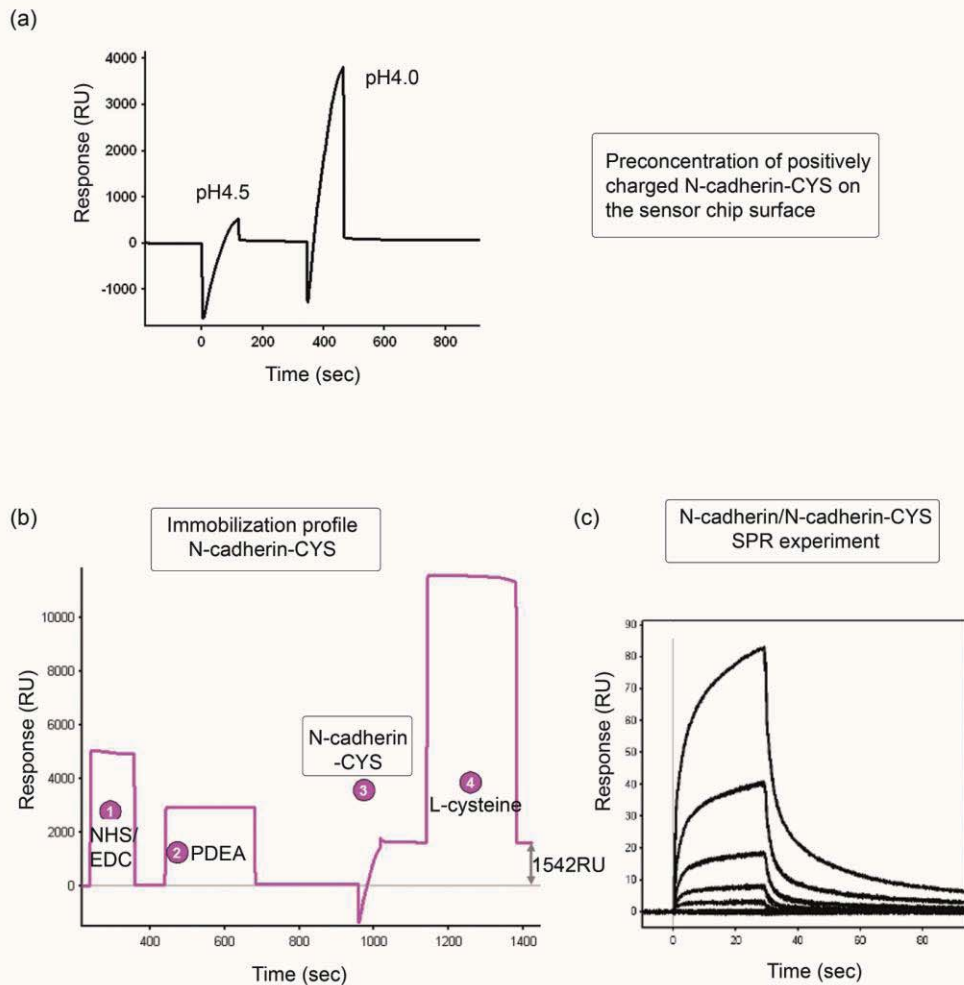


Figure 33: Analysis of N-cadherin-CYS in SPR binding experiments. (a) Preconcentration of N-cadherin-CYS on the CM-dextran surface. Tagged cadherin is injected over the unmodified surface in different pH-acetate buffers. In pH4.0 protein is sufficiently positively charged and concentrates via ionic interactions on the chip surface. (b) Immobilization profile of preconcentrated N-cadherin-CYS via thiol coupling (purple trace). Numbers correspond to reaction scheme for thiol immobilization: 1- activation of CM-dextran with NHS/EDC, 2-introduction of reactive disulfides using PDEA, 3-thiole coupling of reduced N-cadherin-CYS to the surface, 4-deactivation of excess disulfides with L-cysteine. Note that covalent binding of cadherin to the dextran moiety results in a stable surface. 1,542RU corresponds to the total amount of cadherin captured. Grey line marks 'empty' surface. (c) Binding profile of N-cadherin over N-cadherin-CYS surface. Binding is dependent on analyte concentration and is reminiscent of previous N-cadherin homophilic SPR binding studies. Thus the designed C-terminal CYS-tag and thiole coupling are a suitable method to tether functional cadherins to sensor chip surfaces in SPR experiments.

similar to the published results of N-cadherin-Avi**bio* (Katsamba et al., 2009). Due to chemical covalent binding, surfaces were stable during the experiments.

These findings prompt the conclusion that the designed CYS-tag is a new, suitable tag for cadherin binding experiments performed with SPR. We proceeded to use this tag to conduct studies of VE-cadherin binding behavior.

6.2.2 Identification of running buffer for VE-cadherin in SPR experiments

In order to identify cadherin-specific binding, any unspecific binding of VE-cadherin analyte to the chip needs to be disrupted. We passed wild type mouse VE-cadherin in a buffer composed of 150mM NaCl, 10mM Tris-Cl pH8.0, 3mM CaCl₂ over an unmodified chip-surface and observed strong unspecific binding between VE-cadherin and the unmodified CM4 surface (Figure 34a, left panel, unspecific binding). To decrease unspecific interactions, 0.25mg/mL Bovine serum albumin was added to the running buffer and the experiment was repeated. No binding to the unmodified surface could be detected (Figure 34a, right panel, no unspecific binding). Therefore, running buffer for all subsequent experiments was 150mM NaCl, 10mM Tris-Cl pH8.0, 3mM CaCl₂ and 0.25mg/mL Bovine serum albumin.

6.2.3 Assessing homophilic VE-cadherin binding in SPR-experiments

In order to analyze VE-cadherin homophilic and heterophilic binding, VE-cadherin-CYS was immobilized on the CM4 sensor chip as described for N-cadherin-CYS (Section 6.2.1 and 2.2.7.2). As shown in Figure 34b (immobilization) two different flow cells were prepared with distinct concentrations, 1,575RU (low surface, red trace) and 4643RU (high surface, green trace). As observed in the N-cadherin experiment, the surface is stable as VE-cadherin-CYS does not diffuse off the surface due to covalent immobilization (Figure 34b).

Native VE-cadherin was injected over these surfaces in a concentration range of 40μM to 78.1nM in a two-fold dilution series.

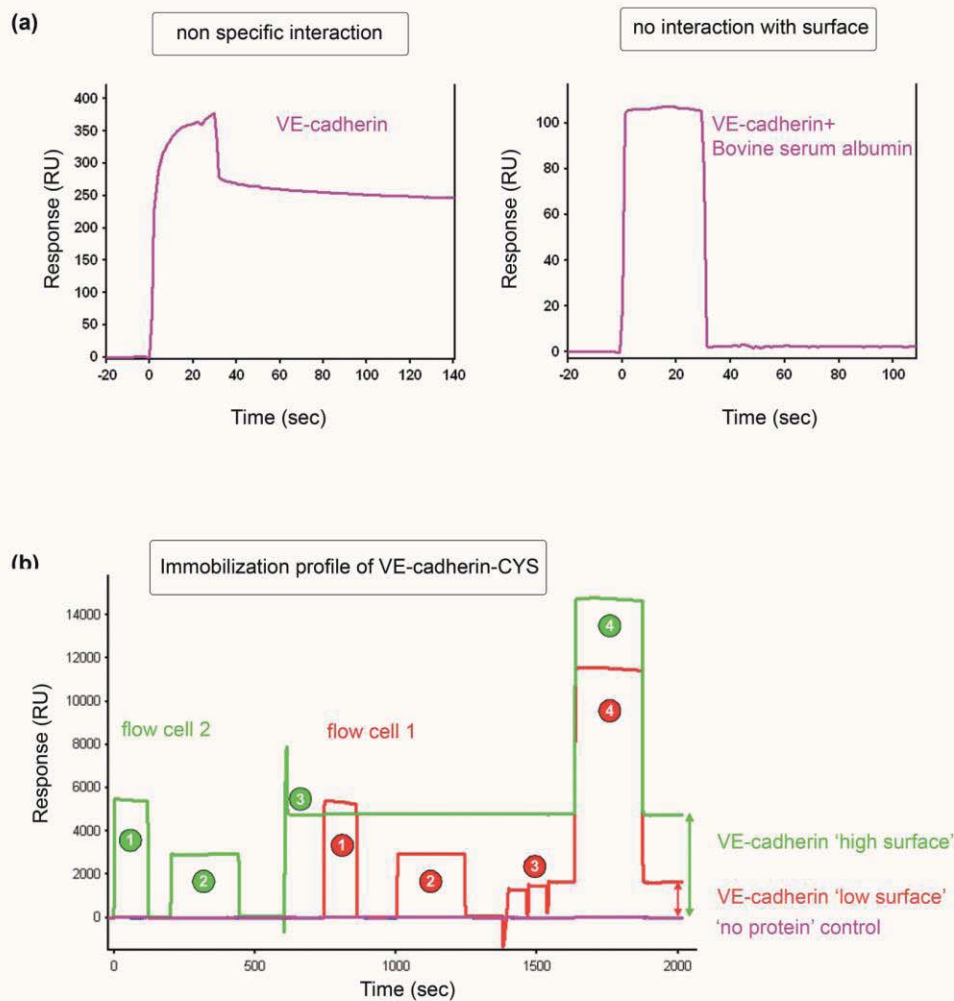


Figure 34: Preparations for VE-cadherin SPR experiments. (a) Determination of correct running buffer. Untagged VE-cadherin unspecifically binds to the unmodified CM-dextran surface (left panel) to minimize unwanted interactions bovine serum albumin is included in the running buffer. Traces show, that VE-cadherin can only be observed during injection (right panel) and no unspecific binding occurs (right panel). (b) VE-cadherin-CYS is immobilized on the sensor chip surface using thiole coupling. Cadherin-CYS is prior immobilization preconcentrated in CM-dextran in acetate buffer at pH4.0 like shown for N-cadherin-CYS. Numbering is identical to that in Figure 33. Two different surfaces are prepared: a high quantity VE-cadherin-CYS surface (4,643RU, red trace, flow cell 1) and a low quantity surface (1,575RU, green trace, flow cell 2). A 'no protein' control serves as reference (same surface treatment, no VE-cadherin).

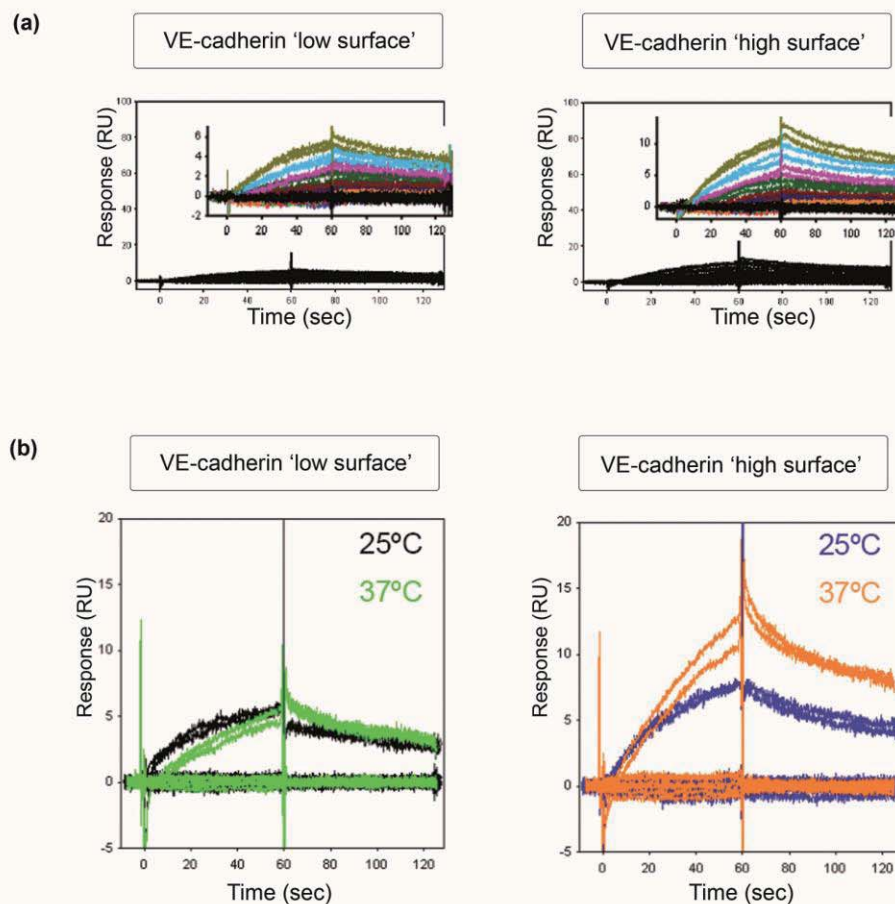


Figure 35: Homophilic binding of VE-cadherin EC1-2 tested in SPR experiments. (a) Binding response shown for VE-cadherin injections over low (left panel) and high (right panel) concentrations of VE-cadherin-CYS on the surface. Different colored traces correspond to a concentration range of 40-0.78 μM in a 2fold dilution series. Inset are close up views of the same binding profiles. Note that VE-cadherin binding response is dependent on concentrations of the analyte and protein on the surface, suggesting homophilic binding. Profiles are reminiscent of those of type II cadherin-6. Though it appears that VE-cadherin homodimerization has 'slow' kinetics in terms of 'on' and 'off' rates. All injections were performed in duplicates, black trace is buffer blank injections. (b) VE-cadherin was injected over the same surfaces at a concentration of 40 μM at 25°C (black trace left panel, blue trace right panel) and 37°C (green trace in left and orange trace in right panel, respectively). Binding responses increase especially for high surface concentrations of VE-cadherin (right panel), but duplicate injections become less reproducible. Due to increase of binding at higher temperature, suggesting acceleration of kinetic on/off rates, it appears that VE-cadherin has a kinetic behavior different from that of other classical cadherins.

A binding response was observed (Figure 35a) in shape reminiscent to that of type II cadherin-6 (Figure 36, (Harrison et al., 2010a)). The binding response produced is approximately 5RU for the low and ~10RU for the high concentration surface and was observed in two independent runs and two independent experiments. The binding response is above the background level, but because it is only ~10RU, it cannot be confidently attributed to homophilic cadherin binding. The low binding response is surprising because both the tagged and analyte VE-cadherin fragments used in the experiments are known to form homodimers in AUC experiments (Table 16). However, VE-cadherin mediates adhesion with very high affinity in comparison to other classical cadherins (Sections 4.2, 5.1 and 6.1), so it is possible, that most of the analyte VE-cadherin molecules and the ones immobilized on the chip are homodimerized leaving only very few proteins present as monomers that are available for interactions (Section 6.2). This would strongly inhibit the binding response only in the case that association and dissociation kinetics of the dimers were insufficiently rapid that little or no exchange between dimers occurs in the time frame of the experiment (~1 minute). This led us to suspect that VE-cadherin binding might be kinetically different from that of other type II cadherins. Type II cadherin-6 appears to have a slower on- and off-rate than type I N-cadherin as suggested by the shallower association and dissociation SPR curves (Figure 33c, Figure 36), but it appears that the rates for VE-cadherin are even lower. Therefore, we tried to shift homodimerization kinetics into a more favorable area by raising the temperature in which experiments are conducted from 25°C to 37°C based on the idea, that higher temperature should accelerate on/off rates and therefore increase availability of free monomer in solution and on the surface. Indeed, it could be observed that binding responses are increased at 37°C and when comparing VE-cadherin high-surface and low-surface result, it appears that the binding response is still concentration dependent (Figure 35b). However, this set-up could not be used in further studies because after temperature increase, reproducibility of the binding responses suffered. This experimental outcome, together with the findings that VE-cadherin and VE-cadherin-CYS are capable of homodimerization in AUC (Table 16) and in addition to size exclusion experiments showing an elution profile of two separate peaks for monomer and dimer (Section 4.3, Figure 16), clearly suggests that low binding responses are produced by unfavorable kinetics for this type of experiment. This phenomenon has also been observed before for cadherins with impaired X-dimer interfaces, which like VE-cadherin failed to produce a strong binding response in SPR experiments despite the fact that they were found to dimerize in AUC and size exclusion studies (Harrison et al., 2010a).

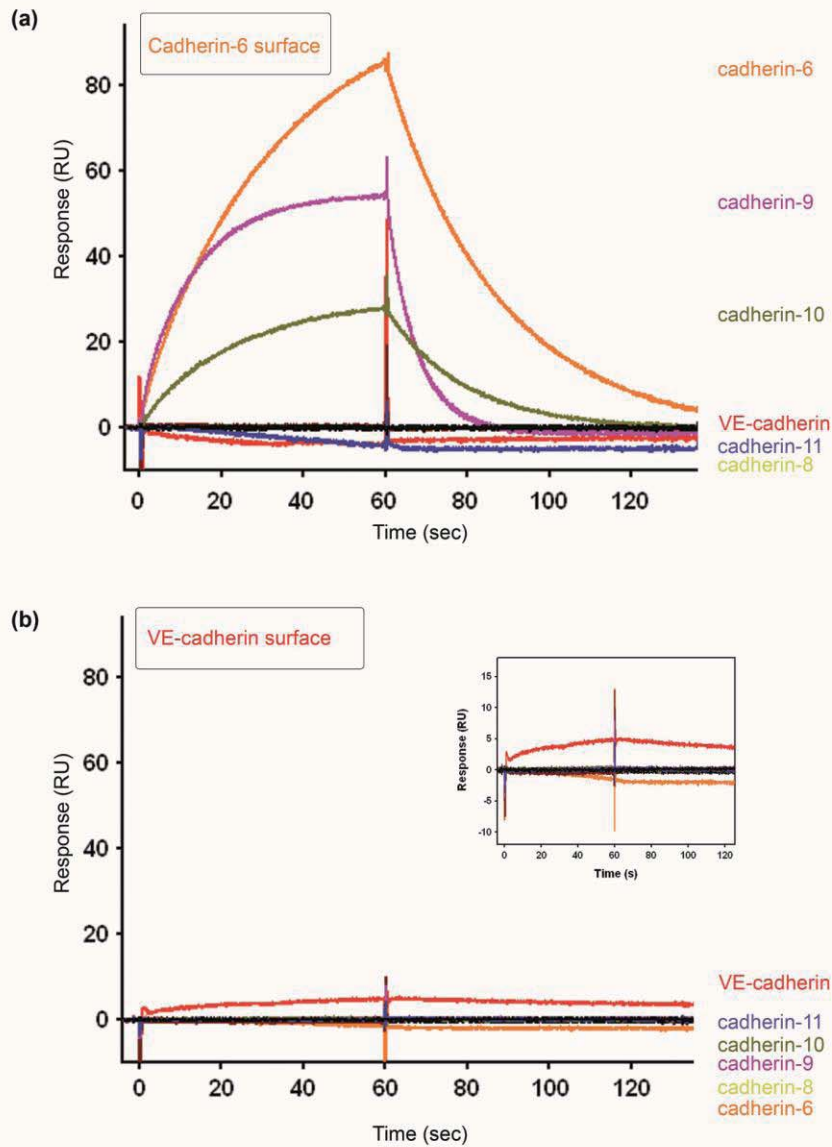


Figure 36: Homophilic and heterophilic type II cadherin binding assessed by SPR experiments. (a) Cadherin-6-Avi*bio is captured on the sensor chip surface and analyte cadherins -6, -8, -9, -10, -11 and VE-cadherin are injected over the surface at calculated free monomer concentrations of 12 μ M. Strongest observed relative binding is homophilic: cadherin6/cadherin-6-Avi*bio (84RU). Strong heterophilic binding can be observed between cadherin-9 and cadherin-6-Avi*bio (54.1RU) and cadherin-10 and the surface (27.6RU). For cadherin-8, 11 and VE-cadherin was no binding response observed. Heterophilic binding observed in this experiment mirrors results of cell-cell-aggregation assays conducted by Shimoyama et al. (2002). (b) The same set of cadherins at identical concentrations as in panel (a) were injected over a VE-cadherin-CYS surface. A binding response is found between VE-cadherin/VE-cadherin (4.8RU). Inset is a close up view of the VE-cadherin binding response, similar to that observed in our initial experiments. Cadherin-6 does not bind heterophilically to VE-cadherin, which corresponds to the experiment in panel (a). None of the other type II cadherins was found to heterophilically interact with VE-cadherin suggesting incompatible specificity. See text for details.

6.2.4 Homophilic and heterophilic adhesive binding of type II cadherins

Cell aggregation studies by Shimoyama et al. (2000) revealed a heterophilic binding specificity pattern for type II cadherins (see Introduction 1.6 and Section 6.2, see also: (Patel et al., 2006; Price et al., 2002)) and SPR was used successfully as method to analyze heterophilic binding of type I N- and E- cadherin (Katsamba et al., 2009). Now we wanted to test if it is also applicable to type II mediated heterophilic binding. It was interesting to examine heterophilic binding between VE-cadherin and other type II cadherins, as VE-cadherin docks Trp2 and Trp4 into an acceptor pocket nearly identical to type II cadherins, but has outside this region a substantially different interface. We decided to assess relative heterophilic adhesive cadherin binding between a set of seven mouse type II cadherins as analytes: cadherin-6, -8, -9, -10, -11 and VE-cadherin to captured cadherin-6-Avi*bio or immobilized VE-cadherin. Notably, cadherin-6, -9, -10 and cadherin-8, -11 share high sequence identity within these subgroups and are closely related by phylogenetic analysis (Table 15 and Figure 30).

Cadherin-6-Avi*bio dimerizes in AUC experiments with a K_D of $2.9 \pm 0.3 \mu\text{M}$ similar to that of the wild type protein and was used previously to study cadherin adhesive interactions (Harrison et al., 2010a; Katsamba et al., 2009). Type II cadherin-6-Avi*bio is captured by NeutrAvidin immobilized on the CM4 sensor chip, which leaves the two domain cadherin fragments oriented in an upright position with their adhesive EC1 domain easily accessible. In order to compare relative binding of different type II cadherins to each other, the concentrations for each analyte were chosen according to their K_D , in order to have equal amounts of calculated free monomer present in SPR experiments. Concentrations for all analyte proteins used in this experiment are summarized in Table 17.

Table 17: Summary of analyte proteins and their concentrations and distribution of monomer and dimer for SPR experiments.

Protein	Protein concentration [μM]	K_D[μM]	Concentration dimer [μM]	Concentration monomer [μM]
VE-cadherin EC1-2	141.8	2.2	64.9	12
Cadherin-6 EC1-2	104	3.13	45.0	12
Cadherin-8 EC1-3	31.2	15	9.6	12
Cadherin-9 EC1-2	30.1	17	8.9	12
Cadherin-10 EC1-2	18.8	42.2	3.4	12
Cadherin-11 EC1-2	20.5	33.8	4.3	12

Binding of each of the cadherin-analytes to immobilized cadherin-6-bio was tested over a time course of 1 minute at 25°C in two repeats with three buffer injections in between sample injections. Wild type, untagged cadherin-6 gives a specific homophilic binding response of 84RU (Figure 36a) which is almost identical to that seen in previously conducted studies (Harrison et al., 2010a; Katsamba et al., 2009). Remarkably, cadherin-9 and cadherin-10 could also be observed to bind to captured cadherin-6 with heterophilic binding responses of 54RU and 28RU, respectively (Figure 36a). In contrast, cadherin-8, -11 and VE-cadherin failed to bind and no response above background could be detected.

In a second experiment, we wanted to investigate if heterophilic binding between VE-cadherin and other type II subfamily members could be detected when VE-cadherin is immobilized on the surface. VE-cadherin-CYS was immobilized as described in the previous section (Figure 34b) and the same set of analytes (Table 17) was consecutively injected. Wild type VE-cadherin produced the typical low homophilic binding response as described in Section 6.2.3 (Figure 35a). However, no binding was detected for cadherin-6, -8, -9, -10 and -11 (Figure 36b) confirming the previous VE-cadherin-cadherin-6-Avi**bio* result.

The observation that VE-cadherin does not bind to captured cadherin-6 or to cadherin-6, -8, -9, -10 and -11 when immobilized on the surface may suggest that VE-cadherin does not engage in heterophilic interactions with other members of the type II cadherin subfamily, with the caveat that even homophilic VE-cadherin binding can only be weakly detected by SPR

probably due to kinetic reasons. Ergo, heterophilic interaction between VE-cadherin and other type II subfamily members might occur, but in relation to an already weak wild type binding response, this result is inconclusive. This issue could be addressed by alternative functional assays such as immunoprecipitation and cell-cell aggregation, which allow longer contact of proteins with each other and are less dependent on binding kinetics.

More broadly, the results of the SPR experiments regarding type II cadherin heterophilic binding on a molecular level correlate perfectly with binding specificities obtained from cell-cell aggregation studies and reveal more subtle differences in binding between related cadherins (Shimoyama et al., 2000). Type II cadherins exhibit a high degree of specificity in heterophilic binding mirroring the phylogenetic tree despite the fact that they all share high levels of sequence identity in their adhesive domains (Table 15). In particular, our results indicate that the separate subgroups of cadherin-6,-9,-10 and cadherin-8,-11 may show binding within but not between groups. Within the cadherin-6,-9,-10 group it appears that even minor sequence differences translate into distinct binding specificity. In general, SPR experiments could be shown to be suitable to assess type II cadherin heterophilic binding properties in a quantitative fashion, which can in future be extended to the entire set of 13 type II cadherins.

6.3 Heterophilic adhesive binding between type I subfamily members and VE-cadherin

Published cell-cell aggregation, SPR and domain shuffling experiments have shown that, while adhesive heterophilic binding is detectable in certain combinations within type I and type II cadherin subfamilies, heterophilic interactions between type I and type II subfamilies are not detected ((Katsamba et al., 2009; Patel et al., 2006; Shimoyama et al., 1999; Shimoyama et al., 2000) and Introduction 1.6). Molecular binding between VE-cadherin and type I cadherins has not been investigated, however, experiments focused on interactions between VE-cadherin and type I subfamily members in the vascular endothelium revealed that VE-cadherin expels from adherens junctions type I N- and P-cadherin, which are *in vivo* co-expressed with VE-cadherin on vascular endothelial cells (Jaggi et al., 2002) and Introduction 1.8.2). To test if there are interactions on a molecular level between adhesive EC1-2 fragments of VE-cadherin and those of type I cadherins, we tested E-, N- and P-

cadherin for potential heterophilic interactions with immobilized VE-cadherin-CYS in SPR assays. Immobilized N-cadherin-CYS was used as a control.

One N-cadherin and two VE-cadherin surfaces (low and high concentration) were prepared as described in Section 6.2 (Figure 33b for N-cadherin-CYS immobilization, 34b for VE-cadherin-CYS immobilization). When wild type, untagged N-cadherin was consecutively injected over the three described surfaces, a strong, concentration dependent homophilic binding response could be detected for the N-cadherin surface, as expected (see Section 6.2). Interestingly, strong binding was also detected between the N-cadherin analyte and both VE-cadherin surfaces. Binding was well above 10RU, thus is likely to represent specific heterophilic binding. We also found that the binding was concentration dependent for both N-cadherin in solution and immobilized VE-cadherin (Figure 37). When soluble, untagged E-cadherin was injected as analyte no binding occurred on VE-cadherin surfaces (Figure 37), but a heterophilic binding response was observed on the N-cadherin surface, which is in agreement with results of previous N- and E-cadherin heterophilic binding studies (Figure 37, (Katsamba et al., 2009)). When P-cadherin was used as the analyte, heterophilic binding to VE- and N-cadherin was detected as minimal binding below 10RU on all three surfaces, with strongest binding, approximately 4RU, to N-cadherin (Figure 37). Lastly, we tested wild type T-cadherin binding to type I N-cadherin and II VE-cadherin, with the result, that no binding could be observed (Figure 37), suggesting that background non-specific binding levels are low such that even minimal binding responses found in these experiments should correspond to specific heterophilic interactions.

N-cadherin bound heterophilically to VE-cadherin surfaces, so we tested if VE-cadherin as analyte would also bind to immobilized N-cadherin. Results showed that only a very minimal binding response could be detected in this combination, which nevertheless was dependent on analyte concentrations (Figure 38). VE-cadherin was suggested to have unfavorable kinetics for SPR experiments (Section 6.2.3), which might explain, why no heterophilic interactions could be observed with VE-cadherin as analyte based on the assumption that molecules can be 'trapped' by slowed kinetics in a dimer state in the analyte more readily than in the immobilized layer.

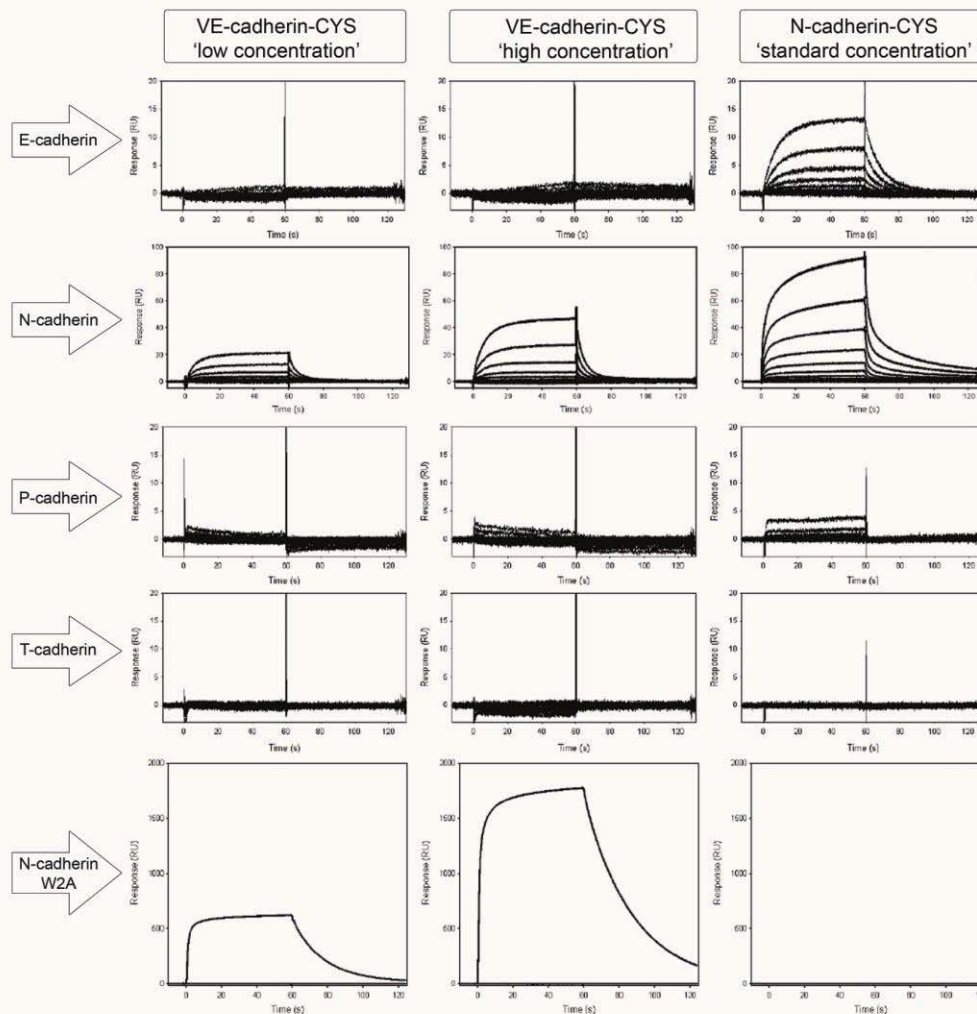


Figure 37: Heterophilic binding of classical type I cadherins E-, N- P- cadherin including N-cadherin strand swap mutant W2A and atypical T-cadherin to type II VE-cadherin and type I N-cadherin. VE-cadherin-CYS (left and middle panel, low and high surface concentration) and N-cadherin-CYS (right panel) were immobilized on the surface as described in Figure 34 and 33, respectively. Shown are from top to bottom panel recorded binding responses of injections of analyte proteins (arrows) at concentrations of 40-0.78 μ M in a 2fold dilution series: type I E-, N-, P-cadherin and atypical T-cadherin. Heterophilic binding responses were found for E- and N-cadherin corresponding to previously published data by Katsamba et al. (2009). N-cadherin interestingly heterophilically interacts with VE-cadherin (21RU left and 46RU middle panel), homophilic N-/N-cadherin binding was also observed. P-cadherin produced a minimal but concentration dependent binding response to VE-cadherin and to N-cadherin (~4RU). Note that VE-, N- and P-cadherin are co-expressed *in vivo* in vascular endothelial cells. Atypical T-cadherin failed to bind to all three surfaces. To test if heterophilic binding between N-/VE-cadherin is mediated by strand swapping, strand swap impaired N-cadherin mutant W2A was injected over all three surfaces (bottom panel) at a single concentration of 40 μ M. N-cadherin W2A produced exorbitant binding responses of 680RU and 1900RU for immobilized VE-cadherin. No binding occurred to N-cadherin (see text for detail).

VE-cadherin has a divergent strand swapped adhesive interface in comparison to type I cadherins, so we tested if the N-/VE-cadherin interaction is dependent on the strand swap mechanism. We used strand swap impaired mutant N-cadherin W2A (Katsamba et al., 2009; Tamura et al., 1998) as the analyte, which was injected over the high and low concentration VE-cadherin surfaces and the N-cadherin surface. We recorded no binding response between N-cadherin mutant W2A and immobilized N-cadherin consistent with prevention of strand swapping. In contrast, strand swapping impaired N-cadherin W2A mutant bound to a high level to VE-cadherin surfaces, which was approximately 35-40fold stronger than the heterophilic binding observed for similar analyte concentrations of wild type N-cadherin, (Figure 37). This heterophilic interaction was also concentration dependent with regard to both VE-cadherin concentration on the surface and analyte mutant N-cadherin concentration, suggesting that this interaction is not artifactual.

Overall, we found that VE-, E- and T-cadherin do not heterophilically interact, but minimal heterophilic interaction between P- and VE-cadherin occurred. Interestingly, N-cadherin and VE-cadherin show strong heterophilic interactions, which can be dramatically enhanced by impairing strand swapping in N-cadherin. Notably, the type I cadherins to which VE-cadherin binds, N-cadherin and P-cadherin, are *in vivo* both present in vascular endothelial cells along with VE-cadherin. In these cells, VE-cadherin is found to expel N-cadherin from junctions, leaving it dispersed over the cell surface (Gentil-Dit-Maurin et al., 2010; Jaggi et al., 2002). Therefore, it is possible that the observed heterophilic interactions may be important *cis* interactions and not adhesive *trans* interactions, supported by the data that N-cadherin wild type and mutant both bind well to immobilized VE-cadherin.

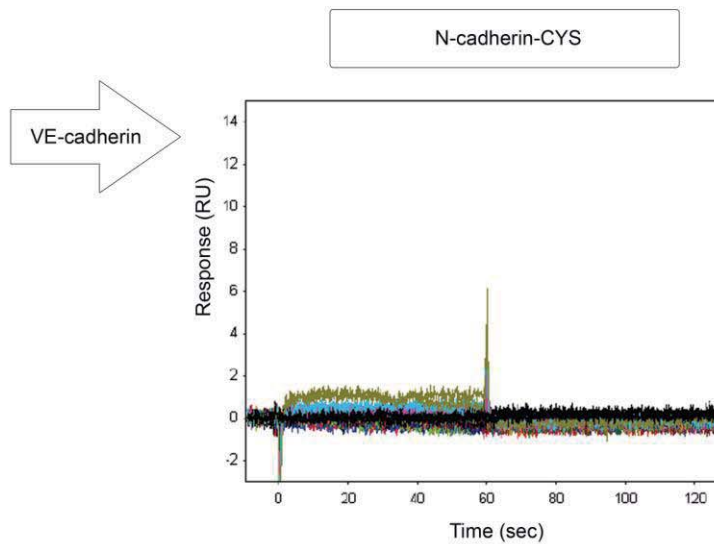


Figure 38: Heterophilic binding of VE-cadherin to immobilized N-cadherin-CYS. Binding response of less than 2RU was observed for the highest two concentrations (40 μ M and 20 μ M, respectively) of VE-cadherin analyte. This is in contrast to the substantial binding response was recorded when N-cadherin was flown over immobilized VE-cadherin-CYS surfaces (Figure 37). Although the recorded traces are extremely weak, they do appear to be dependent on VE-cadherin analyte concentration. Strong homodimerization behavior observed for VE-cadherin with unfavorable kinetics might be the reason, that the binding response is low in this experiment. See text for detail.

6.4 Co-immunoprecipitation assays to detect cadherin high affinity binding

Mouse VE-cadherin EC1-2 produced only minimal binding responses in the SPR experiments described above, but these proteins adhere homophilically with strong affinities in low micromolar range in equilibrium AUC experiments (Section 4.2 and 5.1) and therefore the low SPR response may be due to kinetic effects as discussed in Section 6.2. We sought a complementary method which like AUC can detect cadherin interactions over long time periods and is relatively insensitive to kinetic effects, but that is, like SPR, suitable for detection of both, homophilic and heterophilic interactions. Thus, we conducted co-immunoprecipitation (co-IP) experiments with soluble purified cadherin EC1-2 fragments at high concentrations.

C-terminally tagged two domain cadherins were used in the assays to provide accessible, not sterically impaired antigens for immunoprecipitation and antibody detection. For E- and N-cadherin we used Avi*bio-tags (E-, N-cadherin-Avi*bio), FLAG-tags were used for VE-cadherin (VE-cadherin-FLAG) and C9-tags for VE- and N-cadherin (VE-, N-cadherin-C9). All proteins were previously confirmed by AUC to be able to dimerize in solution with K_{DS} similar to that of wild type untagged proteins (Table 16 in Section 6.2.1).

First, we conducted co-IP assays of homophilic adhesive cadherin binding. Equimolar quantities of N-cadherin-Avi*bio and N-cadherin-C9 were incubated together over a time of three hours to allow dimer formation. The complexes were precipitated by the immune reaction of 1d4 antibody recognizing C9-antigen tagged N-cadherin and pulled down with protein G coated magnetic beads. The pulled down proteins were separated by SDS-PAGE, transferred by western blot and presence of biotinylated N-cadherin in immunoprecipitates and supernatants was detected using NeutrAvidin-HRP (Figure 39). We found biotinylated N-cadherin-Avi*bio in immunoprecipitates of N-cadherin-C9 (Figure 39a Lane 3 and Figure 39b Lane 1), showing that differently tagged N-cadherin proteins dimerized and that these associations were sufficiently stable to be detected in this assay. A negative control, containing only biotinylated N-cadherin, protein G and 1d4 antibody, did not show presence of biotinylated N-cadherin in immunoprecipitates, thus, no unspecific binding between magnetic beads and N-cadherin-Avi*bio and NeutrAvidin-HRP occurred (Figure 39b, Lane 2). These data show that co-immunoprecipitation assays are a suitable method to detect cadherin adhesive binding.

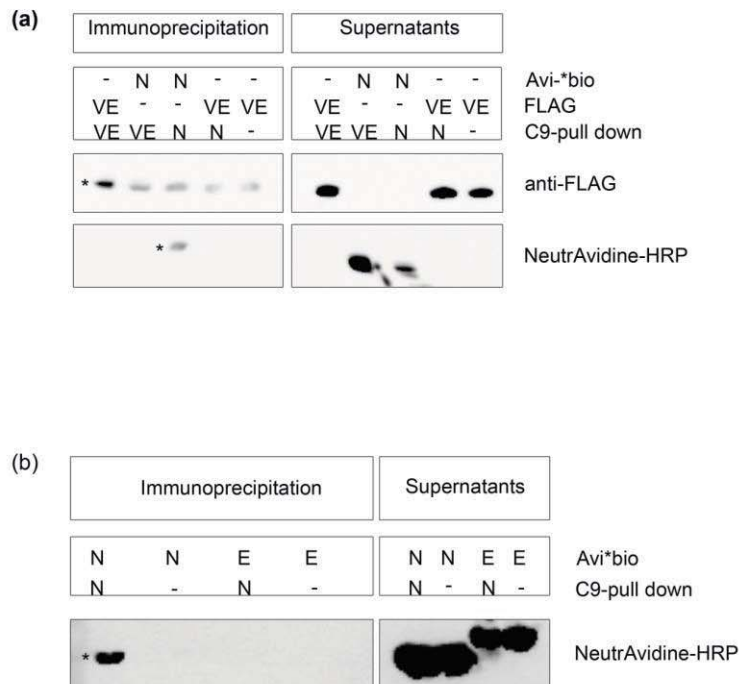


Figure 39: Homophilic and heterophilic cadherin interactions tested in Co-immunoprecipitation assays. (a) VE-cadherin and N-cadherin homophilic and heterophilic binding tested. C-terminally C9-tagged proteins in complexes were pulled down with 1d4 antibodies. Top panel shows FLAG-labelled VE-cadherin. Note that in precipitates background noise at the same size of VE-cadherin occurs (cross reaction of secondary anti-mouse antibody). VE-cadherin-FLAG in lane 1 is well above background noise and can be considered the result of co-ip with VE-cadherin-C9. Biotinylated protein is visualized by NeutrAvidine-HRP in the bottom panel. N-cadherin was precipitated successfully by N-cadherin-C9. Here, too, no heterophilic binding is observed. (b) Biotinylated protein is detected by NeutrAvidine-HRP. Homophilic N-cadherin-Avi*bio/N-cadherin-C9 complexes were pulled down by 1d4 antibody. No heterophilic interactions between biotinylated E-cadherin and N-cadherin could be detected. Heterophilic interactions found in cell aggregation and SPR experiments appear to have a short life and are insufficiently stable to be detected by co-ip experiments. Asterisks denotes co-immunoprecipitated homophilic cadherin complexes. See text for detail.

We performed the same experiment for VE-cadherin, using VE-cadherin-FLAG and VE-cadherin-C9. Magnetic beads coated with antibodies against the C9 tag were used for immunoprecipitation (clone 1d4). VE-cadherin-FLAG was detected in the immunoprecipitates of VE-cadherin-C9 (Figure 39a Lane 1), and could not be detected in the negative control omitting the C9-tagged protein from the reaction (Figure 39a, Lane 5). Therefore, we can conclude that C-terminally tagged VE-cadherins have the ability to homophilically interact with each other. Co-IP experiments allow a long time for protein-protein interaction to occur, so that dimerization of VE-cadherin-C9 and -FLAG can reach equilibrium, potentially overcoming the 'slow' binding kinetics which we suggest to be the cause for only minimal binding responses in SPR experiments.

The homophilic binding results correlate with other biophysical data derived for adhesive cadherin binding, so in the same experiments we tested if heterophilic interactions can also be detected by this method. Therefore, the previously characterized heterophilic binding pair N- and E-cadherin were allowed to interact in form of E-cadherin-Avi*bio and N-cadherin-C9 (Figure 39b). In addition, we investigated heterophilic binding between VE-cadherin and N-cadherin observed in SPR using two combinations: N-cadherin-Avi*bio with VE-cadherin-C9 and N-cadherin-C9 with VE-cadherin-FLAG (Figure 39a). The complexes were pulled down with respective C9-tagged proteins and 1d4 antibody as described before, separated by SDS-PAGE and transferred by western blot. Biotinylated proteins were detected by NeutrAvidin-HRP and VE-cadherin-FLAG by anti-FLAG antibodies in immunoprecipitates and supernatants. E-cadherin-Avi*bio and VE-cadherin-FLAG, were only detectable in the respective supernatants, but not in any of the heterophilic immunoprecipitates (Figure 39a). This suggests that heterophilic cadherin binding, between N- and VE-cadherin or between N- and E-cadherin is too unstable to be detected in this assay system in comparison to homophilic interactions. Our findings suggest in concert with previous data (Shan et al., 2000), that only very stable, high affinity cadherin-cadherin interactions can be detected by co-immunoprecipitation experiments.

Chapter 7:
Homophilic adhesion
without the cadherin strand swap motif

Recently our group published results describing the role of a novel, non-swapped binding interface, named the ‘X-dimer’ interface, in T-cadherin adhesive binding in addition to a role for X-dimer formation in classical cadherin binding (Introduction 1.5, (Ciatto et al., 2010; Harrison et al., 2010a). Although I was not the first author, part of my thesis work contributed to both manuscripts and the impact will be addressed in this section.

7.1 Background and significance

In past extensive studies of the adhesive interface located on EC1 domains of classical type I and type II cadherins revealed that a three dimensional domain swapping mechanism underlies the homophilic binding, in which the N-terminal portion of the A*-strand, Trp2 (type I) or Trp2 and Trp4 (type II), is docked into an hydrophobic acceptor pocket of the partnering molecule. However, the two domain crystal structure of wild type chicken T-cadherin, an outlier of the classical cadherin family, revealed an adhesive dimer involving a similar face of domain EC1, but the region corresponding to the A*-strand of other classical cadherins was not strand swapped. This was named the ‘X-dimer’ interface due to the approximately cross shaped orientation of the protomers. Mutations targeting the novel interface based on the derived structural data were sufficient to abrogate T-cadherin dimerization in equilibrium AUC, SPR, cell aggregation and neuron outgrowth experiments (Ciatto et al., 2010), suggesting a biological role for this interface and supporting a model in which mature adhesive dimers of T-cadherin adopt an X shaped dimer configuration with no contribution of strand swapping.

To test this model different mutations targeted to the strand swap region analogous to mutations known to prevent strand swapping were introduced into T-cadherin and for comparison into E-cadherin (type I) and cadherin-6 (type II), both known to form adhesive interfaces involving A*-strand exchange between partnering molecules. These mutations should diminish adhesive binding in the cadherins which bind via strand swapping, but should have no effect on T-cadherin adhesive properties if the proposed model is correct.

7.2 Strand swap site directed T-cadherin mutations do not affect adhesive binding

We altered in T-, E- and cadherin-6 residues required for strand swap dimer formation in typical classical cadherins to observe the effects on homodimerization in equilibrium AUC

experiments. Several different point mutations were tested. Residues Trp2 (type I) and Trp2 and Trp4 (type II) are crucial for strand swapped dimerization and binding can be prevented by reduction of these side chains to those of alanine (Harrison et al., 2005). Thus, a W2A mutation was introduced into E-cadherin and a W4A mutation in cadherin-6 (single Trp mutation shown for type II VE-cadherin to abolish binding, (May et al., 2005)). In T-cadherin we changed Ile2, found at an equivalent position to that of Trp2 in strand swapping type I cadherins, and mutated it also to alanine. Another crucial interaction, which can be disrupted in order to prevent proper strand swapping, is the salt bridge between glutamic acid (at position 89 in E-cadherin) and the N-terminal amino group of the first residue, which stabilizes the A*-strand in the strand swap dimer conformation. Thus, the mutation E89A was introduced into E-cadherin, reducing the carboxyl side chain of Glu89 to that of alanine. In a different approach, we moved the N-terminal amino group further away from the stabilizing carboxyl group in order to disrupt salt bridge formation by extending the N-terminus of E-cadherin by two alanines (Ala-Ala extension) or methionine and arginine (Met-Arg-extension). Similarly, we extended the N-terminus of T-cadherin by a single glycine residue (Gly-extension) or by Met-Arg. In addition to these mutants targeting a single interaction in the strand swapped dimer, we created an E-cadherin mutant in which both two N-terminal residues Asp1 and Trp2 are deleted, which should prevent salt bridge formation (Asp1) and anchoring of the A*-strand (Trp2) at the same time.

The strand swap dimer targeted mutations were introduced into adhesive EC1-2 fragments of T-cadherin, E-cadherin and cadherin-6 proteins that were produced in bacteria (Section 2.1.2.3). Their homophilic binding was tested in sedimentation equilibrium AUC experiments in order to explore the effect of the introduced mutations. Determined affinities are summarized in Table 18 and profiles of sedimentation AUC experiments are presented in Figure 40. Wild type T-cadherin homodimerizes with a moderate affinity corresponding to a K_D of $41.4 \pm 1.7 \mu\text{M}$, which is in the same range of those of C- and E-cadherin ectodomains described previously, $64 \mu\text{M}$ and $109 \mu\text{M}$, respectively (Chappuis-Flament et al., 2001; Harrison et al., 2010b). Mutant proteins targeting potential strand swapping residues, T-cadherin I2A, Gly- and Met-Arg-extension, were found to form dimers in solution with K_{DS} similar to that of the wild type protein: $37.1 \pm 4.1 \mu\text{M}$ (I2A), $16.5 \pm 0.8 \mu\text{M}$ (Gly-extension) and $34.1 \pm 6.3 \mu\text{M}$ (Met-Arg-extension). Thus, strand swap interface targeted mutations did not inhibit T-cadherin homodimerization significantly. In contrast, equivalent mutations introduced into E-cadherin and cadherin-6 showed strong effects on their homodimerization

behavior and diminished adhesive binding affinities markedly (Figure 40b,c). In strand swap E-cadherin mutant W2A a ten fold decrease of affinity in comparison to that of wild type protein occurred (Figure 40, Table 18) and for cadherin-6 the wild type affinity was decreased by the strand swap W4A mutation even more significantly, resulting in a 100fold weakened affinity of $321\pm 0.5\mu\text{M}$ (Figure 40c, Table 18). The Ala-Ala-extension mutant interfering with the stabilization of the swapped A*-strand and the Asp-Trp deletion E-cadherin mutant, removing part of the swapping strand, diminished the homodimerization properties similarly, resulting in K_{DS} of $811\pm 97\mu\text{M}$ and $662\pm 28.5\mu\text{M}$, respectively. A less severe effect is seen for the E-cadherin E89A mutation, which weakened the affinity approximately by 2.5fold (Figure 40b, Table 18).

Table 18: Dissociation constants K_{DS} from equilibrium AUC analysis for cadherin-6, E- and T-cadherin wild type and strand swapping mutants. Standard error is given.

Protein	Description	K_{D} [μM]
Cadherin-6 EC1-2		
Mouse cadherin-6 EC1-2 ^a	Wild type	3.1 ± 0.1
Mouse cadherin-6 EC1-2 W4A	Strand swapping mutant	321 ± 0.5
E-cadherin EC1-2		
Mouse E-cadherin EC1-2	Wild type	98.6 ± 15.5
Mouse E-cadherin EC1-2 W2A	Strand swapping mutant	916 ± 47
Mouse E-cadherin EC1-2 E89A	Strand swapping mutant	293 ± 11
Mouse E-cadherin EC1-2 Ala-Ala-extension	Strand swapping mutant	811 ± 97
Mouse E-cadherin EC1-2 Met-Arg-extension	Strand swapping mutant	257.5 ± 17.5
Mouse E-cadherin EC1-2 Asp-Trp-deletion	Strand swapping mutant	662 ± 28.5
T-cadherin EC1-2		
Mouse T-cadherin EC1-2	Wild type	41.4 ± 1.7
Mouse T-cadherin EC1-2 I2A	Strand swapping mutant	37.1 ± 4.1
Mouse T-cadherin EC1-2 Gly-extension	Strand swapping mutant	16.5 ± 0.8
Mouse T-cadherin EC1-2 Met-Arg-extension	Strand swapping mutant	34.1 ± 6.3

^a tagged versions of these proteins are listed separately in Table 16.

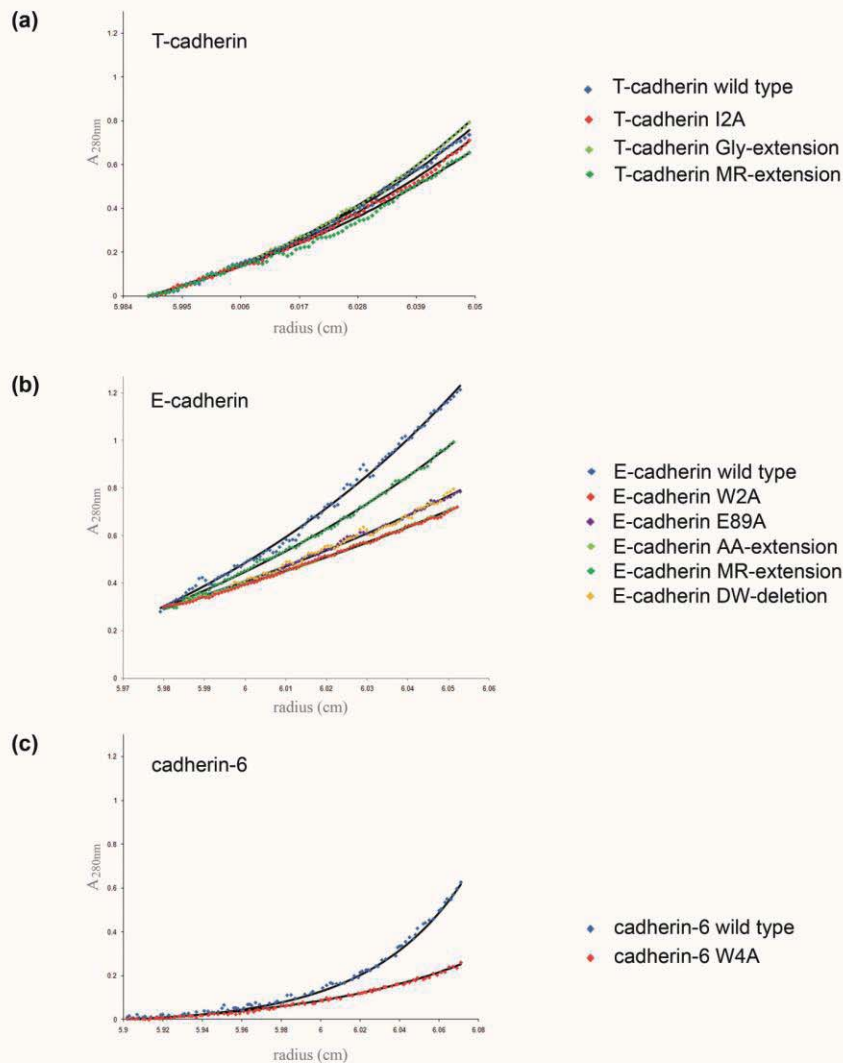


Figure 40: Effects of strand swapping mutations on homodimerization of T-cadherin, E-cadherin and cadherin-6 in equilibrium AUC experiments. (a) Strand swap targeted mutations show no effect on adhesive binding of T-cadherin EC1-2 domains. (b) E-cadherin homophilic binding was inhibited by introduction of strand swap mutations in comparison to wild type AUC profiles (blue diamonds). Most severe influence had Trp2 mutation W2A (red diamonds) and the extension of the A*-strand by a double Ala (light green diamonds). Binding is least altered by the MR-extension. (c) Profile for cadherin-6 wild type (blue diamonds) and mutant W4A (red diamonds) are shown. Binding is substantially reduced by the strand swap targeted mutation. Raw data is represented in all panels as colored diamonds, fittings to dimer models ($A+A=2A$) are depicted as black lines. Calculated K_D values for homodimerization are listed in Table 18.

7.3 Context of the mutational data in the published work

Strand swap mutations had no effect on T-cadherin adhesive binding in equilibrium AUC experiments, which shows that the swapped interface seen in other type I and II cadherins is not involved in T-cadherin mediated adhesion. Together with cell aggregation assays, AUC and SPR experiments showing that mutations targeting the observed novel X-dimer interface result in complete loss of T-cadherin adhesive binding (Ciatto et al., 2010), these data suggest that the X-shaped configuration is the primary adhesive interface of T-cadherin.

Interestingly, although strand swap mutants of type I E-cadherin and type II cadherin-6 were found in AUC experiments to have markedly reduced affinities, they were not monomeric but formed weak homodimers. Structures of E-cadherin W2A, E89A, the Ala-Ala extension mutant and cadherin-6 W4A, determined by other authors and reported in Harrison et al. (2010a) revealed formation of X-shaped dimers closely similar to those of T-cadherin. These structures suggested potential biological relevance of this interface in type I and II cadherins in addition to the well studied strand swap adhesive interface. Mutations targeting the X-dimer interface in these proteins slowed the exchange between monomers and strand swapped dimers considerably such that proteins no longer mediated adhesion in aggregation assays or SPR experiments despite having intact swapping interface regions, suggesting that in classical cadherins the X-dimer interfaces function as a kinetic intermediate indispensable for proper strand swap mediated cadherin adhesion.

Therefore, cadherins appear to employ two different interfaces for homodimerization. One of these, the X-dimer interface, is shared by typical classical cadherins and atypical T-cadherin while the other interface, the strand swap dimer, is specific to typical classical cadherins, mediating mature adhesive cadherin binding.

Chapter 8:

Discussion

8.1 VE-cadherin adhesion is mediated by a classical cadherin dimer

We embarked on an extensive biophysical study of VE-cadherin adhesive behavior to test a novel model for homophilic VE-cadherin adhesive interactions that has been suggested in the literature and is remarkably different from that known for other classical cadherins. The published model is based on solution biophysical data and cryo-EM studies of bacterially produced VE-cadherin EC1-4 fragments and suggests that the adhesive binding unit of VE-cadherin is composed of six molecules which assemble into a hexameric structure based on two sets of interactions (Al-Kurdi et al., 2004; Bibert et al., 2002; Hewat et al., 2007; Lambert et al., 2005; Legrand et al., 2001). One of these, an extensive interaction involving domain EC4, organizes three VE-cadherin molecules laterally into a trimer and the second interaction, mediated by EC1 domains connects two trimers from juxtaposed cell surfaces in a *trans* fashion, which results in the proposed hexamer (Hewat et al., 2007). In contrast, for other type I and type II classical cadherins there is extensive evidence from a wide array of studies for formation of *trans* adhesive dimers between single protomers by 3D domain swapping mediated by EC1 domains (Boggon et al., 2002; Harrison et al., 2010b; Haussinger et al., 2004; Patel et al., 2006; Shapiro et al., 1995). For type I cadherins, there is evidence for subsequent assembly into adherens junctions by weak *cis* interactions (Boggon et al., 2002; Harrison et al., 2010b), but strong trimeric interactions similar to those suggested for VE-cadherin have not been observed for other cadherins. Both, the proposed hexamer model and the known classical cadherin interaction, have in common that EC1 domains mediate *trans* binding, but they differ in the respective *cis* interactions; a suggested strong trimeric interaction mediated by EC4 for VE-cadherin that is sufficiently stable to be detected in solution and a weak *cis* interaction for type I cadherins involving domains EC1 and EC2 that becomes detectable only in the context of adhesion between membranes.

VE-cadherin fragments EC1-4 exhibiting hexameric behavior in cryo-EM and solution biophysics studies were all bacterially produced from inclusion bodies and lacked post-translational modification as well as the membrane proximal domain EC5 (Legrand et al., 2001). Bacterially produced fragments spanning domains EC1-5 also formed hexamers in analytical size exclusion chromatography experiments (Legrand et al., 2001). We embarked on extensive biophysical and imaging studies of VE-cadherin ectodomains produced in mammalian HEK 293 cells to examine hexameric VE-cadherin binding behavior in detail using proteins more closely similar to those *in vivo* in terms of post-translational modification. However, we found that these natively glycosylated VE-cadherin ectodomains uniformly

formed a monomer/dimer equilibrium in solution with no evidence of higher order multimers in analytical ultracentrifugation, gel filtration, multi-angle light scattering and imaging experiments. We also found that isolated, natively glycosylated EC3-5 VE-cadherin fragments are monomeric, consistent with the idea that strong binding interactions of VE-cadherin are mediated only by domains EC1-2. Confirming this, we observed VE-cadherin EC1-2 fragments to dimerize with similar affinities to full-length ectodomains. These data imply that EC4-mediated *cis*-trimer interactions do not form in solution for VE-cadherin ectodomains in their native state. Our findings for VE-cadherin are therefore more similar to behavior observed for other classical cadherins (Boggon et al., 2002; Harrison et al., 2010a; Harrison et al., 2010b; Haussinger et al., 2004; Nagar et al., 1996; Patel et al., 2006; Shapiro et al., 1995).

Furthermore, we identified the likely reason for the discrepancies in VE-cadherin behavior between our findings and previous work in which the hexamer model was proposed. We find that VE-cadherin carries substantial quantities of N-linked glycosylation in comparison with glycosylation found in type I cadherins (Boggon et al., 2002; Harrison et al., 2010b; Liwosz et al., 2006). We identified one glycosylation site at Asn395 (numbering for mature human VE-cadherin) conserved throughout type I and II cadherins, which is located in domain EC4 - the domain responsible for trimerization in the bacterial hexamer model (Bibert et al., 2002; Hewat et al., 2007). As mentioned above, domains EC3-5 of VE-cadherin, when glycosylated, failed to homodimerize and remained monomeric in all biophysical experiments, which is in direct contrast to the prediction of the hexamer model (Bibert et al., 2002). However, removal of N-linked glycosylation from VE-cadherin fragments encompassing the putative trimer site (domains EC3-4 and EC3-5) led to strong dimeric protein interactions or aggregation in analytical ultracentrifugation and appearance of the ability to aggregate liposomes. Similarly, dimerization was also found by Bibert et al (2002) for bacterially produced EC3-4. Although the fragments EC3-4 did not associate into trimers, it has been shown previously, that proteins with non-specific hydrophobic associations can sometimes form complexes composed of unexpected numbers of protomers (Weis et al., 1991). Interestingly, full-length VE-cadherin ectodomains also became prone to non-specific aggregation in AUC experiments and able to more efficiently aggregate liposomes after N-linked glycosylation was reduced enzymatically or by expression in HEK 293 GNTI cells. Our data strongly suggest that EC4-mediated *cis* binding interactions, which are central to the hexamer binding model, are an artifact caused by lack of N-linked glycosylation in VE-cadherin and that expression of VE-cadherin

fragments in bacteria in previous studies (Al-Kurdi et al., 2004; Bibert et al., 2002; Hewat et al., 2007; Legrand et al., 2001) resulted in non-biological, artifactual hexamer assemblies. Interestingly, we find that lack of N-linked glycosylation does not equally affect all cadherins because, in contrast to the findings for VE-cadherin, binding interactions of purified E-cadherin EC1-5 fragments were independent of their N-linked glycosylation. Proteins were stable and adopted the same adhesive binding behavior with highly similar affinity values. Nonetheless, even in type I cadherins, N-linked glycosylation may play a role, albeit a more subtle one, in regulating adhesion at the cell surface (Liwosz et al., 2006).

Our finding of a classical cadherin monomer/dimer behavior for VE-cadherin is in agreement with electron microscopic studies performed by Ahrens et al. (2003), which also used mammalian expressed VE-cadherin ectodomains and suggested VE-cadherin to adopt a homodimerization mechanism similar to classical type I E-, N- and P-cadherins with no occurrence of hexamers (Ahrens et al., 2003). Hexamer interactions have therefore only been described for bacterially expressed constructs (Al-Kurdi et al., 2004; Bibert et al., 2002; Hewat et al., 2007; Lambert et al., 2005; Legrand et al., 2001).

Our AFM imaging studies revealed that VE-cadherin not only homodimerizes in common with other studied classical cadherins, but that protomer and overall dimer arrangement are closely similar to those of type I cadherins based on previous structural data (Boggon et al., 2002; Harrison et al., 2010b). Protomers adopted crescent shaped curved forms, and dimers appear to be composed of two protomers overlapping at their termini in a similar fashion and with similar overall length to those observed in structures and EM studies of E-, N-, P- and C-cadherin (Ahrens et al., 2003; Farquhar and Palade, 1963; McNutt and Weinstein, 1973). Two previous AFM imaging studies of VE- (Baumgartner et al., 2000) and N-cadherin (Harrison et al., 2005) C-terminally attached to Fc domains, could also identify cadherin monomers similar in overall shape and curvature to those we observe, but dimers were not described. As mentioned above, VE-cadherin binding activity was found to reside in domains EC1-2 in solution studies, which lead us to conclude that the overlapping regions seen in our AFM studies are amino terminal.

In addition to similarity in overall dimer configuration between VE-cadherin and previously characterized classical cadherins observed in the above experiments, our structure of the adhesive dimer of chicken VE-cadherin EC1-2 shows that VE-cadherin homodimerization is

mediated by the 3D domain swapping mechanism typical for classical cadherins (Boggon et al., 2002; Haussinger et al., 2004; Patel et al., 2006). However, the adhesive interface reveals features specific to VE-cadherin, as discussed below.

8.2 Variations on a common binding mechanism in classical cadherins

The VE-cadherin structure reported in this work has characteristics of adhesive interfaces found in both type I and II cadherins. The strand swap region and domain orientation of EC1 domains is closely similar to that of other type II cadherins in that the key residues Trp2 and Trp4 located on the A*-strand are docked into the large hydrophobic acceptor pocket of the interacting molecule. However, the interface outside the immediate pocket differs substantially from that of type II cadherins as intermolecular interactions are restricted to the hydrophobic pocket and do not extend along the entire face of the EC1 domain. Absence of these ‘outer’ interactions results in an overall dimer organization of EC1 domains more reminiscent of that of type I cadherins as only the upper half of domain EC1 partakes in homodimerization. VE-cadherin is the only cadherin found so far to combine these characteristics. A unique, almost linear overall arrangement of protomers in the dimer is also found, and accessible surface area per protomer buried in the adhesive interface is approximately intermediate between small type I interfaces and large type II cadherin interfaces. Overall, VE-cadherin is a structurally divergent type II cadherin based on the homodimer structure.

Our structure of VE-cadherin shows clearly how differences on the sequence level, in this case in the region of the extended interface in EC1, translate into substantially divergent adhesive interfaces despite the same underlying strand swap mechanism. Numerous structures of classical cadherins have been reported to date, including full length structures of type I cadherins E-, N- and C-cadherin (Boggon et al., 2002; Harrison et al., 2010b), and a wide array of adhesive EC1, EC1-2 or EC1-3 fragment structures of type II cadherins MN, 8 and 11, (Patel 2006). In addition, in the final stages of preparation of this thesis, I determined a structure of a strand swapped dimer of another type II cadherin, cadherin-10 EC1-2, revealing an adhesive interface sharing the swapped A-strand using Trp2 and Trp4 and the extended non-swapped hydrophobic interface with other typical type II cadherins. Taken together with the newly determined chicken VE-cadherin EC1-2 structure of a divergent type II cadherin interface, we can infer from these numerous structures the diversity in strand swapped

adhesive interfaces within classical cadherins. Broadly, all classical cadherins except T-cadherin (see below) commonly exchange the amino terminal part of the A-strand between EC1 domains, but differ with respect to the exact element that is swapped (Trp2 in type I, Trp2 and Trp4 in type II) and to the involvement of an extended non-swapped interface, which is absent in type I cadherin and atypical type II VE-cadherin dimers.

Indirect evidence from all structures available provide insight to the adhesive mechanism of other cadherin subfamilies with similarity to the classical cadherins, like desmosomal cadherins, for which at present time no binding interface structures are available. Sequence analysis show presence of a tryptophan residue and pocket residues in similar positions to these structural elements in type I cadherins. Cryo electron tomography studies of desmosomes (Al-Amoudi and Frangakis, 2008) together with functional evidence suggest that these proteins are most likely to exchange A-strands for homodimerization, but further investigations are needed to reveal details of adhesion.

But not all classical cadherins facilitate 3D domain swapping for adhesive binding. T-cadherin, a divergent GPI-linked type I cadherin lacking strand swap residue Trp2 and residues lining the type I hydrophobic pocket forms adhesive dimers via a different interface, involving the ‘base’ of the EC1 domain and the ‘top’ of the EC2 domain resulting in an X-shaped dimer configuration (Ciatto et al., 2010). Strand swap targeted mutations in T-cadherin reported here did not impair dimerization and thus the strand swapping mechanism plays no role in T-cadherin adhesion (Ciatto et al., 2010). However, mutations targeting the X-dimer interface abrogated T-cadherin homodimerization completely suggesting this interface to be the only biological important site. Interestingly, when strand swapping was impaired by mutagenesis in type I E-cadherin (Harrison et al., 2010a), N-cadherin (J.V., personal communication) and type II cadherin-6 (Harrison et al., 2010a), structures of these proteins revealed that they use the same interface as observed for T-cadherin. Biophysical evidence suggests the interface to function as a binding intermediate in these cadherins. VE-cadherin also might use the X-dimer as intermediate, based on the remaining ability of strand swap mutant VE-cadherin EC1-5 W2A W4A to form weak dimers in AUC experiments and to aggregate liposomes, however, this remains to be tested by direct mutational studies targeting the X interface.

Outside the classical sub branch of the cadherin superfamily, protocadherins, which have one additional EC domain in comparison to classical and desmosomal cadherins and other even more distantly related members show no conservation of strand swap residues. These will almost certainly employ even more divergent mechanisms to fulfill the task of adhesive binding, which need to be studied in detail in the future.

8.3 Adherens junction assembly – differences within the classical cadherin subfamilies

Although our studies revealed many details about *trans* dimerization of VE-cadherin, certain points remain elusive. How do VE-cadherin and other type II cadherins laterally organize into adherens junctions? We observed cadherin like junction formation in our cryo-EM studies of artificial junctions formed by VE-cadherin between liposomes. In addition, VE-cadherin was also found *in vivo* at adherens junctions in juxtaposed endothelial cells by EM (Uehara, 2006). Adherens junction formation has also been reported for type II cadherin-11 in immunofluorescence studies (Kiener et al., 2006) which show overall similar topology and organization as adherens junctions formed by type I cadherins (Boggon et al., 2002; Harrison et al., 2010b; McNutt and Weinstein, 1973). Abundant evidence from crystal structures, cryo EM of artificial junctions, EM of *in vivo* junctions and functional assays has led to some understanding of adherens junctions assembled by type I cadherins (Boggon et al., 2002; Haussinger et al., 2004; McNutt and Weinstein, 1973). Strand swapped cadherin dimers appear to use a second interface for lateral assembly, the so called *cis* interface, which forms involving β -strands C, F and G of the face of EC1 with contribution of the quasi β -helix on one molecule and B, D and E strands of the face towards the ‘top’ of EC2 on the second molecule (Boggon et al., 2002; Harrison et al., 2010a). Mutational studies targeting this interface reveal that both *trans* and *cis* interactions are essential for E-cadherin to assemble into stable junctions between cells, or into ordered artificial junctions between liposomes (Harrison et al., 2010b). It appears at least for type I cadherins that passive diffusion trap and cytoplasmic interactions are not sufficient to trigger initial clustering of cadherins into junctions (Wu et al., 2010). Therefore it is likely that type I cadherins rely on the described ectodomain mediated mechanism for stable junction formation. For type II cadherins, the requirements for junction assembly are not known. Although the *cis* interface was present in all EC1-2 and EC1-5 structures of mouse type I E-, N- and C-cadherins (Boggon et al., 2002; Harrison et al., 2010a; Harrison et al., 2010b; Haussinger et al., 2004; Parisini et al., 2007), no

similar *cis* interaction was present in type II cadherin EC1-3 and EC1-2 structures of cadherin-8, -11 (Patel et al., 2006) or in the VE-cadherin structure reported here. These findings strongly suggest that the *cis* interface observed for type I cadherins does not have a role in the type II subfamily.

A critical look at EM images of artificial adherens junctions between liposomes reveals that junctions formed by VE-cadherins show a strong midline in the intermembrane density that is not observed in similar preparations of artificial junctions of type I cadherins. This might be therefore indicative of a different *cis* arrangement. Interestingly, desmosomes, which are formed by the classical cadherin-related cadherins desmocollin and desmoglein, also appear different from type I cadherin junctions in cryo-EM and show a broadly similar electron-dense midline to that seen for VE (Al-Amoudi and Frangakis, 2008). Both desmosomal cadherins and type II cadherins also lack a structural element in EC1 referred to as a quasi β -helix, which contributes to the *cis* interface in type I cadherins.

Thus, at the current time we have no evidence for a *cis* interface responsible for lateral junction assembly with physiological relevance for type II cadherins. A full length VE-cadherin structure would elucidate the ectodomain-mediated aspects of junction assembly of this important cadherin crucial to angiogenesis and maintenance of the vascular endothelium and may be relevant to other classical type II cadherins. Physiological relevance of any potential *cis* interface observed could then be assessed by mutagenesis studies, which could also be used to test the relevance of the additional lattice contacts observed in the EC1-2 structure reported here. Trials to obtain diffracting crystals of chicken and human full ectodomains were unsuccessful, so in future experiments a multi species approach will be taken using bovine, mouse, frog and zebrafish (Larson et al., 2004) VE-cadherin, which show 78%, 75%, 55% and 37% sequence identity differences to human VE-cadherin. The substantial sequence differences increase the chance of different behavior in crystallization trials. Another future aim is to elucidate the overall assembly of VE-cadherin junctions and other type II cadherin mediated junctions by cryo electron tomography of artificial adherens junctions between liposomes.

8.4 Type II cadherin specificity – a code to crack

SPR experiments with purified type II cadherins to elucidate the binding specificity pattern within this group showed promiscuous binding between cadherin-6, -9 and -10, but no interactions were observed between cadherin-6 and cadherin-8 and -11. Type II cadherins-6, -9, -10 are more related to each other on sequence level (78-84% sequence identity, EC1-domains) than they are to cadherin-8 and -11 (59-64% sequence identity, EC1 domains). Similarly, cadherin-8 and -11 share with each other a higher similarity on sequence level (72% identity) than to cadherin-6, -9, -10 (59-64%). These data together suggest that there are subgroups within the type II family that engage in restricted heterophilic interactions. Our data agree with promiscuity and selectivity patterns derived from cell aggregation data (Patel et al., 2006; Price et al., 2002; Shimoyama et al., 1999; Shimoyama et al., 2000). From these data we can extract evidence for other subgroups that may interact preferentially, for example cadherin-8 and -11 and cadherin-7 and -14 (Shimoyama et al., 2000).

Because data derived from our SPR studies directly correlates with data from cell aggregation assays we will expand the studies to include all combinations of type II cadherins. Preliminary data from SPR experiments further to those reported in Section 6.2.4 of this thesis show that cadherin-11 coupled to the sensor surface binds heterophilically to cadherin-8, in preference to binding to less related cadherins-6, -9, and -10. This supports our theory that type II cadherin promiscuity and selectivity directly relates to sequence identity and therefore to sub-subfamily organization within the type II family. Future experiments will aim to measure a type II cadherin-wide SPR matrix to test this more fully.

In contrast to cell aggregation assays conducted by Shimoyama et al (2000), in which expression levels of cadherin-9 and -10 were substantially lower, SPR studies conducted on purified proteins had exact same protein concentrations for analyte cadherins, which enables quantitative comparisons of heterophilic binding facilitated by a certain cadherin. SPR experiments provided a more finely grained quantitation, as we can see that cadherin-6 prefers homophilic binding at least 1.5fold over heterophilic binding to cadherin-9 and 3fold over cadherin-10, which is difficult to discern from aggregation assays as for example homophilic cadherin-6 aggregates looked identical to cadherin-6/ cadherin-9 cell aggregates. Nonetheless, the general trend in our data correlates with the findings on cellular level. We see a hierarchy for binding to cadherin-6: homophilic > heterophilic with cadherin-9 > heterophilic with cadherin-10. Notably, cadherin-6 and -10 formed in cell-cell aggregation assays heterophilic

aggregates, with cadherin-6 expressing cells surrounded by cadherin-10 expressing cells (Shimoyama et al., 2000). This kind of heterogeneous aggregate has also been observed in N- and E-cadherin transfected cell aggregates (Katsamba et al., 2009; Patel et al., 2006), in which N-cadherin expressing cells (high affinity homophilic binding) were surrounded by E-cadherin expressing cells (low affinity homophilic binding), which indicated that the organization of cell aggregates was driven by thermodynamical rules/ homophilic binding affinity. In agreement, with cadherin-6 has a homodimerization affinity of $3.1\mu\text{M}$ and cadherin-10 a substantially lower K_D of $42.2\mu\text{M}$. However, affinities of cadherin-6 and -9 are not equal, $3.13\mu\text{M}$ and $17\mu\text{M}$, respectively, but nonetheless homogeneous aggregates are formed, indicating that affinities alone do not govern aggregate morphology.

The observed fine differences in specificity are especially interesting because type II cadherins are all closely similar to each other on sequence and structural levels (Patel et al., 2006) even more so than type I cadherins. For example mouse E- and N-cadherin share in their EC1 domain a sequence identity of 58%, whereas within the type II subfamily, sequence identity reaches up to 84%. The minimal differences in sequence between cadherin-8, -11 and cadherin-6, -9, -10 nonetheless cause homophilic preference over heterophilic interactions as seen in our SPR experiments. For example, cadherin-6 shows preference for homophilic binding over binding with cadherin-9 and -10 (Shimoyama et al., 2000), although on sequence level it shares >82% of identity with specificity governing EC1 domains of the latter cadherins. It will be interesting to relate patterns of binding preference from SPR experiments conducted with all type II cadherins to specific residue differences in the binding interface. Results of these studies could then be applied to mutagenesis studies to determine the minimal set of residues that need to be mutated in order to convert type II cadherins specificity. Such an approach should be facilitated by the small number of non-conserved residues in EC1 for type II cadherins.

It is not uncommon for cell-cell adhesion molecules that very small differences are sufficient to determine binding specificity. For example, in Dscam molecules, which function as important neural cell adhesion and recognition molecules in the fly, as few as one non-conserved residue positioned in an important homophilic binding region localized within parallel β -strands in the dimer is enough to govern specificity (Wojtowicz et al., 2007). This is reminiscent of the fine tuned specificity found in type II cadherins and suggests the possibility that sensitivity of binding affinity to very small binding site differences might be a general

feature of homophilic systems. Considering the knowledge from domain shuffling experiments showing that cadherin domain EC1 governs specificity (Nose et al., 1990; Patel et al., 2006; Price et al., 2002) and structural data for type II cadherins MN, 8, 10 and 11 (Patel et al., 2006), (Brasch, unpublished data), regions in which residue exchanges might have a dramatic effect on specificity must lie outside the core strand swap region, which shows essentially no variation. Thus, the region lining the rim of the acceptor pocket or the extended non swapped hydrophobic interface along domain EC1 are a likely possibility for minor residue changes to translate into specificity.

But does type II cadherin binding specificity play a role *in vivo*? A wide array of type II cadherins are found to be co-expressed in the CNS (Price et al., 2002; Suzuki, 1997) in distinct but overlapping patterns. Also, there is a correlation between expression of certain type II cadherins and segregation of different regions in the CNS (Patel et al., 2006; Suzuki, 1997). Studies of Price et al (2002) elucidated an important role for multiple type II cadherins in motor pools in the spinal cord which are linked to motor organization. Motor pools are small groups of clustered functional subsets of motor neurons in the lateral motor column of the spinal cord (Price et al., 2002). No type I cadherins, except divergent T-cadherin, are found to be expressed in motor pools (Fredette and Ranscht, 1994; Price et al., 2002) which appear to segregate from each other by switching on expression of different sets of type II cadherins, sometimes with different expression levels of each (Price et al., 2002). MN-cadherin for example is abundant in all neurons of this region before distinct motor pools form. Then MN-cadherin expression is lost for most motor pools, but maintained in the Adductor pool, which leads to its segregation from the eF pool, which expresses an identical complement of cadherins except for MN (Price et al., 2002). When MN-cadherin expression is also induced in the eF pool by *in ovo* electroporation to equalize the cadherins,, loss of segregation leading to intermixing is observed (Price et al., 2002). Interestingly, electroporation of a mutant MN-cadherin containing the EC1 domain of cadherin-6b, a cadherin already expressed in both pools, does not cause intermixing suggesting that differences in the adhesive interface of MN and 6b (74% identical in EC1) are sufficient to drive biologically relevant cell sorting (Patel et al., 2006).

One clear exception in the type II cadherin family regarding combinatorial type II cadherin expression is VE-cadherin which is expressed exclusively in the vascular endothelium and is unlikely to be involved in cell sorting processes with other type II cadherins. The divergent

interface we observe is likely to reflect that no selection pressure has acted on VE-cadherin to maintain selective, promiscuous interactions with other type II cadherin subfamily members. Our SPR experiments suggest that VE does not cross interact with any of type II cadherins-6, -8, -9, -10 and -11, which is most likely due to hydrophilic residues in VE-cadherin, where type II cadherins show a non-polar extended interface region. However, SPR experiments involving VE-cadherin binding were hampered by weak homophilic binding responses that were probably due to ‘slow’ kinetics, since VE-cadherin binding in longer time-frame AUC experiments was strong. VE-cadherin kinetic behavior studied in single molecule force microscopy experiments between endothelial cells by Wirtz et al (2006) revealed in comparison to type I cadherins E and N a substantially longer bond lifetime, which is in agreement with the binding responses we observe in SPR experiments. Notably, type II cadherins in general were found to have ‘slower’ kinetics than type I cadherins, which is reflected by the shape of the binding curves in our SPR experiments and in published results of dual pipette assays (Chu et al., 2006). Co-ip experiments could be successfully used to identify homophilic binding between the same VE-cadherin proteins used for SPR experiments, but appear not to be sensitive enough for detection of heterophilic binding such as that between VE- and N-cadherin or between N- and E-cadherin, which appears to be less stable. Nonetheless, if type II cadherin heterophilic binding is more stable, we might be able to assess heterophilic binding with co-ip experiments. Otherwise, cell aggregation assays of VE-cadherin transfected cells with those expressing other type II cadherins will be needed in order to confirm our results that show no binding between VE-cadherin and other members of the type II subfamily. Surprisingly, VE-cadherin has never been tested before in cell aggregation assays with other type II cadherins, published cell studies are limited to type I E-, N- and P-cadherin expressing cells.

8.5 Interactions between cadherins in vascular endothelial cells

VE-cadherin, a divergent type II cadherin crucial for angiogenesis and vascular maintenance, is expressed exclusively in the vascular endothelium and forms adherens junctions between endothelial cells (Breier et al., 1996; Dejana, 1996; Dejana et al., 1996; Gentil-Dit-Maurin et al., 2010; Lampugnani et al., 1992; Vittet et al., 1997). Co-expressed in the endothelium alongside VE-cadherin are type I N-cadherin and in low levels P-cadherin which do not co-localize in adherens junctions in endothelial cells in which VE-cadherin is present (Gentil-Dit-Maurin et al., 2010; Jaggi et al., 2002; Liaw et al., 1990; Navarro et al., 1998; Salomon et al., 1992). This is in contrast to other tissues, in which N-cadherin and P-cadherin are

junctional (Gentil-Dit-Maurin et al., 2010; Jaggi et al., 2002; Navarro et al., 1998). VE-cadherin displaces N-cadherin actively from endothelial adherens junctions, leaving it evenly dispersed over the cell surface (Jaggi et al., 2002; Navarro et al., 1998; Salomon et al., 1992). This is not a general activity of VE-cadherin but is specific for N-cadherin because E-cadherin and P-cadherin junction formation in transfected cells was not disturbed by co-expressed VE-cadherin (Jaggi et al., 2002). In our SPR experiments we found very surprisingly a strong heterophilic binding of N-cadherin wild type or strand swap mutant protein to VE-cadherin. This is the first time that a strong interaction has been observed between a type I and type II cadherin; in most experiments conducted to investigate heterophilic binding no interactions were observed between type I and II cadherins, for example between cadherin-6 and N- or E-cadherin (Katsamba et al., 2009; Nakagawa and Takeichi, 1995; Patel et al., 2006; Shimoyama et al., 1999; Shimoyama et al., 2000). The interaction between VE- and N-cadherin was independent from strand swap exchange, as W2A strand swap mutant protein of N-cadherin was also observed to bind to VE-cadherin surfaces. This is in agreement with the fact that both proteins have remarkably different adhesive strand swap interfaces and also with previous results from plate-cell adhesion assays, in which cells transfected with either N- or VE-cadherin failed to heterophilically bind to each other (Breviario et al., 1995; Navarro et al., 1998). Therefore, it can be excluded that this interaction is mediating *trans*-adhesion, indicating it to be lateral. It is interesting to speculate that this interaction could trigger the displacement of N-cadherin by VE-cadherin from vascular endothelial adherens junctions. Interestingly, in transfection experiments the N-cadherin extracellular domain was shown to be involved in the displacement, supporting this possibility.

Despite strong evidence of binding between VE- and N-cadherin in SPR experiments, this interaction could not be observed in co-ip experiments, which might be due to instability and short bond life time, which appears likely considering the traces suggesting fast on/off binding rates in SPR experiments. In the future, we need to expand our studies and test if VE-cadherin strand swap mutants also bind heterophilically to N-cadherin in SPR experiments to determine if the interaction is fully independent of the strand swap interface. In addition, we plan to investigate if the putative complex can be purified by size exclusion chromatography of N-cadherin VE-cadherin mixtures to confirm our SPR binding data and potentially to allow us to determine a crystal structure of the complex to shed light on this novel interaction on a molecular level.

9. Future Directions

The described work provides detailed and extensive insight into the structure and binding mechanism of VE-cadherin, which is the major cell-cell adhesion receptor found in adherens junctions in the vascular endothelium, where it plays a critical role in vascular angiogenesis and maintenance. The adhesive dimer of VE-cadherin was found to utilize the 3D domain swapping mechanism in common with other classical cadherins, however, the adhesive interface was shown to be unique to this particular cadherin as it shares features of adhesive interfaces observed for type I and type II cadherins and exhibiting remarkably strong binding affinities. However, the molecular mechanism underlying VE-cadherin assembly in adherens junctions remains elusive. Electron micrographs of artificial junctions between liposomes are different from those of type I cadherins, suggesting that the junction assembly of VE-cadherin and maybe other type II cadherins, too, is different from that reported for type I cadherins. Therefore, crystallization of full length ectodomains of VE-cadherin of different species will be attempted so that potential ectodomain-mediated interfaces involved in clustering at junctions can be determined. In parallel we will examine the organization of VE-cadherin in junctions formed between liposomes by electron microscopy tomography. Additionally, relevance of crystal contacts other than the adhesive dimer observed in the VE-cadherin EC1-2 crystal structure will be tested by targeted mutagenesis studies.

An experimental set up was designed for systematic binding studies with the aim to understand promiscuous adhesive binding inherent to classical type II cadherins. Based on results reported here, which confirm and extend previous cell aggregation data, it was possible to propose for the first time a binding code underlying the regulation type II cadherin-mediated cell-cell adhesion in the CNS. This binding code will be tested in future by extending these experiments to an overall binding matrix including the 13 known classical type II cadherins. Binding preferences for the cadherins tested can then be used to relate specificity to the small set of non-conserved residues in the adhesive domain EC1. It will be of great interest to identify the minimal set of residues responsible for adhesive specificity in these cadherins.

For the first time we observed binding between a type I and type II classical cadherin, N- and VE-cadherin, which are co-expressed in the vasculature. Based on our findings, this interaction appears to be independent from the strand swap mechanism and likely to be a

lateral interaction. This novel interaction needs to be validated in future experiments. The complexes formed between VE- and N-cadherin can be tested for stability by size exclusion chromatography and then could be co-crystallized, which would provide detail on this novel interface on atomic level.

Overall, this work provides an extensive study of structural and biophysical adhesive binding features of VE-cadherin and insight into the binding code of classical type II cadherins, which contributes to the understanding of the binding interface diversity and specificity in cadherin cell-cell adhesion.

10. List of References

- Abedin, M., and King, N. (2008). The premetazoan ancestry of cadherins. *Science* 319, 946-948.
- Ahrens, T., Lambert, M., Pertz, O., Sasaki, T., Schulthess, T., Mege, R.M., Timpl, R., and Engel, J. (2003). Homoassociation of VE-cadherin follows a mechanism common to "classical" cadherins. *J Mol Biol* 325, 733-742.
- Al-Amoudi, A., and Frangakis, A.S. (2008). Structural studies on desmosomes. *Biochem Soc Trans* 36, 181-187.
- Al-Kurdi, R., Gulino-Debrac, D., Martel, L., Legrand, J.F., Renault, A., Hewat, E., and Venien-Bryan, C. (2004). A soluble VE-cadherin fragment forms 2D arrays of dimers upon binding to a lipid monolayer. *J Mol Biol* 337, 881-892.
- Baumgartner, W., Hinterdorfer, P., Ness, W., Raab, A., Vestweber, D., Schindler, H., and Drenckhahn, D. (2000). Cadherin interaction probed by atomic force microscopy. *Proc Natl Acad Sci U S A* 97, 4005-4010.
- Bennett, M.J., Schlunegger, M.P., and Eisenberg, D. (1995). 3D domain swapping: a mechanism for oligomer assembly. *Protein Sci* 4, 2455-2468.
- Bibert, S., Jaquinod, M., Concord, E., Ebel, C., Hewat, E., Vanbelle, C., Legrand, P., Weidenhaupt, M., Vernet, T., and Gulino-Debrac, D. (2002). Synergy between extracellular modules of vascular endothelial cadherin promotes homotypic hexameric interactions. *J Biol Chem* 277, 12790-12801.
- Boggon, T.J., Murray, J., Chappuis-Flament, S., Wong, E., Gumbiner, B.M., and Shapiro, L. (2002). C-cadherin ectodomain structure and implications for cell adhesion mechanisms. *Science* 296, 1308-1313.
- Breier, G., Breviario, F., Caveda, L., Berthier, R., Schnurch, H., Gotsch, U., Vestweber, D., Risau, W., and Dejana, E. (1996). Molecular cloning and expression of murine vascular endothelial-cadherin in early stage development of cardiovascular system. *Blood* 87, 630-641.
- Breviario, F., Caveda, L., Corada, M., Martin-Padura, I., Navarro, P., Golay, J., Introna, M., Gulino, D., Lampugnani, M.G., and Dejana, E. (1995). Functional properties of human vascular endothelial cadherin (7B4/cadherin-5), an endothelium-specific cadherin. *Arterioscler Thromb Vasc Biol* 15, 1229-1239.
- Carmeliet, P., Lampugnani, M.G., Moons, L., Breviario, F., Compernelle, V., Bono, F., Balconi, G., Spagnuolo, R., Oosthuysen, B., Dewerchin, M., *et al.* (1999). Targeted deficiency or cytosolic truncation of the VE-cadherin gene in mice impairs VEGF-mediated endothelial survival and angiogenesis. *Cell* 98, 147-157.
- Chappuis-Flament, S., Wong, E., Hicks, L.D., Kay, C.M., and Gumbiner, B.M. (2001). Multiple cadherin extracellular repeats mediate homophilic binding and adhesion. *J Cell Biol* 154, 231-243.
- Charlton, C.A., Mohler, W.A., Radice, G.L., Hynes, R.O., and Blau, H.M. (1997). Fusion competence of myoblasts rendered genetically null for N-cadherin in culture. *J Cell Biol* 138, 331-336.
- Chen, C.P., Posy, S., Ben-Shaul, A., Shapiro, L., and Honig, B.H. (2005). Specificity of cell-cell adhesion by classical cadherins: Critical role for low-affinity dimerization through beta-strand swapping. *Proc Natl Acad Sci U S A* 102, 8531-8536.
- Chu, Y.S., Eder, O., Thomas, W.A., Simcha, I., Pincet, F., Ben-Ze'ev, A., Perez, E., Thiery, J.P., and Dufour, S. (2006). Prototypical type I E-cadherin and type II cadherin-7 mediate very distinct adhesiveness through their extracellular domains. *J Biol Chem* 281, 2901-2910.

Ciatto, C., Bahna, F., Zampieri, N., VanSteenhouse, H.C., Katsamba, P.S., Ahlsen, G., Harrison, O.J., Brasch, J., Jin, X., Posy, S., *et al.* (2010). T-cadherin structures reveal a novel adhesive binding mechanism. *Nat Struct Mol Biol* *17*, 339-347.

Corada, M., Liao, F., Lindgren, M., Lampugnani, M.G., Breviario, F., Frank, R., Muller, W.A., Hicklin, D.J., Bohlen, P., and Dejana, E. (2001). Monoclonal antibodies directed to different regions of vascular endothelial cadherin extracellular domain affect adhesion and clustering of the protein and modulate endothelial permeability. *Blood* *97*, 1679-1684.

Corada, M., Mariotti, M., Thurston, G., Smith, K., Kunkel, R., Brockhaus, M., Lampugnani, M.G., Martin-Padura, I., Stoppacciaro, A., Ruco, L., *et al.* (1999). Vascular endothelial-cadherin is an important determinant of microvascular integrity in vivo. *Proc Natl Acad Sci U S A* *96*, 9815-9820.

Cruciani, V., and Mikalsen, S.O. (2006). The vertebrate connexin family. *Cell Mol Life Sci* *63*, 1125-1140.

Dejana, E. (1996). Endothelial adherens junctions: implications in the control of vascular permeability and angiogenesis. *J Clin Invest* *98*, 1949-1953.

Dejana, E. (2004). Endothelial cell-cell junctions: happy together. *Nat Rev Mol Cell Biol* *5*, 261-270.

Dejana, E., Tournier-Lasserre, E., and Weinstein, B.M. (2009). The control of vascular integrity by endothelial cell junctions: molecular basis and pathological implications. *Dev Cell* *16*, 209-221.

Dejana, E., Zanetti, A., and Del Maschio, A. (1996). Adhesive proteins at endothelial cell-to-cell junctions and leukocyte extravasation. *Haemostasis* *26 Suppl 4*, 210-219.

Duguay, D., Foty, R.A., and Steinberg, M.S. (2003). Cadherin-mediated cell adhesion and tissue segregation: qualitative and quantitative determinants. *Dev Biol* *253*, 309-323.

Farquhar, M.G., and Palade, G.E. (1963). Junctional complexes in various epithelia. *J Cell Biol* *17*, 375-412.

Foty, R.A., and Steinberg, M.S. (2005). The differential adhesion hypothesis: a direct evaluation. *Dev Biol* *278*, 255-263.

Fredette, B.J., and Ranscht, B. (1994). T-cadherin expression delineates specific regions of the developing motor axon-hindlimb projection pathway. *J Neurosci* *14*, 7331-7346.

Frieden, C., and Goddette, D.W. (1983). Polymerization of actin and actin-like systems: evaluation of the time course of polymerization in relation to the mechanism. *Biochemistry* *22*, 5836-5843.

Gavard, J. (2009). Breaking the VE-cadherin bonds. *FEBS Lett* *583*, 1-6.

Gentil-Dit-Maurin, A., Oun, S., Almagro, S., Bouillot, S., Courcon, M., Linnepe, R., Vestweber, D., Huber, P., and Tillet, E. (2010). Unraveling the distinct distributions of VE- and N-cadherins in endothelial cells: A key role for p120-catenin. *Exp Cell Res*.

Goridis, C., and Brunet, J.F. (1992). NCAM: structural diversity, function and regulation of expression. *Semin Cell Biol* *3*, 189-197.

Gumbiner, B.M. (1996). Cell adhesion: the molecular basis of tissue architecture and morphogenesis. *Cell* *84*, 345-357.

Harris, E.S., and Nelson, W.J. (2010). VE-cadherin: at the front, center, and sides of endothelial cell organization and function. *Curr Opin Cell Biol* *22*, 651-658.

Harrison, O.J., Bahna, F., Katsamba, P.S., Jin, X., Brasch, J., Vendome, J., Ahlsen, G., Carroll, K.J., Price, S.R., Honig, B., *et al.* (2010a). Two-step adhesive binding by classical cadherins. *Nat Struct Mol Biol* *17*, 348-357.

Harrison, O.J., Corps, E.M., Berge, T., and Kilshaw, P.J. (2005). The mechanism of cell adhesion by classical cadherins: the role of domain 1. *J Cell Sci* *118*, 711-721.

Harrison, O.J., Jin, X., Hong, S., Bahna, F., Ahlsen, G., Brasch, J., Wu, Y., Vendome, J., Felsovalyi, K., Hampton, C.M., *et al.* (2010b). The extracellular architecture of adherens junctions revealed by crystal structures of type I cadherins. Submitted.

Hatta, K., Nose, A., Nagafuchi, A., and Takeichi, M. (1988). Cloning and expression of cDNA encoding a neural calcium-dependent cell adhesion molecule: its identity in the cadherin gene family. *J Cell Biol* *106*, 873-881.

Haussinger, D., Ahrens, T., Aberle, T., Engel, J., Stetefeld, J., and Grzesiek, S. (2004). Proteolytic E-cadherin activation followed by solution NMR and X-ray crystallography. *EMBO J* *23*, 1699-1708.

He, W., Cowin, P., and Stokes, D.L. (2003). Untangling desmosomal knots with electron tomography. *Science* *302*, 109-113.

Hewat, E.A., Durmort, C., Jacquamet, L., Concord, E., and Gulino-Debrac, D. (2007). Architecture of the VE-cadherin hexamer. *J Mol Biol* *365*, 744-751.

Hong, C.Q., Ran, Y.G., Chen, J.Y., Wu, X., and You, Y.J. (2010). [Study on promoter methylation status of E-cadherin gene in nasopharyngeal carcinoma cell lines.]. *Zhonghua Bing Li Xue Za Zhi* *39*, 532-536.

Huber, A.H., and Weis, W.I. (2001). The structure of the beta-catenin/E-cadherin complex and the molecular basis of diverse ligand recognition by beta-catenin. *Cell* *105*, 391-402.

Huber, O. (2003). Structure and function of desmosomal proteins and their role in development and disease. *Cell Mol Life Sci* *60*, 1872-1890.

Hulpiau, P., and van Roy, F. (2009). Molecular evolution of the cadherin superfamily. *Int J Biochem Cell Biol* *41*, 349-369.

Hynes, R.O., and Zhao, Q. (2000). The evolution of cell adhesion. *J Cell Biol* *150*, F89-96.

Inoue, T., Tanaka, T., Takeichi, M., Chisaka, O., Nakamura, S., and Osumi, N. (2001). Role of cadherins in maintaining the compartment boundary between the cortex and striatum during development. *Development* *128*, 561-569.

Ishiyama, N., Lee, S.H., Liu, S., Li, G.Y., Smith, M.J., Reichardt, L.F., and Ikura, M. (2010). Dynamic and static interactions between p120 catenin and E-cadherin regulate the stability of cell-cell adhesion. *Cell* *141*, 117-128.

Jaggi, M., Wheelock, M.J., and Johnson, K.R. (2002). Differential displacement of classical cadherins by VE-cadherin. *Cell Commun Adhes* *9*, 103-115.

Kapadia, S.E. (1984). Ultrastructural alterations in blood vessels of the white matter after experimental spinal cord trauma. *J Neurosurg* *61*, 539-544.

Katsamba, P., Carroll, K., Ahlsen, G., Bahna, F., Vendome, J., Posy, S., Rajebhosale, M., Price, S., Jessell, T.M., Ben-Shaul, A., *et al.* (2009). Linking molecular affinity and cellular specificity in cadherin-mediated adhesion. *Proc Natl Acad Sci U S A* *106*, 11594-11599.

Kiener, H.P., Stipp, C.S., Allen, P.G., Higgins, J.M., and Brenner, M.B. (2006). The cadherin-11 cytoplasmic juxtamembrane domain promotes alpha-catenin turnover at adherens junctions and intercellular motility. *Mol Biol Cell* *17*, 2366-2376.

Kitagawa, M., Natori, M., Murase, S., Hirano, S., Taketani, S., and Suzuki, S.T. (2000). Mutation analysis of cadherin-4 reveals amino acid residues of EC1 important for the structure and function. *Biochem Biophys Res Commun* *271*, 358-363.

Klingelhofer, J., Troyanovsky, R.B., Laur, O.Y., and Troyanovsky, S. (2000). Amino-terminal domain of classic cadherins determines the specificity of the adhesive interactions. *J Cell Sci* *113* (Pt 16), 2829-2836.

Kobielak, A., and Fuchs, E. (2004). Alpha-catenin: at the junction of intercellular adhesion and actin dynamics. *Nat Rev Mol Cell Biol* *5*, 614-625.

Koch, A.W., Farooq, A., Shan, W., Zeng, L., Colman, D.R., and Zhou, M.M. (2004). Structure of the neural (N-) cadherin prodomain reveals a cadherin extracellular domain-like fold without adhesive characteristics. *Structure* *12*, 793-805.

Koval, M. (2006). Claudins--key pieces in the tight junction puzzle. *Cell Commun Adhes* *13*, 127-138.

Lambert, O., Taveau, J.C., Him, J.L., Al Kurdi, R., Gulino-Debrac, D., and Brisson, A. (2005). The basic framework of VE-cadherin junctions revealed by cryo-EM. *J Mol Biol* 346, 1193-1196.

Lampugnani, M.G., Corada, M., Caveda, L., Breviario, F., Ayalon, O., Geiger, B., and Dejana, E. (1995). The molecular organization of endothelial cell to cell junctions: differential association of plakoglobin, beta-catenin, and alpha-catenin with vascular endothelial cadherin (VE-cadherin). *J Cell Biol* 129, 203-217.

Lampugnani, M.G., Resnati, M., Raiteri, M., Pigott, R., Pisacane, A., Houen, G., Ruco, L.P., and Dejana, E. (1992). A novel endothelial-specific membrane protein is a marker of cell-cell contacts. *J Cell Biol* 118, 1511-1522.

Larson, J.D., Wadman, S.A., Chen, E., Kerley, L., Clark, K.J., Eide, M., Lippert, S., Nasevicius, A., Ekker, S.C., Hackett, P.B., *et al.* (2004). Expression of VE-cadherin in zebrafish embryos: a new tool to evaluate vascular development. *Dev Dyn* 231, 204-213.

Legrand, P., Bibert, S., Jaquinod, M., Ebel, C., Hewat, E., Vincent, F., Vanbelle, C., Concord, E., Vernet, T., and Gulino, D. (2001). Self-assembly of the vascular endothelial cadherin ectodomain in a Ca²⁺-dependent hexameric structure. *J Biol Chem* 276, 3581-3588.

Liaw, C.W., Cannon, C., Power, M.D., Kiboneka, P.K., and Rubin, L.L. (1990). Identification and cloning of two species of cadherins in bovine endothelial cells. *EMBO J* 9, 2701-2708.

Lim, M.J., Chiang, E.T., Hechtman, H.B., and Shepro, D. (2001). Inflammation-induced subcellular redistribution of VE-cadherin, actin, and gamma-catenin in cultured human lung microvessel endothelial cells. *Microvasc Res* 62, 366-382.

Liu, H., Komiyama, S., Shimizu, M., Fukunaga, Y., and Nagafuchi, A. (2007). Involvement of p120 carboxy-terminal domain in cadherin trafficking. *Cell Struct Funct* 32, 127-137.

Liwoz, A., Lei, T., and Kukuruzinska, M.A. (2006). N-glycosylation affects the molecular organization and stability of E-cadherin junctions. *J Biol Chem* 281, 23138-23149.

Matsunami, H., Miyatani, S., Inoue, T., Copeland, N.G., Gilbert, D.J., Jenkins, N.A., and Takeichi, M. (1993). Cell binding specificity of mouse R-cadherin and chromosomal mapping of the gene. *J Cell Sci* 106 (Pt 1), 401-409.

May, C., Doody, J.F., Abdullah, R., Balderes, P., Xu, X., Chen, C.P., Zhu, Z., Shapiro, L., Kussie, P., Hicklin, D.J., *et al.* (2005). Identification of a transiently exposed VE-cadherin epitope that allows for specific targeting of an antibody to the tumor neovasculature. *Blood* 105, 4337-4344.

McNutt, N.S., and Weinstein, R.S. (1973). Membrane ultrastructure at mammalian intercellular junctions. *Prog Biophys Mol Biol* 26, 45-101.

Murphy-Erdosh, C., Yoshida, C.K., Paradies, N., and Reichardt, L.F. (1995). The cadherin-binding specificities of B-cadherin and LCAM. *J Cell Biol* 129, 1379-1390.

Nagafuchi, A., Shirayoshi, Y., Okazaki, K., Yasuda, K., and Takeichi, M. (1987). Transformation of cell adhesion properties by exogenously introduced E-cadherin cDNA. *Nature* 329, 341-343.

Nagar, B., Overduin, M., Ikura, M., and Rini, J.M. (1996). Structural basis of calcium-induced E-cadherin rigidification and dimerization. *Nature* 380, 360-364.

Nakagawa, S., and Takeichi, M. (1995). Neural crest cell-cell adhesion controlled by sequential and subpopulation-specific expression of novel cadherins. *Development* 121, 1321-1332.

Nakagawa, S., and Takeichi, M. (1998). Neural crest emigration from the neural tube depends on regulated cadherin expression. *Development* 125, 2963-2971.

Navarro, P., Caveda, L., Breviario, F., Mandoteanu, I., Lampugnani, M.G., and Dejana, E. (1995). Catenin-dependent and -independent functions of vascular endothelial cadherin. *J Biol Chem* 270, 30965-30972.

Navarro, P., Ruco, L., and Dejana, E. (1998). Differential localization of VE- and N-cadherins in human endothelial cells: VE-cadherin competes with N-cadherin for junctional localization. *J Cell Biol* *140*, 1475-1484.

Nollet, F., Kools, P., and van Roy, F. (2000). Phylogenetic analysis of the cadherin superfamily allows identification of six major subfamilies besides several solitary members. *J Mol Biol* *299*, 551-572.

Nose, A., Tsuji, K., and Takeichi, M. (1990). Localization of specificity determining sites in cadherin cell adhesion molecules. *Cell* *61*, 147-155.

Ozaki, C., Yoshioka, M., Tominaga, S., Osaka, Y., Obata, S., and Suzuki, S.T. (2010). p120-Catenin is essential for N-cadherin-mediated formation of proper junctional structure, thereby establishing cell polarity in epithelial cells. *Cell Struct Funct* *35*, 81-94.

Ozawa, M., Baribault, H., and Kemler, R. (1989). The cytoplasmic domain of the cell adhesion molecule uvomorulin associates with three independent proteins structurally related in different species. *EMBO J* *8*, 1711-1717.

Ozawa, M., Hoschutzky, H., Herrenknecht, K., and Kemler, R. (1990). A possible new adhesive site in the cell-adhesion molecule uvomorulin. *Mech Dev* *33*, 49-56.

Parisini, E., Higgins, J.M., Liu, J.H., Brenner, M.B., and Wang, J.H. (2007). The crystal structure of human E-cadherin domains 1 and 2, and comparison with other cadherins in the context of adhesion mechanism. *J Mol Biol* *373*, 401-411.

Patel, S.D., Chen, C.P., Bahna, F., Honig, B., and Shapiro, L. (2003). Cadherin-mediated cell-cell adhesion: sticking together as a family. *Curr Opin Struct Biol* *13*, 690-698.

Patel, S.D., Ciatto, C., Chen, C.P., Bahna, F., Rajebhosale, M., Arkus, N., Schieren, I., Jessell, T.M., Honig, B., Price, S.R., *et al.* (2006). Type II cadherin ectodomain structures: implications for classical cadherin specificity. *Cell* *124*, 1255-1268.

Perret, E., Benoliel, A.M., Nassoy, P., Pierres, A., Delmas, V., Thiery, J.P., Bongrand, P., and Feracci, H. (2002). Fast dissociation kinetics between individual E-cadherin fragments revealed by flow chamber analysis. *EMBO J* *21*, 2537-2546.

Pertz, O., Bozic, D., Koch, A.W., Fauser, C., Brancaccio, A., and Engel, J. (1999). A new crystal structure, Ca²⁺ dependence and mutational analysis reveal molecular details of E-cadherin homoassociation. *EMBO J* *18*, 1738-1747.

Pokutta, S., Herrenknecht, K., Kemler, R., and Engel, J. (1994). Conformational changes of the recombinant extracellular domain of E-cadherin upon calcium binding. *Eur J Biochem* *223*, 1019-1026.

Posy, S., Shapiro, L., and Honig, B. (2008). Sequence and structural determinants of strand swapping in cadherin domains: do all cadherins bind through the same adhesive interface? *J Mol Biol* *378*, 954-968.

Potter, M.D., Barbero, S., and Cheresch, D.A. (2005). Tyrosine phosphorylation of VE-cadherin prevents binding of p120- and beta-catenin and maintains the cellular mesenchymal state. *J Biol Chem* *280*, 31906-31912.

Price, S.R., De Marco Garcia, N.V., Ranscht, B., and Jessell, T.M. (2002). Regulation of motor neuron pool sorting by differential expression of type II cadherins. *Cell* *109*, 205-216.

Ranscht, B., and Dours-Zimmermann, M.T. (1991). T-cadherin, a novel cadherin cell adhesion molecule in the nervous system lacks the conserved cytoplasmic region. *Neuron* *7*, 391-402.

Redies, C., Treubert-Zimmermann, U., and Luo, J. (2003). Cadherins as regulators for the emergence of neural nets from embryonic divisions. *J Physiol Paris* *97*, 5-15.

Reynolds, A.B., and Carnahan, R.H. (2004). Regulation of cadherin stability and turnover by p120ctn: implications in disease and cancer. *Semin Cell Dev Biol* *15*, 657-663.

Salomon, D., Ayalon, O., Patel-King, R., Hynes, R.O., and Geiger, B. (1992). Extrajunctional distribution of N-cadherin in cultured human endothelial cells. *J Cell Sci* *102 (Pt 1)*, 7-17.

Sano, K., Tanihara, H., Heimark, R.L., Obata, S., Davidson, M., St John, T., Taketani, S., and Suzuki, S. (1993). Protocadherins: a large family of cadherin-related molecules in central nervous system. *EMBO J* *12*, 2249-2256.

Sato, M., and Ohashi, T. (2005). Biorheological views of endothelial cell responses to mechanical stimuli. *Biorheology* *42*, 421-441.

Shan, W., Yagita, Y., Wang, Z., Koch, A., Fex Svenningsen, A., Gruzglin, E., Pedraza, L., and Colman, D.R. (2004). The minimal essential unit for cadherin-mediated intercellular adhesion comprises extracellular domains 1 and 2. *J Biol Chem* *279*, 55914-55923.

Shan, W.S., Tanaka, H., Phillips, G.R., Arndt, K., Yoshida, M., Colman, D.R., and Shapiro, L. (2000). Functional cis-heterodimers of N- and R-cadherins. *J Cell Biol* *148*, 579-590.

Shapiro, L., Fannon, A.M., Kwong, P.D., Thompson, A., Lehmann, M.S., Grubel, G., Legrand, J.F., Als-Nielsen, J., Colman, D.R., and Hendrickson, W.A. (1995). Structural basis of cell-cell adhesion by cadherins. *Nature* *374*, 327-337.

Shimoyama, Y., Takeda, H., Yoshihara, S., Kitajima, M., and Hirohashi, S. (1999). Biochemical characterization and functional analysis of two type II classic cadherins, cadherin-6 and -14, and comparison with E-cadherin. *J Biol Chem* *274*, 11987-11994.

Shimoyama, Y., Tsujimoto, G., Kitajima, M., and Natori, M. (2000). Identification of three human type-II classic cadherins and frequent heterophilic interactions between different subclasses of type-II classic cadherins. *Biochem J* *349*, 159-167.

Sivasankar, S., Zhang, Y., Nelson, W.J., and Chu, S. (2009). Characterizing the initial encounter complex in cadherin adhesion. *Structure* *17*, 1075-1081.

Sopko, R., and McNeill, H. (2009). The skinny on Fat: an enormous cadherin that regulates cell adhesion, tissue growth, and planar cell polarity. *Curr Opin Cell Biol* *21*, 717-723.

Sotomayor, M., and Schulten, K. (2008). The allosteric role of the Ca²⁺ switch in adhesion and elasticity of C-cadherin. *Biophys J* *94*, 4621-4633.

Steinberg, M.S., and Gilbert, S.F. (2004). Townes and Holtfreter (1955): directed movements and selective adhesion of embryonic amphibian cells. *J Exp Zool A Comp Exp Biol* *301*, 701-706.

Suzuki, S., Sano, K., and Tanihara, H. (1991). Diversity of the cadherin family: evidence for eight new cadherins in nervous tissue. *Cell Regul* *2*, 261-270.

Suzuki, S.C., Furue, H., Koga, K., Jiang, N., Nohmi, M., Shimazaki, Y., Katoh-Fukui, Y., Yokoyama, M., Yoshimura, M., and Takeichi, M. (2007). Cadherin-8 is required for the first relay synapses to receive functional inputs from primary sensory afferents for cold sensation. *J Neurosci* *27*, 3466-3476.

Suzuki, S.T. (1997). [Adhesion complex and biological roles of cadherins]. *Seikagaku* *69*, 1269-1271.

Takai, Y., Miyoshi, J., Ikeda, W., and Ogita, H. (2008). Nectins and nectin-like molecules: roles in contact inhibition of cell movement and proliferation. *Nat Rev Mol Cell Biol* *9*, 603-615.

Takeichi, M. (1990). Cadherins: a molecular family important in selective cell-cell adhesion. *Annu Rev Biochem* *59*, 237-252.

Takeichi, M. (1991). Cadherin cell adhesion receptors as a morphogenetic regulator. *Science* *251*, 1451-1455.

Takeichi, M., Hatta, K., Nose, A., and Nagafuchi, A. (1988). Identification of a gene family of cadherin cell adhesion molecules. *Cell Differ Dev* *25 Suppl*, 91-94.

Tamura, K., Shan, W.S., Hendrickson, W.A., Colman, D.R., and Shapiro, L. (1998). Structure-function analysis of cell adhesion by neural (N-) cadherin. *Neuron* *20*, 1153-1163.

Taveau, J.C., Dubois, M., Le Bihan, O., Trepout, S., Almagro, S., Hewat, E., Durmort, C., Heyraud, S., Gulino-Debrac, D., and Lambert, O. (2008). Structure of artificial and natural VE-cadherin-based adherens junctions. *Biochem Soc Trans* *36*, 189-193.

Tomschy, A., Fauser, C., Landwehr, R., and Engel, J. (1996). Homophilic adhesion of E-cadherin occurs by a co-operative two-step interaction of N-terminal domains. *EMBO J* 15, 3507-3514.

Troyanovsky, R.B., Sokolov, E., and Troyanovsky, S.M. (2003). Adhesive and lateral E-cadherin dimers are mediated by the same interface. *Mol Cell Biol* 23, 7965-7972.

Tuckwell, D.S., and Humphries, M.J. (1993). Molecular and cellular biology of integrins. *Crit Rev Oncol Hematol* 15, 149-171.

Uehara, K. (2006). Distribution of adherens junction mediated by VE-cadherin complex in rat spleen sinus endothelial cells. *Cell Tissue Res* 323, 417-424.

Usui, T., Shima, Y., Shimada, Y., Hirano, S., Burgess, R.W., Schwarz, T.L., Takeichi, M., and Uemura, T. (1999). Flamingo, a seven-pass transmembrane cadherin, regulates planar cell polarity under the control of Frizzled. *Cell* 98, 585-595.

Vendome, J., Posy, S., Jin, X., Bahna, F., Ahlsen, G., Shapiro, L., and Honig, B. (2010). Molecular design principles underlying affinity and specificity in classical cadherins. Submitted.

Vestweber, D., and Kemler, R. (1985). Identification of a putative cell adhesion domain of uvomorulin. *EMBO J* 4, 3393-3398.

Vittet, D., Buchou, T., Schweitzer, A., Dejana, E., and Huber, P. (1997). Targeted null-mutation in the vascular endothelial-cadherin gene impairs the organization of vascular-like structures in embryoid bodies. *Proc Natl Acad Sci U S A* 94, 6273-6278.

Volk, T., Geiger, B., and Raz, A. (1984). Motility and adhesive properties of high- and low-metastatic murine neoplastic cells. *Cancer Res* 44, 811-824.

Weis, W.I., Kahn, R., Fourme, R., Drickamer, K., and Hendrickson, W.A. (1991). Structure of the calcium-dependent lectin domain from a rat mannose-binding protein determined by MAD phasing. *Science* 254, 1608-1615.

Wojtowicz, W.M., Wu, W., Andre, I., Qian, B., Baker, D., and Zipursky, S.L. (2007). A vast repertoire of Dscam binding specificities arises from modular interactions of variable Ig domains. *Cell* 130, 1134-1145.

Wu, Y., Jin, X., Harrison, O., Shapiro, L., Honig, B.H., and Ben-Shaul, A. (2010). Cooperativity between trans and cis interactions in cadherin-mediated junction formation. *Proc Natl Acad Sci U S A* 107, 17592-17597.

11. Table of Figures

Figure	Description
Figure 1	Schematic representation of the domain organization of various subfamilies of the superfamily of cadherins.
Figure 2	Domain organization and structural architecture of classical cadherins.
Figure 3	Molecular basis of classical cadherin adhesive binding.
Figure 4	EC1 domains govern cadherin mediated adhesion in classical and desmosomal cadherins.
Figure 5	The adhesive interface found in T-cadherin adopts an X-shaped conformation.
Figure 6	Cadherins are the major cell adhesion protein in adherens junctions.
Figure 7	VE-cadherin, the major adhesion molecule of the vascular endothelium, is proposed to form adhesive hexamers.
Figure 8	Mammalian expressed and purified human and chicken VE-cadherin at concentrations of 1mg/mL examined by SDS-PAGE and stained with coomassie brilliant blue.
Figure 9	Schematic representation of alterations in N-linked glycosylation.
Figure 10	Mammalian expressed VE-cadherin carries substantial quantities of N-linked glycosylation in contrast to type I E-cadherin.
Figure 11	N-linked glycosylation sites in the VE-cadherin ectodomain.
Figure 12	SDS-PAGE of purified VE-cadherin fragments of three different species.
Figure 13	SDS PAGE of purified EC1-2 and EC1-3 fragments of classical type I and type II cadherin.
Figure 14	SDS-PAGE of two domain C-terminally tagged wild type cadherins.
Figure 15	Sedimentation equilibrium analytical ultracentrifugation experiments showing similar profiles of different VE-cadherin ectodomains.
Figure 16	Comparison of elution profiles from analytical size exclusion experiments with human VE-cadherin EC1-5 (blue), double tryptophan mutant W2A W4A (green) and EC3-5 (orange) at a concentration of 0.5mg/mL.
Figure 17	Liposome aggregation by VE- and E-cadherin ectodomains
Figure 18	Electron micrographs of VE-cadherin on liposomes.
Figure 19	AFM-imaging of full ectodomains of VE-cadherin deposited on poly-L-lysine mica reveals monomer and dimer forms.
Figure 20	VE-cadherin behaves differently with and without complex N-linked glycosylation.
Figure 21	Chicken VE-cadherin EC1-2 crystals.
Figure 22	Diffraction pattern from chicken VE-cadherin EC1-2 crystal in space group $P4_3 2_1 2$

with unit cell dimensions of $a=b=99.973$, $c=105.987$ and $a=b=c=90$.

- Figure 23 Images of crystals of human and mouse chicken VE-cadherin EC1-2.
- Figure 24 Crystal structure of the EC1-2 domain of chicken VE-cadherin showing a strand swapped cadherin dimer.
- Figure 25 Chicken VE-cadherin calcium coordination and detailed view of interactions in the strand swapped dimer.
- Figure 26 Comparison of the strand swapped dimer interface of VE-cadherin with those of type I and type II cadherins.
- Figure 27 VE-cadherin uses a different set of residues for trans-dimerization than type II cadherins.
- Figure 28 Superposed α -carbon traces from crystal structures of VE-cadherin and type I and type II classical cadherins.
- Figure 29 Molecular surface presentation of crystal contacts found in the crystallographic asymmetric unit of chicken VE-cadherin.
- Figure 30 Phylogenetic tree branch of strand swap cadherins on the basis domain EC1 adapted from Nollet (2000).
- Figure 31 Surface Plasmon Resonance experiments with cadherins.
- Figure 32 Stability of antibody captured VE-cadherin-FLAG and VE- and N-cadherin-C9 surfaces.
- Figure 33 Analysis of N-cadherin-CYS in SPR binding experiments.
- Figure 34 Preparations for VE-cadherin SPR experiments.
- Figure 35 Homophilic binding of VE-cadherin EC1-2 tested in SPR experiments.
- Figure 36 Homophilic and heterophilic type II cadherin binding assessed by SPR experiments.
- Figure 37 Heterophilic binding of classical type I cadherins E-, N- P- cadherin including N-cadherin strand swap mutant W2A and atypical T-cadherin to type II VE-cadherin and type I N-cadherin.
- Figure 38 Heterophilic binding of VE-cadherin to immobilized N-cadherin-CYS.
- Figure 39 Homophilic and heterophilic cadherin interactions tested in Co-immunoprecipitation assays.
- Figure 40 Effects of strand swapping mutations on homodimerization of T-cadherin, E-cadherin and cadherin-6 in equilibrium AUC experiments.
-

12. List of Tables

Table	Content
Table 1	Classical type I and II cadherins identified in mouse and human
Table 2	Immobilization levels of antibodies and NeutrAvidin used in SPR studies.
Table 3	Statistics of mammalian produced cadherins.
Table 4	Glycosylation quantities found on mammalian produced VE- and E-cadherin ectodomains
Table 5	Summary of bacterial produced cadherins.
Table 6	Summary of C-terminally tagged classical mouse cadherins and associated experiments.
Table 7	Dissociation constants (K_D) for homodimerization of mammalian produced VE-cadherin and E-cadherin.
Table 8	Molecular weight for human VE-cadherin EC1-5 and EC3-5 and mouse E-cadherin W2A K14E determined by MALS.
Table 9	Different glycosylation pattern of human VE-cadherin protein fragments results in different behavior in equilibrium AUC experiments.
Table 10	Dissociation constants (K_D) for homodimerization of VE-cadherin EC1 and EC1-2 fragments.
Table 11	Crystallographic data and refinement statistics.
Table 12	Buried accessible surface area (BSA) for type I and type II cadherin interfaces, BSA value for one protomer given.
Table 13	Root mean square deviations between superposed EC1 (yellow), EC2 (red) and EC12 (blue) domains of type I and type II cadherins.
Table 14	Dissociation constants (K_D) for homodimerization of wild type classical type II cadherins.
Table 15	Sequence identities given in percent between EC1 (lavender) and EC1-2 (light blue) domains of all strand swapping classical cadherins used in our studies.
Table 16	Dissociation constants (K_D) for homodimerization of C-terminally tagged classical type I and II cadherins EC1-2 from mouse. Standard Error is reported.
Table 17	Summary of analyte proteins and their concentrations and distribution of monomer and dimer for SPR experiments.
Table 18	Dissociation constants K_{DS} from equilibrium AUC analysis for cadherin-6, E- and T-cadherin wild type and strand swapping mutants. Standard error is given.

13. Acknowledgements

I would like to thank Prof. Dr. Shapiro for the opportunity to join his lab and conduct my external thesis work under his supervision at Columbia University in the City of New York, USA, in collaboration with the Gottfried Wilhelm Leibniz Universität Hannover, Germany. It was an awesome, interesting, challenging and experience-rich time and I am deeply grateful for all the encouraging discussions, fun talks, the shared knowledge and all the help, trust and support I received during my studies and the interesting topic I was obliged to work on. I enjoyed every minute of it.

Ich möchte mich von ganzem Herzen bei meinen Doktorvätern Prof. Dr. Müller und Prof. Dr. Otto für ihre fachliche Unterstützung, ihr Vertrauen in meine Person und dafür danken, dass Sie immer für mich da waren und diese Arbeit möglich gemacht haben.

In addition, I would also like to thank Prof. Dr. Honig for the guidance and advice throughout my time at Columbia University.

Meinen Eltern danke ich für meine unglaublich schöne Kindheit voller Wärme, Liebe, Freude und Geborgenheit. Von euch habe ich gelernt, auf das Leben neugierig zu sein und dass es auf jedes ‚warum‘ eine Antwort gibt.

I am also deeply grateful to my colleagues, especially to Goran Ahlsen, PhD, for all the analytical ultracentrifugation experiments, we performed and encouraging discussions and to Phinikoula Strati-Katsamba for her help with all the VE-cadherin SPR experiments and encouraging discussions about heterophilic binding and the world. You guys are a milestone to the completion of this work.

Fabiana Bahna, thank you that you were always there for me – from the first minute I set foot into the ‘big city’, you taught me the deep secrets of successful protein purification and protein crystallography and that work is always more fun when you can laugh and have a special person to share it with. Thank you for being such a great friend!

Dear Oliver Harrison, you always have been and always will be my personal hero. With deepest love, Jules.

14. List of Publications

Brasch J, Harrison OJ, Ahlsen G, Carnally SM, Henderson RM, Honig B, Shapiro L. (2010) **Structure and binding mechanism of vascular endothelial cadherin, a divergent classical cadherin.** *Journal of Molecular Biology*, 408 (1): 57-73.

Harrison OJ, Jin, X, Hong S, Bahna F, Ahlsen G, **Brasch J**, Wu Y, Vendome J, Felsovalyi K, Hampton CM, Troyanovsky RB, Ben-Shaul A, Frank J, Trojanovksy SM, Shapiro L, Honig B. (2010) **The extracellular architecture of adherens junctions revealed by crystal structures of type I cadherins.** *Structure*, 19 (2): 244-56.

Harrison OJ, Bahna F, Katsamba PS, Jin X, **Brasch J**, Vendome, J, Ahlsen, G, Carrol KJ, Price SR, Honig B, Shapiro L. (2010) **Two-step adhesive binding by classical cadherins.** *Nature Structural Molecular Biology*, 17 (3): 348-57.

Ciatto C, Bahna F, Zampieri N, CanSteenhouse HC, Katsamba PS, Ahlsen G, Harrison OJ, **Brasch J**, Jin X, Posy S, Vendome J, Ranscht B, Jessel TM, Honig B, Shapiro L. (2010) **T-cadherin structures reveal a novel adhesive binding mechanism.** *Nature Structural Molecular Biology*, 17 (3): 339-47.

Koehnke J, Jin X, Trbovic N, Katsamba PS, **Brasch J**, Ahlsen G, Scheiffele P, Honig B, Palmer AG 3rd, Shapiro L. (2008) **Crystal structures of beta-neurexin 1 and beta-neurexin 2 ectodomains and dynamics of splice insertion sequence 4.** *Structure* 16 (3): 410-21.

15. Curriculum vitae

Persönliche Daten

Name	Julia Brasch
Geburtstag	16. Januar 1982
Geburtsort	Braunschweig, Deutschland

Promotion

04/2007-04/2011	Gottfried Wilhelm Leibniz Universität Hannover, Deutschland in Kollaboration mit der Columbia University in the City of New York, USA Thema der Dissertation: <i>Structural and Biophysical Studies of Adhesive Binding by Classical Cadherins</i>
21.04.2011	Tag der Promotion; bestanden mit Gesamtnote „ausgezeichnet“

Studium

10/2001-01/2007	Gottfried Wilhelm Leibniz Universität Hannover, Deutschland Studium im Fach: Biochemie
06/2006-11/2006	Externe Diplomarbeit an der Columbia University in the City of New York, USA Thema der Diplomarbeit: <i>Characterisation of Neurexin-Neurologin Interactions</i>
05/2006	Diplomprüfung Biochemie; bestanden mit Gesamtnote „sehr gut“ mit Nebenfächern: Organische Chemie und Pharmakologie
08/2003	Biochemie Vordiplom
10/2010	Aufnahme des Studienganges Biochemie an der Gottfried Wilhelm Leibniz Universität Hannover

Schulausbildung

Juni 2001	Abitur; bestanden mit Gesamtnote 1,9
1994-2001	Otto-Hahn-Gymnasium Gifhorn, Deutschland
1992-1994	Orientierungsstufe Meinersen, Deutschland
1988-1992	Grundschule Leiferde, Deutschland
